2014-02-03

Metamodeling methods and their direct methanol fuel cell applications

Yang, Qinwen

UNIVERSITY OF CALGARY

Metamodeling Methods and Their Direct Methanol Fuel Cell Applications

by

Qinwen Yang

A THESIS

SUBMITTED TO THE FACULTY OF GRADUATE STUDIES

IN PARTIAL FULFILMENT OF THE REQUIREMENTS FOR THE

DEGREE OF DOCTOR OF PHILOSOPHY

DEPARTMENT OF MECHANICAL AND MANUFACTURING ENGINEERING

CALGARY, ALBERTA

NOVEMBER, 2013

Abstract

Direct methanol fuel cells (DMFCs) have emerged in recent years as potential power sources for portable electronic devices due to the high energy density of methanol and low power requirements of the portable electronic devices. Fuel cell system modeling plays an important role in the design of DMFC systems. Despite the progress in modeling of DMFCs, most of these models considered only some of the key operating parameters with overly simplified geometric shapes. In addition, since extensive simulations are usually required in design and control of DMFC systems, advanced modeling tools with high computation quality and efficiency are expected. This research focuses on study of adaptive metamodeling methods and applications of these methods in modeling and design of DMFC systems.

A semi-empirical model is developed to build the relationships between all important operating parameters and DMFC performance measures. Coefficients of this semi-empirical model are obtained through experiments and data fitting. The semi-empirical model provides a basis to identify the optimal operating parameters of the DMFC system considering different power requirements. In addition, adaptive metamodeling has been employed to describe the electrochemical relationships in a computational fluid dynamics (CFD) based DMFC model to study influences of both geometric parameters and operating parameters on DMFC performance. The CFD-based DMFC model can be used in optimal design of geometric parameters and optimal control of operating parameters.

Metamodeling methods, which were initially developed as “surrogates” of the expensive simulation process, can be used to model the relationship between input and output parameters in DMFC systems. Influences of two factors, noise level and initial sample size, on quality of adaptive metamodeling considering different metamodel schemes and test functions are studied in this work. Guidelines have been developed for selection of the proper adaptive metamodeling methods. In addition, a new sampling method namely weighted sequential sampling (WSS) method is introduced in this research to improve the accuracy of adaptive metamodeling considering influences of sample quality measures in both input and output parameter spaces. Quality of the global optimization can be improved based on the metamodel built using the WSS method.

Acknowledgements

I would like to thank several people who assisted me during the research process for my doctorial degree and the composition of my thesis. My appreciation and thanks must go to my supervisor, Dr. Deyi Xue, for his continuous guidance and training throughout my Ph.D. program. I learned a lot from him not only in research, but also in many other aspects of my life. I also wish to thank my supervisory committee members, Dr. Theodor Freiheit and Dr. Simon Park, for providing valuable insights, discussions, and encouragements to my research.

I gratefully acknowledge the financial support provided by the Canadian School of Energy and Environment (CSEE) and the Natural Science and Engineering Research Council (NSERC) of Canada for completing my Ph.D. program. Without their financial help, this research would not have been achievable.

I wish to thank the following students, Dong Zhao, Gang Hong, Biao Yu and Amir Kianimanesh, for their valuable assistance, support, encouragement, and discussions during my program.

Finally, I would like to extend my appreciation and grateful thanks to my mother Huifan Tong. Without her love, encouragement, and consistent support, my greatest achievement to date would not have been possible.

Dedication

This thesis is dedicated to my mother and the loving memory of my father.

Table of Contents

List of Tables

List of Figures and Illustrations

CHAPTER 1 INTRODUCTION

1.1 Background

The pursuit of sustainable alternative energy systems is vital for modern industrialized countries especially due to the environmental concerns and volatile petroleum market. Among various alternative energy sources, fuel cells are considered with great potential to replace the batteries or work as power generators (Larminie and Dicks, 2003). A fuel cell is a device that converts the chemical energy from a fuel into electrical energy through a chemical reaction. The interest in developing fuel cell technology has increased due to its following advantages:

- Efficiency. Fuel cells are generally more efficient than combustion engines. The maximum possible (theoretical) efficiency of a fuel cell with fuel of hydrogen is 80%. The efficiency limit for heat engines, such as steam and gas turbines, is 52% (Zhang, 2008).
- Simplicity. The essential parts of a fuel cell are relative simple.
- Low emissions. When hydrogen is used as the fuel, the main by-product of the fuel cell reaction is pure water.
- Silence. Fuel cells are quiet, even those with extensive extra fuel processing equipment. This feature is important for both the portable power generators and stationary power generators (Larminie and Dicks, 2003).

Various types of fuel cells have been developed in the past. These fuel cells include proton exchange membrane (PEM) fuel cells, alkaline fuel cells, phosphoric acid fuel cells (PAFCs), solid oxide fuel cells (SOFCs), and molten carbonate fuel cells (MCFC). Among these fuel cells, the proton exchange membrane (PEM) fuel cells are primarily used as batteries. In a PEM fuel cell, the electrolyte is a solid polymer with mobile protons. The PEM fuel cells usually use hydrogen as the fuel running at a low temperature. Sophisticated catalysts have to be used in PEM fuel cells to improve the reaction rates. In addition, relative pure hydrogen must be used for the PEM fuel cells.

One alternative fuel to hydrogen for PEM fuel cells is methanol. The direct methanol fuel cell (DMFC), which is also a kind of PEM fuel cell, has emerged in the recent years as a potential

power source for portable electronic devices such as laptop computers and cell phones due to the high energy density of methanol and low power requirements of the portable electronic devices (Dillon et al., 2004). Methanol has the advantage that it is easier to transport and refill compared with hydrogen. The complex steam reforming process to produce hydrogen is also eliminated in DMFC systems. In addition, since methanol is fed with a large amount of water to the anode, humidification and water management problems associated with other types of PEM fuel cells are also avoided.

To design and control DMFC systems that can be used in different applications, good understanding and accurate modeling of DMFC behaviors are necessary. From an engineering application point of view, fuel cell behaviors are usually described by performance measures such as output voltage and current density which are influenced by design and operating parameters. Typical design parameters include the type of proton exchange membrane, the catalyst and its preparation, the electrode structure, and the geometric shapes of the fuel cell components. Typical operating parameters include temperature, methanol concentration, flow rates of methanol and air, and pressures of methanol and air.

In principle, the performance measures of fuel cell systems can be achieved through experiments. However, the experiments are usually expensive and time-consuming. To solve this problem, modeling of fuel cell systems based on sophisticated computer analysis programs, such as finite element analysis (FEA) and computational fluid dynamics (CFD), has become standard industry practice. However, the effective use of these computer simulation tools is largely hindered by the diversified model complexities and the computing intensity of simulations. Despite the advancement of computer technology, the cost to run complex and high fidelity computer analysis programs remains high, especially for engineering optimizations based on these simulation systems. In addition, these simulation tools do not help to discover the underling relationships between input and output parameters (Simpson et al., 2001) which are usually required to achieve the optimal product and operating parameters in fuel cell system design.

A technique called *computer experiment* was introduced to achieve the relationships between input and output parameters (Sacks et al., 1989). In the computer experiment, a series of design points with different values of input parameters are generated first by using design of experiment

(DOE) techniques. Second, computer simulations are carried out on these design points to obtain the output parameter values in the form of performance measures. Finally, the results from these computer simulations are collected and an approximation model is built based on the data of input and output parameters by using some statistical methods (Fang et al., 2006). This approximation model is often called *metamodel* (Kleijnen, 1987). The created metamodel can be used to partially replace the sophisticated computer analysis programs with advantages in the following aspects: (1) efficient modeling of the relationships between input and output parameters, (2) easy integration of computer simulation programs, and (3) fast exploration of design space by using approximation models and efficient analysis tools for optimization (Simpson et al., 2001).

Metamodeling techniques have been developed from many different disciplines including engineering disciplines. These metamodels were initially developed as "surrogates" of the expensive simulation process for improving the overall computation efficiency and quality (Wang and Shan, 2007). Kriging method, radial basis function method, and multivariate polynomial method are popular metamodeling methods (Zhao and Xue, 2010).

In the past decade, metamodeling has gained increasing popularity in developing industry applications (Chen et al., 2006). However, the effective use of metamodels is largely dependent on the selected metamodeling method and the sample points which are used to train the metamodels. For the complicated relationships between input and output parameters, sufficient sample points are required to build an accurate metamodel in the traditional metamodeling methods. The large number of sample size leads to the low efficiency in metamodel construction. Depending on whether all the samples are collected at the same time, metamodeling methods are classified into two categories: non-adaptive metamodeling and adaptive metamodeling (Crombecq, 2011). The traditional methods to collect all the data once and build the metamodels using these data belong to the non-adaptive metamodeling approach. In these methods, data sampling strategies are selected, such as the data in the input parameter space are uniformly distributed, to improve quality of metamodeling. In adaptive metamodeling, the data are sampled sequentially. First an initial set of data is sampled to build an initial metamodel. The initial metamodel is then used to determine location of the input parameters to collect the next sample based on the requirement. The new sample is subsequently used to update the metamodel. The

iterative process of identifying the new input location for sampling based on the presently developed metamodel, sampling the new data at the new input location, and updating the metamodel using the new sample is continued until the modified metamodel satisfies the requirement.

From the above discussions, it can be seen that modeling of DMFC systems and development of accurate and efficient metamodels for modeling of the DMFC systems are of great importance in optimal design and control of DMFC systems.

1.2 Problem Statements

Considerable research results have been obtained in the past decade for direct methanol fuel cell (DMFC) modeling (Yang et al., 2011) and metamodeling (Wang and Shan, 2007). However, a number of problems are still needed to be further addressed. These problems in DMFC system modeling and metamodeling are summarized as follows.

1.2.1 Problems in Direct Methanol Fuel Cell System Modeling

Modeling of all important operating parameters for optimal DMFC system control

Despite the progress in research on modeling of relationships between DMFC operating parameters and their corresponding behaviors, these developed models focused on two key operating parameters: temperature and methanol concentration (Song et al., 2004; Arisetty et al., 2009). Although the influences of methanol flow rate and air flow rate have been studied through experiments (Yang et al., 2010), a systematic approach to model the relationships between all important operating parameters and the DMFC performance measures is still required for the optimal control of a DMFC system.

Modeling of both operating parameters and design parameters for optimal DMFC system design

Furthermore, the research on modeling of relationship between DMFC operating parameters and behaviors focused on one specific DMFC (Yang et al., 2011). In order to model DMFC in a more general way, both design and operating parameters need to be considered. For the modeling of the relationships between design/operating parameters and performance measures, most models

found in the literature considered only a single channel with simple geometric shapes at the anode and cathode sides (Baxter et al., 1999; Scott and Argyropoulos, 2004). The impacts of geometric parameters at the anode and cathode on performance measures have not been well studied in DMFC system design. Although Ge and Liu (2006) stated their models had the potential to predict DMFC performance with new geometries, only data collected from a DMFC with the same geometric configuration were used in their model. In addition, the physical and/or chemical model parameters have to be calibrated manually to match the models with the experimental data (Yu et al., 2013).

1.2.2 Problems in Adaptive Metamodeling Considering Accuracy and Efficiency

Selection of the adaptive metamodeling method considering characteristics of the selected application

Many popular metamodeling schemes, including kriging, radial basis function and multivariate polynomial, have been developed and employed in the past for adaptive metamodeling (Crombecq, 2011). The accuracy and efficiency of these adaptive metamodeling methods are influenced by many factors such as the characteristics of the relationship between input and output parameters, the size of the sample data, the uncertainty of the collected sample data, and the initial sample size. Therefore comparative studies to investigate the impacts of influencing factors on accuracy and efficiency of different adaptive metamodeling methods need to be conducted, such that the right metamodeling method can be selected based on the characteristics of the application.

Sequential sampling for adaptive metamodeling considering qualities in both the input and output parameter spaces

The adaptive metamodeling based optimization approach is effective to find the optimum through creating the sample data and searching near the optimum point. Since the sample quality in the whole input parameter space is not considered, the constructed metamodel may only be accurate at specific locations. Therefore the true global optimal solution may not be identified properly. Therefore development of a sampling method considering both input and output parameter spaces has to be conducted to build an accurate global metamodel. In the developed

sequential sampling methods considering sample qualities in both input and output parameter spaces, contributions of the sample qualities in input and output parameter spaces are not changed in the whole adaptive metamodeling process (Jin et al., 2002). With the increase of sample size in adaptive metamodeling, accuracy of the constructed metamodel is also improved and the sample data are more scatted in the input parameter space. Therefore a new sequential sampling method needs to be developed to put more weight on quality of the samples in input parameter space at early iterations in the adaptive metamodeling process while to put more weight on quality of samples in output parameter space at late iterations in the adaptive metamodeling process. Furthermore, a global optimization method based on an accurate metamodel in the whole design space is still needed.

1.3 Research Objectives

Based on the problems stated in Section 1.2, the overall objective of this research is to further improve the accuracy and efficiency of metamodeling and adaptive metamodeling methods and to employ these methods to model DMFC systems considering influences of design and operating parameters.

The specific research objectives are in the following two aspects.

Objective 1: Modeling of Direct Methanol Fuel Cell System Considering Both Design and Operating Parameters

(1.1) Development of a DMFC system modeling method considering all important operating parameters for optimal DMFC system control

(1.2) Development of a DMFC system modeling method considering both operating parameters and design parameters for optimal DMFC system design

Objective 2: Improvement of Accuracy and Efficiency of Adaptive Metamodeling Methods

(2.1) Comparative study considering impacts of influencing factors on accuracy and efficiency of adaptive metamodeling methods

(2.2) Development of a new sequential sampling method considering different contributions of qualities in input and output parameter spaces in different stages of adaptive metamodeling

1.4 Research Summary

Considerable research results have been obtained to achieve the research objectives. These research results are summarized in the following two categories.

(1) Modeling of Direct Methanol Fuel Cell System Considering Both Design and Operating Parameters

(1.1) Development of a semi-empirical model to describe the relationship between operating parameters and performance behaviors of a direct methanol fuel cell system

A systematic approach to model the relationship between the operating parameters and the direct methanol fuel cell performance was introduced first in our study (Yang et al., 2011). Four operating parameters, including temperature, methanol concentration, flow rate of methanol and flow rate of air, are considered in this work. In this research, the relationship is described by a semi-empirical model by integrating theoretical and approximation models. Experiments were designed for collecting performance data under different operating conditions. These experimental data were used to obtain the coefficients of the semi-empirical model. The accuracy of this semi-empirical model was also analyzed. Compared with the theoretical models that require complicated processes to obtain the physical/chemical parameters, the coefficients in our semi-empirical model can be obtained easily through numerical data fitting using the data collected from experiments. Characteristics of this research are summarized as follows:

- A better understanding of the DMFC behaviors was obtained through an analysis of the influences of operating parameters on the DMFC performance based on the semi-empirical model.
- The modeling of the relationships between the operating parameters and the DMFC performance measures could also provide a basis to identify the optimal operating parameters of the DMFC system considering different power requirements.

(1.2) Development of a CFD model with semi-empirical electrochemical relationships to study the influences of geometric and operating parameters on DMFC performance

A three-dimensional computational fluid dynamics (CFD) model was developed to investigate the influences of geometric and operating parameters on performance of a direct methanol fuel cell (DMFC) (Yu et al., 2013). This research was based on the research results by Yang et al. (2011) for DMFC modeling considering influences of only operating parameters. In this work, semi-empirical relationships were introduced to describe the electrochemical behaviors required in the CFD governing equations. Coefficients in these semi-empirical relationships were fitted using experimental data. Two geometric configurations with serpentine channels at the anode and cathode were considered in this work. Temperature, methanol concentration, and methanol flow rate were selected as the operating parameters. Due to the computational effort of CFD, an adaptive metamodeling method was developed to reduce the number of data-fitting iterations for obtaining the coefficients in the semi-empirical relationships. The research on CFD modeling was conducted by Biao Yu, a visiting Ph.D. student in the University of Calgary. The research on adaptive metamodeling was considered as contribution of this thesis work. This research has the following two advantages:

- Compared with the existing CFD models where only simple geometric shapes are considered, sophisticated geometric shapes with serpentine channels were considered in this work. Therefore, in addition to studying the influences of geometric and operating parameters on DMFC performance, the CFD model has the potential to be used in optimal design of geometric parameters and optimal control of operating parameters for developing DMFC systems.
- This research introduced a systematic approach to model the relationships between geometric/operating parameters and performance measures based on CFD. In the existing CFD models, some physical/chemical parameter values must be calibrated manually based on experience or heuristics to fit the data to the model. In this CFD modeling approach, semi-empirical relationships were used to describe the electrochemical relationships. The coefficients in these semi-empirical relationships were fitted automatically using data collected from experiments.

(2) Improvement of Accuracy and Efficiency of Adaptive Metamodeling Methods

(2.1) Comparative study on influencing factors in adaptive metamodeling

In this research, influences of two factors in adaptive metamodeling, noise level of samples and initial size of samples, were investigated through comparative study. Two cases of adaptive metamodeling considering the best output point for optimization and the best fit in a specific output parameter space were considered. Three different metamodels, kriging, radial basis function and multivariate polynomial, were employed in this study. Various test functions were used to create the sample data and evaluate the accuracy and efficiency of the adaptive metamodeling methods considering influences of noise and initial size of samples. The results of this research provide guidelines for selecting appropriate adaptive metamodeling methods to solve various engineering problems. The developed guidelines were used in the selection of adaptive metamodeling methods in the design of DMFC systems. The theoretical contributions and findings identified through this research are summarized as follows.

- A new type of adaptive metamodeling problem considering uniformity in a specific output space was introduced. Compared with the traditional metamodeling methods where uniformity in input parameter space is considered to improve metamodeling quality, the adaptive metamodeling considering uniformity in specific output space can improve the quality of metamodeling in that specific space such that better input parameter values can be identified to achieve a given target output parameter value.
- The influences of noise level on different adaptive metamodeling methods were studied. Low noise level and high noise level were selected to test their influences on different metamodeling methods including kriging method, radial basis function method and multivariate polynomial method.
- The influences of initial sample size on different adaptive metamodeling methods were investigated. In both adaptive metamodeling for optimization and adaptive metamodeling for uniformity in specific output space, large initial sample size and too small initial sample size can lead to large total sample size. Selection of an appropriate small sample size can improve the efficiency and accuracy in adaptive metamodeling.

(2.2) Development of a weighted sequential sampling method considering influences of sample qualities in input and output parameter spaces for global optimization

A new sampling method namely weighted sequential sampling (WSS) method was introduced in this research to improve accuracy and efficiency of adaptive metamodeling considering influences of sample quality measures in both input and output parameter spaces. In this WSS method, sample quality measures in input and output parameter spaces are associated with weighting factors. Values of these weighting factors are changed in sequential sampling considering the different levels of contributions of these sample quality measures in the input and output parameter spaces during the adaptive metamodeling process. Since quality of the metamodel developed through weighted sequential sampling is good in the whole design space, quality of the global optimization can be improved through adaptive metamodeling based on weighted sequential sampling. Effectiveness of the developed method has been demonstrated through comparative studies using test functions. The developed method has been employed in the optimal design of a direct methanol fuel cell system. The contributions and findings through this research are summarized as follows.

- For different problems with different relationships between input and output parameters, influences of sample qualities in input and output parameter spaces on the quality of the metamodel constructed through adaptive metamodeling approach with different sampling methods are different.
- The levels of contributions of quality measures in input and output parameter spaces at different stages in the sequential sampling process are different. The sample quality in input parameter space plays a more important role in early sampling stages while the sample quality in output parameter space plays a more important role in late sampling stages.
- The newly developed two-step global optimization method can improve the quality of global optimization by developing an accurate metamodel considering influences of both input and output parameter spaces, and searching for the optimal points by incorporating the uniformity measure in input parameter space into the optimization objective function to ensure the sample points are well scatted in the input parameter space to prevent the solution from falling into a local optimum.

1.5 Thesis Structure

This thesis is composed of 7 chapters. The research results presented in four major chapters and their relationships are summarized in Figure 1.1.

In Chapter 2, literature reviews on DMFC modeling and metamodeling are provided. The relevant methods, advantages and limitations of these methods, and their applications are discussed.

In Chapter 3, a semi-empirical model is developed to build the relationship between operating parameters and performance considering a single-cell DMFC system.

In Chapter 4, a single-phase 3D CFD model is introduced to study the performance of two DMFC systems with serpentine flow channels at anode and cathode sides considering influences of both geometric and operating parameters.

In Chapter 5, a series of experiments are investigated to examine the impacts of influencing factors on accuracy and efficiency of adaptive metamodeling methods considering three typical metamodeling schemes and different test functions.

In Chapter 6, a new sampling method namely weighted sequential sampling method is introduced to improve accuracy and efficiency of adaptive metamodeling considering influences of sample quality measures in both input and output parameter spaces. Adaptive metamodeling based on weighted sequential sampling is used to improve the quality of global optimization.

In Chapter 7, the major contributions and findings of this research work are summarized and future work is discussed.

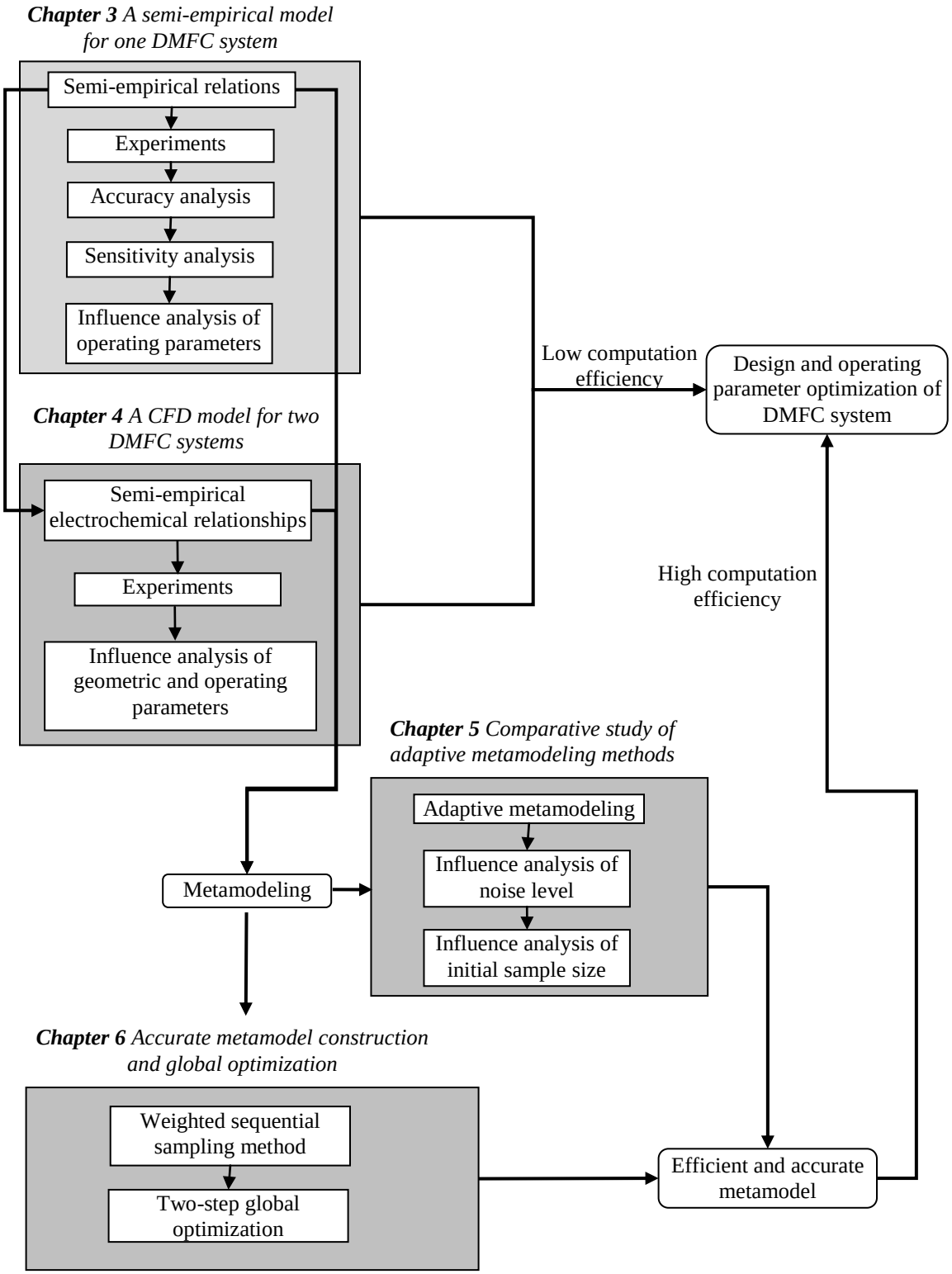

Figure 1.1. Research results and their relations in the thesis.

CHAPTER 2 LITERATURE REVIEW

2.1 Overview

Since this research focuses on modeling of direct methanol fuel cell systems and development of metamodeling methods for improving quality in modeling of direct methanol fuel cell systems, the two relevant research areas, (1) modeling of direct methanol fuel cell systems and (2) data sampling and metamodel construction, are reviewed in this chapter.

In Section 2.2., a brief introduction to direct methanol fuel cell systems is first provided. Modeling of fuel cell systems considering influences of operating parameters and geometric parameters is then discussed. In Section 2.3, several research areas related to metamodeling, including design of experiment techniques, metamodeling methods, influencing factors for metamodeling, and metamodel validation and comparison, are summarized.

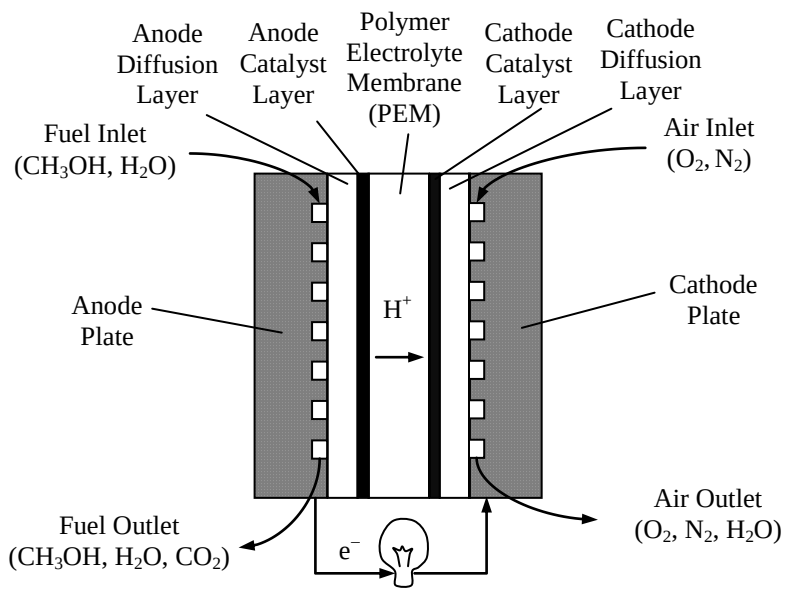

Figure 2.1. Schematic diagram of a direct methanol fuel cell (DMFC).

2.2 Modeling of Direct Methanol Fuel Cell Systems

A direct methanol fuel cell, as shown in Figure 2.1, uses methanol as fuel to generate electricity through reaction with the oxygen in the air. The overall reaction is described by (Larminie and

Dicks, 2003):

$$CH_3OH + \frac{3}{2}O_2 \rightarrow 2H_2O + CO_2 \tag{2.1}$$

A DMFC is primarily composed of a polymer electrolyte membrane (also called proton exchange membrane, or PEM), catalyzed electrodes at the anode and cathode sides, and end plates. The polymer electrolyte membrane and catalyzed electrodes form a membrane electrode assembly (MEA). Nafion by DuPont is often used as the membrane. The electrodes, including the anode and cathode, are thick layers of carbon paper or cloth with Pt-Ru and Pt catalysts deposited on the anode and cathode, respectively. The carbon paper or cloth of the anode and cathode also diffuses methanol and oxygen to the catalysts for reaction. The graphite end plates at anode and cathode sides are used to provide methanol and air through their channels, and withdrawn current. A number of MEAs can be connected by bipolar plates, where channels are provided on both sides of each plate, to form a stack.

The reaction at the anode side is described by:

$$CH_3OH + H_2O \rightarrow 6H^+ + 6e^- + CO_2 \tag{2.2}$$

At the anode, the protons permeate the polymer electrolyte membrane to the cathode side, while the electrons travel through the external circuit to the cathode side to generate current. The required water comes from the methanol solution (e.g., 1 M methanol solution with 3.2% methanol and 96.8% water by mass).

The reaction in the cathode side is described by:

$$\frac{3}{2}O_2 + 6H^+ + 6e^- \rightarrow 3H_2O \tag{2.3}$$

The researches on modeling of DMFC systems are classified into two categories: (1) modeling of the relationship between operating parameters and DMFC performance for one specific DMFC, and, (2) modeling of the relationship between geometric/operating parameters and DMFC performance for DMFC with different designs.

2.2.1 Modeling of Relationship between Operation Parameters and DMFC Performance

The influences of operating conditions on DMFC performance have been extensively studied through experiments (Dillon et al., 2004; Ge and Liu, 2005). In this research area, Song et al. (2004) investigated the influences of temperature and methanol concentration on the crossover of methanol, and consequently on the open circuit voltage and cell performance. They observed that the crossover rate increases as the methanol concentration and temperature increase. They also found out that the performance improves as the temperature increases despite an increase in methanol crossover. At low methanol flow rates, the methanol concentration is too low in the catalyst layer due to mass transfer resistance resulting in low current density. When the flow rate is high enough, any further increase in the flow rate has no significant effect on the methanol concentration in the catalyst layer, thus providing no influence on cell current density. Arisetty et al. (2009) studied the impact of methanol concentration on DMFC performance. Low methanol concentration reduces the reaction rate at the anode, thus resulting in a low operating voltage. However voltage does not simply increase with the increase of methanol concentration due to crossover. Yang et al. (2010) studied the influences of temperature, methanol concentration, and methanol flow rate on the impedance of the fuel cell. At low temperature (e.g., 30 ^{o}C), the slow methanol oxidation reaction and oxygen reduction reaction lead to poor fuel cell performance due to high charge-transfer resistance (CTR). At high temperature (e.g., 50 ^{o}C or 70 ^{o}C), both the enhanced kinetics and the low ohmic losses significantly improve fuel cell performance.

Since experimental research is expensive and time consuming, development of sophisticated mathematical models plays a key role in understanding the physical-chemical processes of DMFCs. Scott et al. (1999) developed a model to describe the methanol transport process that can be used to predict the effective methanol concentration at the catalyst surface and polarization at the anode. They used this model, together with an empirical model of the open circuit voltage and a cathode overpotential model, to predict the voltage and current density of the DMFC. Argyropoulos et al. (2003) and Scott et al. (2006) developed semi-empirical models considering the influences of methanol concentration and temperature on DMFC performance. Through DMFC experiments, Dohle and Wippermann (2004) investigated the influences of operating conditions on the anode, the cathode, and methanol permeation to determine the parameters for a DMFC model. Wang et al. (2008b) developed a semi-empirical model to derive

a nonlinear equivalent circuit from a special group of impedance fuel cell models. Wang et al. (2008a) developed a DMFC performance model based on adaptive-network-based fuzzy inference with methanol concentration, temperature, and current as inputs and cell voltage as output. Celik and Mat (2010) studied the concentration of methanol through experiments and numerical methods.

2.2.2 Modeling of Relationship between Geometric/Operating Parameters and DMFC Performance Based on CFD

Semi-empirical relationships can be used to investigate the relationship between the operating parameters and DMFC performance for one specific DMFC. In order to consider both operating parameters and geometric parameters to obtain a general model for one type of fuel cell, mechanistic model should be used. Mechanistic models are transport models with differential and algebraic equations developed based on electrochemical and physical governing phenomena. In mechanistic models, the phenomena of heat, momentum, multi-component mass transport, multi-phase transportation, and electrochemical processes are considered. Mechanistic models developed based on CFD can be classified into three categories: one-dimensional (1D), two-dimensional (2D), and three-dimensional (3D) models. Figure 2.2 shows a DMFC that is composed of an anode with anode flow channel (AFC), anode diffusion layer (ADL), anode catalyst layer (ACL), proton exchange membrane (PEM), cathode catalyst layer (CCL), cathode diffusion layer (CDL), and cathode with cathode flow channel (CFC). In 1D models, the physical and chemical behaviors are considered only along a single direction, i.e., the X-direction from the anode to the cathode as shown in Figure 2.2. In 2D models, the physical and chemical behaviors are considered along both X-direction and Y-direction (i.e., the direction from inlet to outlet in a channel shown in Figure 2.2). Three-dimensional models are complete models where the physical and chemical behaviors are considered in all three directions. Computational fluid dynamics (CFD) is an effective tool for building mechanistic models in research on DMFCs.

Baxter et al. (1999) developed a one-dimensional model that considers the anode as a porous electrode consisting of an electronically conducting catalyst structure thinly coated with an ion-selective polymer electrolyte. Scott and Argyropoulos (2004) introduced another one-dimensional model to focus on DMFC anode catalyst. This model used a metal mesh supported

electro-catalysts structure and analyzed the multi-reaction paths of methanol oxidation. Oliveira et al. (2008) developed a steady-state, one-dimensional model considering coupled heat and mass transfer, along with the electrochemical reactions occurring in the DMFC. This model can be used to predict the correct trends considering the influences of current density and methanol feed concentration on both methanol and water crossovers. This model was further employed to study the influences of methanol crossover and water crossover on performance of DMFC (Oliveira et al., 2009). Ko et al. (2010) presented a one-dimensional, two-phase model (i.e., liquid and air phases) in which the two-phase species transport behavior through the porous DMFC components was formulated based on the Maxwell-Stefan multi-component diffusion equations, while the capillary-induced liquid flow in the porous media was described by Darcy's law.

Kulikovsky (2000) introduced a two-dimensional numerical model based on mass and current conservation equations. The velocity of the liquid in this model is governed by the gradients of membrane phase potential and pressure. Birgersson et al. (2003) developed an isothermal two-dimensional liquid phase model for the conservation of mass, momentum, and species in the anode of a DMFC. Divisek et al. (2003) developed a two-dimensional model that treats the diffusion layer as a water-gas system in the pore space, with saturation and permeability varying according to capillary effects. Bigersson et al. (2004) further introduced an isothermal two-phase ternary mixture model that takes into account conservation of mass, momentum, and species in the anode of the DMFC. Rice and Faghri (2006) developed a 2-dimensional, transient, multi-phase, multi-component model for a passive DMFC. This model can capture evaporative effects, as water and fuel management issues are crucial. Yang and Zhao (2007) introduced an isothermal, two-dimension, two-phase transport model for liquid-feed DMFC. The two-phase mass transport behaviors in the anode and cathode porous regions were formulated based on the classical multiphase flow in porous media without invoking the assumption of constant gas pressure in the unsaturated porous medium flow theory.

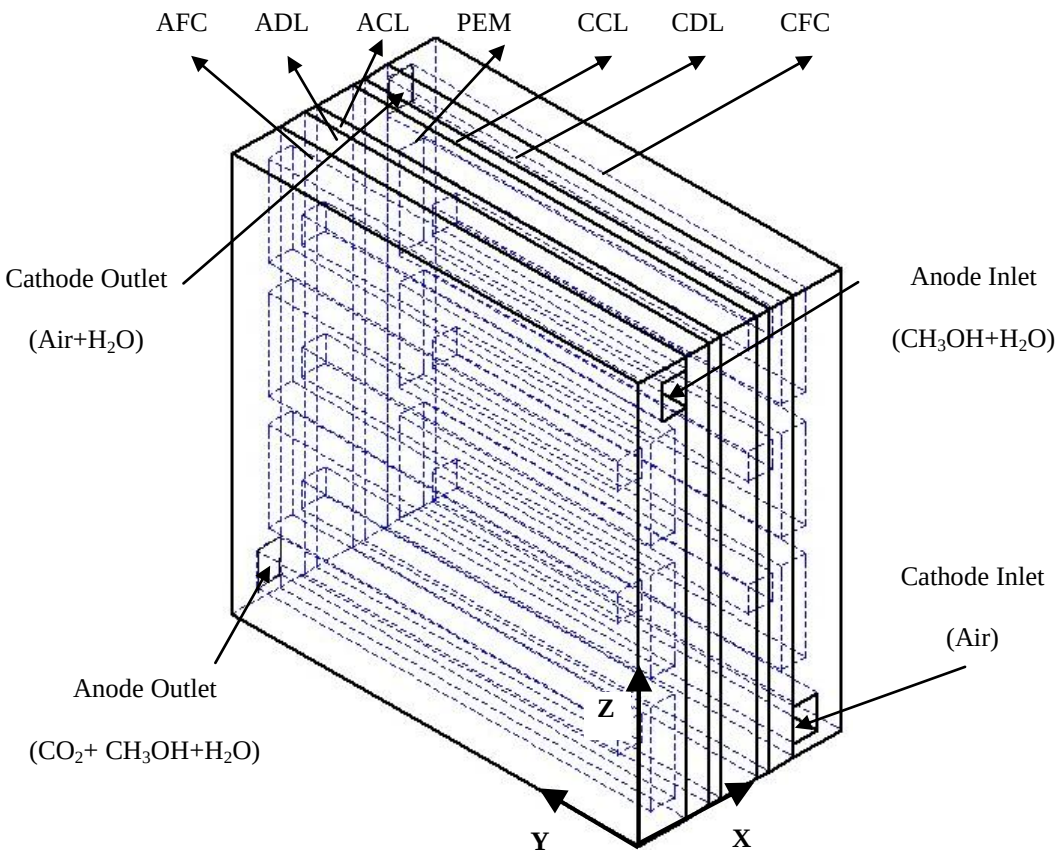

Figure 2.2. Schematic diagram of a direct methanol fuel cell (DMFC).

Although the one-dimensional and two-dimensional CFD models are easier to use, they are not as accurate as three-dimensional CFD models. Ge and Liu (2006) developed a three-dimensional single phase (i.e., liquid phase at the anode and gas phase at the cathode), multi-component model of a DMFC. Danilov et al. (2006) presented a three-dimensional, two-phase CFD model for describing gas evolution and current distribution in a DMFC. Ge and Liu (2007) improved their previous three-dimensional single-phase model into a three-dimensional, two-phase, multi-component model. Liu and Wang (2007) developed a three-dimensional, two-phase, isothermal model for DMFC to investigate the effect of electron transport through the backing layer and the land in bipolar plates. Yang et al. (2007) developed a three-dimensional steady-state model.

2.3 Data Sampling and Metamodel Construction

As mentioned in Section 2.2, modeling of direct methanol fuel cell systems is usually based on experiments and simulations. However, experiments and simulation are often expensive and/or time-consuming. To solve this kind of problem, an approach called computer experiment, which employs design of experiment techniques and approximation methods, was developed for surrogating complicated mathematical models and exploring design space in complex computer simulations (Fang et al., 2006). A computer experiment is usually carried out in two steps: design of experiment and metamodeling.

2.3.1 Design of Experiment

Design of experiments refers to the process of planning, designing and analyzing the experiment such that valid and objective conclusions can be achieved effectively and efficiently. Statistical methods are usually required for developing the experimental design methodologies (Antony, 2003).

In physical experiments, replication, blocking and randomization are considered as the three basic principles for design of experiment to control noise and bias (Santner et al., 2003). Replication is a process to observe the system response at the same design point several times for estimating the magnitude and distribution of random errors. Blocking is a process to classify design points into different groups according to their different characteristics. The relationships between design points and their corresponding system responses are first examined in each individual group and then combined together. Randomization is a process to reduce bias. The overall bias on a system response could be minimized by exploring how the system response changes when other controllable random factors are assigned along with input parameters. Based on the three basic principles, several popular methods such as orthogonal array design, factorial design, and optimal design have been developed and widely used for the design of physical experiments in engineering practice (Atkinson and Donev, 1992).

Considering the difference between physical experiments and computer experiments, the principles of design of experiment are also changed correspondingly. As mentioned by Santner et al. (2003), in computer experiments the observation at a design point should be conducted only

once and design points should provide information in all parts of experimental region. Based on these principles, space filling design has been developed for the computer experiment design. The basic idea behind space filling design is to generate a small number of samples to spread all over the design space and capture the maximum of information about the unknown relationships between inputs and outputs. Typical space filling design methods include random sampling design, Latin hypercube design (McKay et al., 1979), and uniform design (Fang, 1980). In the rest of this subsection, these typical space filling designs are reviewed.

Simple random sampling

Simple random sampling is a basic stochastic method for design of experiment, in which a sequence of design points are generated randomly according to a specific distribution in the s dimensional unit cube $C^s = [0,1]^s$ (Fang et al., 2006).

Simple random sampling could be very useful in some situations, where by sampling design points according to some distributions in the input space and evaluating their corresponding system outputs, the distributions of system outputs can be observed and used for analysis of prediction uncertainty.

One main drawback associated with the simple random sampling is that the design points generated in the s dimensional unit cube are usually not evenly distributed over the experimental region. It could be even worse, for instance, to use simple random sampling for high dimensional problems, where the design points generated by simple random sampling are usually clustered in some parts of the experimental region. Another issue associated with simple random sampling is related to input factors. In simple random sampling, even with more points spreading throughout the experimental region, the generated design points can still not be projected evenly for each of the input parameters in consideration (Santner et al., 2003).

Latin hypercube sampling

Latin hypercube sampling was first proposed by McKay et al. (1979). The basic idea of Latin hypercube sampling is to divide the design space C^s into n strata of equal marginal probability $1/n$ and then sample once from each stratum (Fang et al., 2006). The goal is to ensure that each input variable has all parts of its range represented (Sacks et al., 1989).

Latin hypercube sampling has several obvious advantages over other sampling methods: (1) its sample mean value has a smaller variance compared with simple random sampling (McKay et al., 1979), (2) it could be used for generating design points, when the number of input variables is large and a great many runs are required, (3) it is cheap in computing and easy for implementation compared with other complex sampling methods used in the area of computer experiment.

Some issues associated with classical Latin hypercube sampling method have also been identified and several general guidelines such as (1) to reduce the variance of sample means (Owen, 1992; Tang, 1993), (2) to satisfy symmetric property (Park, 1994; Morris and Mitchell, 1995), and (3) to satisfy column orthogonality (Ye, 1998) have also been developed for improving overall sampling performances.

By applying optimization techniques, some experimental design optimality criteria such as integrated mean squared error (IMSE) (Sacks et al., 1989), maximum entropy (Shewry and Wynn, 1987), and minimax and maximin distance (Johnson et al., 1990) have also been developed and the optimized Latin hypercube sampling on the basis of these criteria is thus called optimal Latin hypercube sampling. However, as pointed out by Wang and Shan (2007), the optimality criteria do not directly relate to the comprehensiveness in capturing functional features and their effectiveness for improving engineering design optimization is not yet proved.

Uniform sampling

Uniform sampling method was initially proposed by Fang (1980). Unlike Latin hypercube sampling, uniform sampling is a deterministic method. This indicates that the samples obtained from a uniform sampling with n runs and s factors should always be the same. The basic idea of uniform sampling is to optimize samples according to a specific optimality criterion - uniformity. In practice, discrepancy, instead of uniformity, is usually used in uniform sampling. The lower the value of discrepancy measure is, the more uniform the distribution of samples is. Several popular discrepancy measures developed in the past include L_2 star discrepancy (Warnock, 1972), centered L_2 discrepancy (Hickernell, 1998a), and wrap around L_2 discrepancy (Hickernell, 1998b).

To build a uniform design with *n* runs and *s* factors to achieve a specific discrepancy measure is a NP (non-deterministic polynomial) hard problem (Fang et al., 2006). Several methods have been developed in the past for tackling this NP hard problem. Good lattice point method (Korobov, 1959), Latin square method (Fang et al., 1999), expending orthogonal array method (Fang, 1995) and cutting method (Ma and Fang, 2004) are popular ones.

Several advantages of uniform sampling, such as its robustness against model change (Fang et al., 2006) and deterministic characteristic, have been recognized. However, as a promising technique for design of experiment, additional studies are still needed considering characteristics of uniform sampling and its applications in the field of computer experiment (Wiens, 1991).

Sequential sampling

When sufficient sample data are collected, an accurate metamodel can usually be constructed based on the samples collected from one-time random sampling, such as Latin hypercube sampling and uniform sampling. However, when experiments and simulations are expensive and/or time-consuming to sample the required data, adaptive metamodeling through sequential sampling is often employed to build the metamodel with the required quality using only small number of sample data. In sequential sampling, initial samples are first collected to build an initial metamodel. Then location of the input parameters to sample the next data is determined based on the requirement (e.g., to minimize the output parameter value) and the input-output relationship defined in the metamodel. The output value corresponding to the newly selected input parameters is then sampled, and this new sample data with input and output parameter values is subsequently used to update the metamodel. The process of data sampling and metamodel updating is continued until a metamodel with good quality is achieved. Several sequential sampling methods have been developed in the past decade (Crombecq, 2011). Jin et al. (2002) introduced the mean squared error (MSE) method for global metamodeling. Xiong et al. (2007) developed a variable fidelity optimization method to reduce the uncertainty of surrogate models in engineering design. Yao et al. (2009) introduced a gradient-based sequential radial basis function neural network modeling method to improve the approximation accuracy. Wei et al. (2012) introduced a new sequential sampling method using a metamodel described by radial basis function to improve accuracy and efficiency in metamodeling.

As the initial samples may not be sufficient to build an accurate metamodel such that the right location of the input parameters for the next sample can be obtained especially when the relationship between input and output parameters is complex, the sequential sampling process should rely less on the constructed metamodel at the very beginning of adaptive metamodeling to avoid sampling the data at poor location due to the poorly developed metamodel. Several sequential sampling methods have been developed to identify the location of the new sample by considering the sample quality measures in the input parameter space, which are independent of the currently constructed metamodel, in addition to the sample quality measures in the output parameter space, which are predicted using the currently constructed metamodel. In this research area, Jin et al. (2002) introduced a hybrid sequential sampling (HSS) method to search for a new sample by maximizing the product of the predicted error considering the output parameter space and the minimum distance between this sample and other existing sample points considering the input parameter space. Busby et al. (2007) employed a flexible two-stage method to combine adaptive domain refinement with sequential experimental design. Crombecq et al. (2011) introduced a hybrid sequential design strategy, which uses Monte-Carlo based approximation of a Voronoi tessellation for exploration and local linear approximation of a simulator for exploitation. Gramacy and Lee (2009) developed a method to automatically explore the input parameter space while simultaneously fitting the response surface using the predicted uncertainty to guide the subsequent experimental runs. Wei et al. (2012) introduced an evaluation criterion to search for the optimal sampling point by maximizing the product of the response surface curvature in the output parameter space and the squared minimum distance to other input parameter locations.

2.3.2 Metamodeling Methods

Metamodeling methods are used in computer experiments to build the approximate mathematical relationships between design inputs and their corresponding system responses. In addition to the basic functionality of model approximation, metamodeling methods can also be used for design space exploration, problem formulation and engineering design optimizations (Wang and Shan, 2007).

In order to develop a metamodeling method, some issues that need to be considered are the performance of fitting and prediction, prediction uncertainty, model complexity, model flexibility, computation efficiency, and the requirements on design of experiment. Several typical metamodeling methods developed in the past include kriging method (Sacks et al., 1989), radial basis functions method (Hardy, 1971), and multivariate polynomial method (Myers and Montgomery, 1995).

Kriging method

Kriging method was initially proposed by Krige (1951) for analysis of data mining. Subsequently, this work was further improved by others such as Matheron (1963) who developed the Gaussian kriging method for modeling spatial data in geostatistics. Kriging method was systematically introduced into the area of computer experiment by Sacks et al. (1989) as a popular metamodeling method.

In kriging method, the random output is assumed to be obtained from a linear combination of regression functions plus a Gaussian random process factor as follows:

$$Y = \sum_{j=0}^{N} \beta_j f_j(\boldsymbol{x}) + Z(\boldsymbol{x}) \tag{2.4}$$

where N+1 is the number of regression functions, $f_j(\cdot)$ is a regression function, β_j is the coefficient for $f_j(\cdot)$, $\boldsymbol{x}$ is the design point, and $Z(\cdot)$ is the Gaussian random process function. It is assumed in kriging method that the random factor is from a Gaussian random process with zero mean, variance σ^2, and a correlation function defined by the following equation:

$$Cov(Z(\boldsymbol{x}_1), Z(\boldsymbol{x}_2)) = r(\theta, \boldsymbol{x}_1, \boldsymbol{x}_2) \tag{2.5}$$

where $Cov(\cdot)$ is the correlation function, $\boldsymbol{x}_1$ and $\boldsymbol{x}_2$ are two design points, and θ is a structural parameter to be optimized. The correlation function could be defined in several different ways such as exponential, Gaussian, linear, spherical, cubical, and spline (Lophaven et al., 2002). When the linear part in kriging method is assumed to be a constant, this kind of kriging method is called ordinary kriging, which is the most widely used method of kriging in engineering practice.

The best linear unbiased predictor (BLUP) is used here for prediction. The best linear unbiased predictor satisfies the following three requirements (Fang et al., 2006): (1) it is a linear combination of the training data outputs:

$$\hat{g}(\boldsymbol{x}) = \sum_{i=1}^{M} c_i(\boldsymbol{x}) y_i \tag{2.6}$$

where $\hat{g}$ is the estimated output value, M is the number of design points in the training data, y_i is an output in the training data, and c_i is the coefficient for y_i; (2) it is unbiased in prediction; and (3) it is of the least prediction variance.

Compared with radial basis functions method and multivariate polynomial method introduced later on, kriging method is more complicated in computation and sensitive to the noises in data due to its interpolative nature. However, by properly choosing from different forms of correlation functions, kriging method can be adjusted for smoothing data instead of just interpolating data (Simpson et al., 2001).

Recently, with the availability of well developed computer programs (Lophaven et al., 2002), kriging method is widely adopted as the metamodeling tool in the research community. In addition, because of its flexibility in interpolating the sample points and its accuracy in dealing with nonlinear problems, kriging method is now considered as one of the most important methods in the field of metamodel-based design optimization (Wang and Shan, 2007).

Radial basis function (RBF) method

Radial basis function method was initially developed as an exact interpolation technique for data in multi-dimensional space (Powell, 1987).

In radial basis function method, a series of center points ($\boldsymbol{x}_{j1}$, $\boldsymbol{x}_{j2}$, …, $\boldsymbol{x}_{jm}$) are chosen first from the design points ($\boldsymbol{x}_1$, $\boldsymbol{x}_2$, …, $\boldsymbol{x}_n$) based on some criteria. Then the basis functions are constructed by using these center points as:

$$B_i(\boldsymbol{x}) = f\left(\left\|\boldsymbol{x} - \boldsymbol{x}_{ji}\right\|\right) \tag{2.7}$$

where $\boldsymbol{x}$ is the design point, $\boldsymbol{x}_{ji}$ is the center point for $B_i(\cdot)$, and $\| \boldsymbol{x}-\boldsymbol{x}_{ji} \|$ is the Euclidian distance between the two points. The radial basis function f could have different forms such as linear,

cubic, thin-plate, spline, Gaussian, multi-quadratic, and inverse multi-quadratic (Powell, 1987). The relationship between inputs and outputs is constructed as a linear combination of radial basis functions:

$$\hat{g}(\boldsymbol{x}) = \beta_0 + \sum_{j=1}^{N} B_j(\boldsymbol{x})\beta_j \tag{2.8}$$

where $\hat{g}$ is the estimated output value, $B_j(\cdot)$ is a basis function, N is the number of basis functions, β_0 is a constant, and β_j is the coefficient for $B_j(\cdot)$.

Radial basis function method suffers from the problem of inefficiency in modeling large scale problems. When sample size is increased, more design points have to be considered for the selection of center points, and the number of basis functions is also increased. The efficiency of building a radial basis function model is thus decreased significantly.

On the other hand, by selecting from different forms of f, radial basis function method can be adapted to solve different kinds of problems.

Multivariate polynomial method

Multivariate polynomial method is one of the most fundamental metamodeling methods used in computer experiment. It is mostly known from response surface method (Myers and Montgomery, 1995), which employs quadratic polynomial in the field of engineering design optimization.

In multivariate polynomial method, basis functions are built directly by using input variable components ($\boldsymbol{x} = [x_1, x_2, \ldots, x_n]$) and their interactions such as:

$$B_0(\boldsymbol{x}) = 1,\ \ B_1(\boldsymbol{x}) = x_1,\ \ B_2(\boldsymbol{x}) = x_2,\ \ \ldots,\ \ B_n(\boldsymbol{x}) = x_n \tag{2.9}$$

$$B_{11}(\boldsymbol{x}) = x_1^2,\ \ B_{12}(\boldsymbol{x}) = x_1 x_2,\ \ \ldots,\ \ B_{1n}(\boldsymbol{x}) = x_1 x_n$$

…

A multivariate polynomial is constructed as the weighted sum of these basis functions:

$$\hat{g}(\boldsymbol{x}) = \beta_0 + \sum_{j=1}^{N} B_j(\boldsymbol{x})\beta_j \tag{2.10}$$

where $\hat{g}$ is the estimated output value, $B_j(\cdot)$ is a basis function, N is the number of basis functions, β_0 is a constant, and β_j is the coefficient for $B_j(\cdot)$.

Due to the way of basis functions construction, when the number of input variables and the order of polynomial are increased (e.g., for highly nonlinear problems), the number of basis functions will be increased significantly. Thus, the number of required samples also increases dramatically, leading to a big burden for complex computer simulations. In addition, stability problems could also occur in this case (Barton, 1992). Fortunately, this issue could be improved within a certain limit by removing unimportant basis functions. Some popular methods such as stepwise selection method based on C_p (Mallows, 1973), AIC (Akaike, 1974), BIC (Schwarz, 1978), and φ-criterion (Hannan and Quinn, 1979) have been developed to address this issue.

However, because of its easy construction, being capable in smoothing noises and efficient in computation, multivariate polynomial method, especially quadratic polynomial method, is still the most widely used metamodeling method in engineering applications (Simpson et al., 2001).

2.3.3 Adaptive Metamodeling

As mentioned in Chapter 1, depending on whether all the samples are collected at the same time, metamodeling methods are classified into two categories: non-adaptive metamodeling and adaptive metamodeling. Different from the traditional metamodeling methods to collect all the data once and build the metamodels, the data are sampled sequentially in adaptive metamodeling. All the popular metamodeling methods, like kriging, radial basis function, multivariate polynomial, can be used for adaptive metamodeling. First an initial set of data is sampled to construct an initial metamodel, which is then used to determine location of the input parameters to collect the next sample based on the requirement. The new sample is subsequently used to update the metamodel. The iterative process of searching the new input location for sampling based on the present metamodel, sampling the new data at the new input location, and updating the metamodel using the new sample is continued until the modified metamodel satisfies the requirement.

Adaptive metamodeling methods were primarily developed to solve two types of problems: (1) optimization to identify the input parameter values that lead to the minimum or maximum output

measure, and (2) accurate approximation of the relationship between input and output parameters within the whole or certain input and/or output spaces.

When adaptive metamodeling is used for optimization, the currently developed metamodel is used as guidance to identify the new sample points that have potential to lead to the optimum. In this research area, Jones et al. (1998) introduced a response surface method to model the nonlinear and multimodal relationships for efficient global optimization. Wang et al. (2004) introduced a global optimization method based on a novel mode-pursuing sampling (MPS) approach to systematically generate more sample points in the neighborhood of the potential optimum while statistically covering the entire search space. Jeong et al. (2005) used the kriging metamodel to improve the accuracy of response surface for objective function evaluation in the optimization process. In this work, the expected improvement (EI) measure was defined and used to select additional sample points to explore the global optimum efficiently. Villemonteix et al. (2007) introduced informational approach to global optimization (IAGO) to address the optimization problem in which stepwise uncertainty reduction strategy was used for selecting the next sample point. Li et al. (2008) presented a new multi-objective design optimization approach in which the kriging-based metamodeling was embedded in multi-objective genetic algorithms. Hassing et al. (2010) developed an RBF-based adaptive metamodel for optimization of the 12 material parameters used in McGinty's Model for AL 6022.

When adaptive metamodeling is used for obtaining accurate approximation of the relationship between input and output parameters, the whole metamodeling space and/or some critical regions are usually considered. Various sequential sampling methods, such as Sobol sequence method (Sobol 1967), minimax method and maximin method (Johnson et al., 1990), can be used in adaptive metamodeling for accurate approximation. In this research area, mean squared error (MSE) approach was introduced by Jin et al. (2002) for global metamodeling. Mourelatos et al. (2006) presented a method to use both global and local metamodels to detect the critical regions and then to obtain accurate approximation. Yao et al. (2009) developed a gradient-based sequential radial basis function neural network modeling method. In this method, the gradient information of the presently constructed metamodel is used to expand the sample set and refine the metamodel sequentially in order to improve the approximation accuracy effectively. Lovison and Rigoni (2010) developed Lipschitz sampling method through evaluation of output data to

build an accurate metamodel efficiently. Li et al. (2010a) introduced an adaptive approach to sample more design points in regions where the simulation responses are expected to be highly nonlinear and multi-modal to build an accurate metamodel with limited sample points. Picheny et al. (2010) developed an adaptive metamodeling strategy to improve the accuracy in the target regions.

2.3.4 Influencing Factors for Metamodeling

The metamodeling efficiency and accuracy are closely related to quality of samples. The three sampling quality merits, including sample uniformity, sample size and sample noise, are considered three main influencing factors for metamodeling (Zhao and Xue, 2010).

Sample uniformity

Uniformity is a measure for evaluating how uniform a point set is scattered in a space. Let $D_n = \{\boldsymbol{x}_1, \boldsymbol{x}_2, ..., \boldsymbol{x}_n\}$ be a set of sample points in the p-dimensional unit cube C^p, and $[\boldsymbol{0}, \boldsymbol{x}) = [0, x_1) \times [0, x_2), \cdots, \times [0, x_p)$ be the Cartesian space defined by $\boldsymbol{x}$. The number of sample points of D_n falling in the Cartesian space $[\boldsymbol{0}, \boldsymbol{x})$ is denoted by $N(D_n, [\boldsymbol{0}, \boldsymbol{x}))$. The ratio $N(D_n, [\boldsymbol{0}, \boldsymbol{x}))/n$ should be as close as possible to the volume of the Cartesian space $Vol([\boldsymbol{0}, \boldsymbol{x}))$. As a measure for evaluating uniformity, L_q *star discrepancy* was defined by Hua and Wang (1981) as follows:

$$D_q(D_n) = \left\{ \int_{C^p} \left| \frac{N(D_n, [\boldsymbol{0}, \boldsymbol{x}))}{n} - Vol([\boldsymbol{0}, \boldsymbol{x})) \right|^q \right\}^{\frac{1}{q}} \tag{2.11}$$

where q=2 is usually selected. The value of L_q star discrepancy changes from 0 to 1. The smaller the value of L_q star discrepancy is, the more uniform the samples are scattered in the design space. As an instance, a point set D_n in Figure 2.2 is scattered in a unit square C^2. Based on the uniformity definition, the ratio of the number of points falling in the enclosed area $[0, x_1) \times [0, x_2)$ to the total number of points in D_n should be close to the area of $[0, x_1) \times [0, x_2)$.

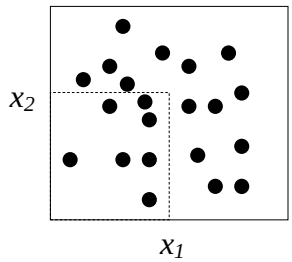

Figure 2.3. Uniformity explained using C^2.

However, L_q *star discrepancy* is expensive to compute. Several modified L_q discrepancies were developed by Hickernell (1998a) and *centered* L_2 *discrepancy* is often selected because of its easiness in calculation. This evaluation measure can be obtained by:

$$(CD(D_n))^2 = \left(\frac{13}{12}\right)^p - \frac{2}{n}\sum_{j=1}^{n}\prod_{i=1}^{p}\left[1+\frac{1}{2}\left|x_{ji}-0.5\right|-\frac{1}{2}\left|x_{ji}-0.5\right|^2\right]$$

$$+\frac{1}{n^2}\sum_{k=1}^{n}\sum_{j=1}^{n}\prod_{i=1}^{p}\left[1+\frac{1}{2}\left|x_{ki}-0.5\right|+\frac{1}{2}\left|x_{ji}-0.5\right|-\frac{1}{2}\left|x_{ki}-x_{ji}\right|\right] \tag{2.12}$$

where n is the number of design points, p is the dimension of the inputs, and x_{ji} is the i-th component of the j-th design point. The value of centered L_2 discrepancy changes between 0 and 1. The smaller the value of centered L_2 discrepancy is, the higher uniformity the samples are of.

<u>*Sample size*</u>

Two types of sample sizes are considered in adaptive metamodeling: initial sample size and total sample size. Initial sample size refers to the small group of points sampled for building the initial metamodel at the very beginning in adaptive metamodeling. Total sample size is the number of samples when the adaptive metamodeling process is stopped. When the accuracy requirement is given, the total sample size can be used as a criterion to evaluate the efficiency of metamodeling. For the non-adaptive metamodeling, total sample size is the number of samples from the one-time sampling before building the metamodel.

Sample noise

Sample noises are introduced due to the uncertainties in metamodeling, such as the uncertainties of the measurement devices to obtain the sampling data. Sample noise can be measured using probability evaluation measures such as variances or standard deviations.

When a given mathematical function $f(\boldsymbol{x})$ is used for evaluation of the influences of noise factors, artificial noises are added to the values of the output parameter using (Zhao and Xue, 2010):

$$Y = f(x) + \alpha Z \tag{2.13}$$

where α is a scaling factor, and Z is a random number sampled from the uniform distribution in the region (-1,1).

2.3.5 Validation and Comparison of Metamodels

Metamodel validation

A metamodel needs to be validated before being used as a "surrogate" of the computation-intensive process (Wang and Shan, 2007).

Some popular metrics for performance measures such as R square, mean squared errors (MSE), root mean squared errors (RMSE), relative average absolute error (RAAE) and relative maximum absolute error (RMAE) can be found in literatures (Jin et al., 2001) and are widely used in engineering applications. Extra conformation samples, in addition to the sample points for constructing the model, are often required to evaluate the constructed metamodels.

Cross validation, for which no extra samples are needed, is another type of popular method used in the field of computer experiment for model validation. In the leave-*k*-out approach (Wang and Shan, 2007), samples are grouped into *N* groups where *k* groups out of the *N* groups are used for prediction and the rest *N*-*k* groups used for training. A special case of the leave-*k*-out is the so-called leave-one-out approach (Mitchell and Morris, 1992) in which just one group is used for prediction and the rest for training. The errors collected from all possible runs of a cross validation process are used for the performance evaluation of a metamodel. It was suggested to use the leave-one-out approach for low-order multivariate polynomial method and radial basis functions method, but leave-*k*-out approach for kriging method (Meckesheimer et al., 2002).

However, as speculated by some researchers, a metamodel that is insensitive to cross validation does not mean that this metamodel is accurate, and it is advised that the results achieved from cross validations should be used carefully along with other measures for the performance evaluation of a metamodel (Lin, 2004).

Metamodel comparison

After different metamodels have been constructed, even if they are based on the same sample points, the performance would be different from one to the other. The relationships among different metamodeling methods have been widely investigated. For instance, Fang et al. (2006) revealed through an analytical investigation that the predictors of the metamodeling methods such as kriging method, local polynomial regression method, and radial basis function (RBF) method could all be written as a linear combination of kernel functions. These metamodeling methods differ from each other only in their choices of kernel functions and the applied regression methods.

Considering the complexities involved in the unknown relationships between design inputs and outputs, the interaction between metamodeling methods and different sampling methods, different computing algorithms used in metamodeling methods, and different performance evaluation measures, it is usually difficult to find the best metamodeling method for a specific problem. For solving this problem, the performance measures of metamodeling methods in specific cases have been observed and several insights on selection of metamodeling methods have also been obtained through comparative studies in the past (Wang and Shan, 2007).

Jin et al. (2001) conducted a systematic comparative study about four metamodeling methods: multivariate polynomial method, kriging method, multivariate adaptive regression splines (MARS) method, and RBF method. Fourteen mathematical and engineering problems representing different nonlinearities and dimensionalities were tested. In addition to the traditional performance aspects such as accuracy, computing efficiency, and modeling robustness, model transparency and simplicity were also studied in their research. Several significant conclusions from their work are summarized as follows: (1) radial basis functions method performs the best in terms of accuracy and robustness and is not sensitive to sample size; (2) multivariate polynomial method is the best for test problems with noise, but kriging method is

very sensitive to noises; (3) multivariate polynomial method is the best in terms of efficiency while kriging method performs the worst; (4) design of experiment plays a very significant role in determining if a test will fail or success, especially for kriging method and RBF method; (5) multivariate polynomial method and MARS have good transparency, which is very helpful to reduce the scale of a problem by removing insignificant factors; (6) considering simplicity, multivariate polynomial method and RBF method are the easiest to implement.

Chen et al. (2006) compared the performances of different metamodeling methods in different kinds of designs of experiments. Seven metamodeling methods (i.e., multivariate polynomial method, RBF method, kriging method, multivariate adaptive regression splines method, regression trees method, artificial neural network method, and least interpolating polynomials method) were considered in their study. Only the predictive root mean squared error was selected as the measure for performance evaluation. Several important conclusions from their study regarding metamodeling methods are listed as: (1) kriging method is accurate at the training sample sites, but it is slow in parameter estimation and its assumptions are difficult to verify; (2) RBF method is flexible in model structures and the speed of programs running is from fast to moderate, however, it is slow in calibrating model parameters and may have artificial periodicity problem; (3) multivariate polynomial method is very fast but not flexible in terms of adapting model forms for different kinds of problems.

Li et al. (2010b) gave a systematic comparison of metamodeling techniques for simulation. Overall performance has been compared among support vector regression (SVR), kriging and RBF. SVR and kriging can be effectively adopted for problems with low dimension, small error size and homogeneous error. For complicated problems with higher dimension, larger error size and heterogeneous error characteristics, RBF is preferable in terms of efficiency although RBF, SVR and kriging are all good metamodeling choices.

Zhao and Xue (2010) carried out a comparative study of metamodeling methods considering sample quality merits. Three sampling merits, sample size, sample uniformity and sample noise, were considered. Four performance measures, accuracy, confidence, robustness and efficiency, were selected. The performances of four metamodeling methods (kriging, RBF, multivariate polynomial and Bayesian neural network) were analyzed according to different performance

measures, based on sample points with different sampling merits. No one metamodeling method could performance the best for each of the performance measures based on the collected sample points.

From the above discussions, we can see that different metamodeling methods behave differently for different applications. No one method is superior to all the others under all different application environments. Thus analyses of the influencing factors for metamodeling and selection of the proper metamodeling method according to the specific application environment are still needed.

CHAPTER 3 A SEMI-EMPIRICAL MODEL CONSIDERING THE INFLUENCES OF OPERATING PARAMETERS ON PERFORMANCE FOR A DMFC SYSTEM

3.1 Introduction

To design and control direct methanol fuel cell (DMFC) systems that can be used in different applications, good understanding and accurate modeling of DMFC behavior are necessary. Generally speaking, the behaviors of the fuel cells are modeled at two different levels: (1) the semi-empirical cell model to describe the relationships between the operating parameters and the fuel cell evaluation measures, and (2) the simulation-based cell model to describe the relationships between design/operating parameters and the fuel cell evaluation measures.

In DMFC, four operating parameters, including temperature, methanol concentration, flow rate of the methanol, and flow rate of the air, play the important roles to contribute to fuel cell behaviors. The fuel cell evaluation measures are primarily described by the performance measures, such as output voltages and power densities at different current densities. The cost measures, such as manufacturing cost and operation cost, can also be used to evaluate designs and operating conditions. In the semi-empirical cell model, instead of using theoretical relationships, approximation relationships with coefficients are used to simplify the theoretical relationships to avoid the difficulty for obtaining the values of the physical parameters. The coefficients in the semi-empirical model are achieved through training using the data collected by experiments. First design of experiment (DOE) method was used to identify the test cases considering the four operating parameters: temperature, methanol concentration, flow rate of the methanol, and flow rate of the air. For each test case, the four operating parameters were assigned with the desired values, and the output of the fuel cells, including the output voltages and their corresponding current densities, were recorded. The coefficients of the semi-empirical model were then achieved from the collected data sets using the least-square curve-fitting method, a simple metamodeling method.

The simulation-based fuel cell model, on the other hand, was developed based on the physical/chemical relationships between design/operating parameters and fuel cell behaviors. The simulation-based analysis tools, primarily the computational fluid dynamics (CFD) analysis tools, were used to achieve the fuel cell performance measures considering different design and

operating parameters. The finite element analysis (FEA) tools were also used for structure analysis. In the simulation-based fuel cell model, in addition to the four operating parameters, the design parameters, primarily the geometric parameters of the channels, the diffusion layers and the catalyst layers at both the anode and cathode sides, are also considered. The physical properties and their relationships in the fuel cell are governed by the built-in equations of the CFD system. The activities in chemical reactions, such as the consumption and creation of chemical substances, are modeled by custom programs using C++. To simplify the theoretical relationships and avoid the difficulty for obtaining the values of the physical parameters, the semi-empirical relationships with coefficients are used to model the chemical reaction activities. The coefficients of these semi-empirical relationships can be obtained through data training using the least square approximation method, a simple metamodeling method. Due to the high computation efforts of the CFD-based simulation, adaptive metamodeling method is required to achieve the values of the coefficients in the semi-empirical relationships. Since different fuel cells with different geometric parameters provide different performance measures, experiments considering multiple designs have to be conducted to collect the required data.

The semi-empirical fuel cell model is primarily used for optimization of operating parameters in the fuel cell operation stage. The simulation-based fuel cell model, on the other hand, is mainly used for optimization of geometric parameters in the design stage.

This chapter focuses on modeling of the relationships between operating parameters and performance measures for a single stack direct methanol fuel cell (DMFC) using a semi-empirical approximation model. The simulation-based CFD model will be introduced in Chapter 4.

3.2 Direct Methanol Fuel Cell (DMFC) and Its Behaviors

The structure of a DMFC and its behaviors have been briefly introduced in Section 2.2. The fuel cell behavior is usually described by the relationship between current density, j (A cm^{-2}), and output cell voltage, V_{cell} (V), as shown in Figure 3.1.

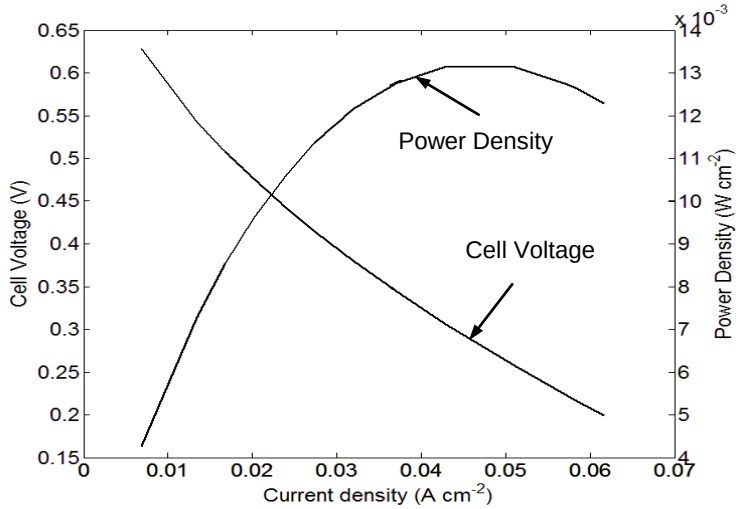

Figure 3.1. Curves to model fuel cell performance.

The power density, P_{cell} (W cm^{-2}), can be calculated by:

$$P_{cell} = V_{cell} \cdot j \tag{3.1}$$

The cell voltage, V_{cell}, can be calculated by (Larminie and Dicks, 2003):

$$V_{cell} = E_o - \eta_R - \eta_{act,a} - \eta_{act,c} - \eta_{con,a} - \eta_{con,c} \tag{3.2}$$

where E_o is the open circuit voltage, η_R is the voltage loss due to ohmic polarization, $\eta_{act,a}$ and $\eta_{act,c}$ are the voltage losses at the anode and cathode due to activation polarization, and $\eta_{con,a}$ and $\eta_{con,c}$ are the voltage losses at the anode and cathode due to concentration polarization. The voltage loss is also called overpotential.

The ohmic overpotential η_R is calculated by:

$$\eta_R = R_e j \tag{3.3}$$

where R_e ($\Omega \cdot$cm^2) is the area-specific resistance of the fuel cell, particularly contributed to by the resistance of the membrane in DMFC. The area-specific resistance, R_e, is primarily influenced by the absolute temperature T (K) (Scott et al., 2006):

$$R_e = R_0 \exp\left(\frac{B}{T} - \frac{B}{T_0}\right) \tag{3.4}$$

where T_0 and R_0 are the reference temperature and area-specific resistance, respectively, and B is a constant determined from experimental data.

According to Scott et al. (2006), the open circuit voltage, E_o, can be calculated by:

$$E_o = \frac{1}{\beta_c + \beta_{ME}} \left[\beta_{ME} E_{ME}^0 + \beta_c E_{O_2}^0 - \ln\left(\frac{j_0 p_O^{ref}}{j_{0c} (p_O)^{N_o}} \right) - N \ln \frac{C_{ME}}{C_{ME}^{ref}} \right] \tag{3.5}$$

where E_{ME}^0 and $E_{O_2}^0$ are the standard potentials at the anode and cathode when polarization is not considered, j_0 and j_{0c} are the exchange current densities at the anode and cathode, p_O^{ref} and p_o are the reference partial pressure and actual partial pressure of oxygen, N and N_o are orders of reaction for methanol oxidation and oxygen reduction defined as the powers to which the concentration terms in the rate equations are raised, and C_{ME}^{ref} and C_{ME} are the reference methanol concentration and actual methanol concentration. In Equation (3.5), β_i is calculated by:

$$\beta_i = \frac{\alpha_i n_i F}{RT}, \ (\mathrm{i} = \mathrm{ME,c}) \tag{3.6}$$

where α_i is the transfer coefficient, n_i is the stoichiometric number of electrons for a methanol molecule consumed in the reaction, F is the Faraday constant (96,485 C mol^{-1}), R is the gas constant (8.314472 J (mol·K)$^{-1}$), and T is the absolute temperature.

Calculation of the overpotential measures considering activation and concentration polarizations at the anode and cathode is a non-trivial task. Scott et al. (2006) combined the activation and concentration overpotential measures separately at the anode and cathode. In their model, the total overpotential due to activation and concentration polarizations at the anode, η_a, is calculated by:

$$\eta_a = \frac{RT}{\alpha_a F} \left[\ln \frac{j C_{ME}^{ref}}{j_0 (C_{ME})^N} - N \ln\left(1 - \frac{j}{n F k_{eff} C_{ME}} \right) \right] \tag{3.7}$$

where α_a is the transfer coefficient at anode, n is the stoichiometric number of electrons for a methanol molecule consumed in the electrode reaction, and k_{eff} is the effective mass transfer coefficient, which increases with the increase in temperature and methanol concentration.

According to Scott et al. (2006), the total overpotential due to activation and concentration polarizations at the cathode, η_c, is calculated by:

$$\eta_c = \frac{RT}{\alpha_c F}\left[\ln\frac{jp_O^{ref}}{j_{0c}(p_O)^{N_O}} - N_O \ln\left(1-\frac{j}{nFk_{1O}p_O}\right)\right] \tag{3.8}$$

where α_c is the transfer coefficient at cathode, and k_{1O} is the mass transfer coefficient at cathode.

Assuming the reduction of oxygen does not proceed under mass transport limitations (Scott et al., 2006), the second term in Equation (3.8) is not needed to calculate the η_c. Therefore the total overpotential at anode and cathode due to activation and concentration polarizations can be calculated by:

$$\eta_a + \eta_c = \frac{RT}{\alpha_a F}\left[\ln\frac{jC_{ME}^{ref}}{j_0(C_{ME})^N} - N\ln\left(1-\frac{j}{nFk_{eff}C_{ME}}\right)\right] + \frac{RT}{\alpha_c F}\ln\frac{jp_O^{ref}}{j_{0c}(p_O)^{N_O}} \tag{3.9}$$

Although the theoretical models are effective in describing the physical and chemical behaviors of DMFCs, these models are difficult to employ for the design and control of DMFC systems due to the complexity involved in obtaining the values of the parameters for these models. In this work, a semi-empirical model is developed to simplify this complexity while maintaining good quality for modeling DMFC behaviors.

3.3 A Semi-empirical Model

The semi-empirical model introduced in this research has been developed based on the theoretical models provided in the literature, particularly the equations given by Scott et al. (2006), where the relationships between operating conditions, including temperature and methanol concentration, and DMFC performance were extensively discussed. In our semi-empirical model, the flow rates of methanol and air are also considered. Many parameters given in Scott et al. (2006) were combined and simplified as coefficients in our semi-empirical model, and the values of these coefficients were obtained through an approximation process using the data collected from experiments.

In our semi-empirical model, the fuel cell voltage, V_{cell}, is described by:

$$V_{cell} = E_o - \eta_R - \eta_{ac} \tag{3.10}$$

where E_o is the open circuit voltage, η_R is the overpotential due to ohmic polarization, and η_{ac} is the total overpotential due to activation and concentration polarizations at both the anode and the cathode. Three sub-models, including a resistance sub-model, an open circuit sub-model and a closed circuit sub-model, have been developed to predict ohmic overpotential, open circuit voltage, and activation/concentration overpotential.

3.3.1 The Resistance Sub-model

The resistance sub-model aims at identifying the area-specific resistance of the DMFC, R_e, so the ohmic overpotential, η_R, can be calculated by Equation (3.3).

According to Scott et al. (2006), resistance of the DMFC is dominated by the resistance of the polymer electrolyte membrane. Temperature is the major factor that influences the resistance of the DMFC. Based on these observations, the area-specific resistance, R_e, in units of Ω cm^2 in our resistance sub-model is described by:

$$R_e = a_1 e^{(\frac{a_2}{T} - a_3)} \tag{3.11}$$

where T is the absolute temperature in Kelvin, and a_1, a_2 and a_3 are experimentally determined coefficients.

3.3.2 The Open Circuit Sub-model

The open circuit sub-model aims at identifying the open circuit voltage E_o in Equation (3.10). From Equations (3.5) and (3.6) and the research result of Qi and Kaufman (2002), the open circuit voltage is primarily influenced by temperature, methanol concentration, and partial pressure of oxygen. Since the partial pressure of oxygen is coupled with the flow rate of air, in this research the open circuit voltage is modeled as a function of temperature, methanol concentration and air flow rate in the open circuit sub-model:

$$E_o = E_o^{(R)} + b_1 T + b_2 T \ln C_{ME} + b_3 T \ln(F_{AIR}) + b_4 \tag{3.12}$$

where $E_o^{(R)}$ is the reversible "no-loss" cell voltage, T is the temperature, C_{ME} is the molar concentration of methanol, F_{AIR} is the flow rate of air in the unit of ccm (cubic centimeters per minute), and b_1-b_4 are experimentally determined coefficients. The reversible "no-loss" cell voltage, $E_o^{(R)}$, is calculated by Larminie and Dicks (2003) as:

$$E_o^{(R)} = \frac{-\Delta\overline{g_f}}{nF} = \frac{-(-698.5\times10^3)}{6\times96485} = 1.21\,\text{V} \tag{3.13}$$

where $\Delta\overline{g_f}$ is the molar Gibbs energy released from the methanol reaction ($\Delta\overline{g_f}$ = –698.5×10^3 J·mol^{-1}), n is the number of electrons transferred for each molecule of methanol (n = 6), and F is the Faraday constant.

3.3.3 The Closed Circuit Sub-model

The closed circuit sub-model aims at identifying the total overpotential, η_{ac}, due to activation and concentration polarizations at both the anode and cathode. According to Equation (3.9), η_{ac} is influenced by temperature, methanol concentration, and flow rates of the methanol and air.

To simplify the calculation, Equation (3.9) is first transformed into:

$$\begin{aligned}\eta_{ac} = \eta_a + \eta_c &= \frac{RT}{\alpha_a F}\left[\ln j + \ln\left(\frac{C_{ME}^{ref}}{j_0}\right) - N\ln(C_{ME}) - N\ln\left(1 - \frac{1}{nFk_{eff}C_{ME}}j\right)\right] \\ &+ \frac{RT}{\alpha_c F}\left[\ln j + \ln\left(\frac{p_O^{ref}}{j_{0c}}\right) - N_o\ln(p_o)\right]\end{aligned} \tag{3.14}$$

The transfer coefficients at the anode and cathodes, α_a and α_c, are influenced by temperature, methanol concentration and current density (Vera, 2007). The partial pressure of oxygen, p_o, is coupled with the flow rate of air. In addition, the flow rate of methanol also plays a role in the activation and concentration polarizations. Based on the above considerations, the overpotential, η_{ac}, is modeled as a function of the four operating parameters by:

$$
\begin{aligned}
\eta_{ac} = & \left[c_1 j^3 + c_2 j^2 + c_3 j + c_4 T + c_5 C_{ME}^2 + c_6 C_{ME} + c_7\right] \\
& \times \left[\ln j + c_8 - c_9\left(\ln(C_{ME}) + \ln\left(1 - \frac{1}{c_{10} e^{(-c_{11}/T)} C_{ME}^2} j\right)\right)\right] \\
& + \left[c_{12} j^3 + c_{13} j^2 + c_{14} j + c_{15} T + c_{16} C_{ME}^2 + c_{17} C_{ME} + c_{18}\right] \\
& \times \left[\ln j + c_{19} - c_{20} \ln(F_{AIR})\right] - c_{21} j^2 \ln(F_{ME})
\end{aligned}
\tag{3.15}
$$

where j is the current density in units of A cm^{-2}, T is the absolute temperature in Kelvin, C_{ME} is the molar concentration of methanol, F_{ME} and F_{AIR} are the methanol and air flow rates in ccm (cubic centimeters per minute), and c_1-c_{21} are 21 experimentally determined coefficients.

3.3.4 The Overall Semi-empirical Model

The overall semi-empirical model considering the influences of the four operating parameters on the DMFC performance is determined by combining Equations (3.3), (3.10)-(3.13), and (3.15):

$$
\begin{aligned}
V_{cell} = & 1.21 + b_1 T + b_2 T \ln C_{ME} + b_3 T \ln(F_{AIR}) + b_4 - a_1 e^{(\frac{a_2}{T} - a_3)} j \\
& - \left[c_1 j^3 + c_2 j^2 + c_3 j + c_4 T + c_5 C_{ME}^2 + c_6 C_{ME} + c_7\right] \\
& \times \left[\ln j + c_8 - c_9\left(\ln(C_{ME}) + \ln\left(1 - \frac{1}{c_{10} e^{(-c_{11}/T)} C_{ME}^2} j\right)\right)\right] \\
& - \left[c_{12} j^3 + c_{13} j^2 + c_{14} j + c_{15} T + c_{16} C_{ME}^2 + c_{17} C_{ME} + c_{18}\right] \\
& \times \left[\ln j + c_{19} - c_{20} \ln(F_{AIR})\right] + c_{21} j^2 \ln(F_{ME})
\end{aligned}
\tag{3.16}
$$

Values of the coefficients in the semi-empirical model for a DMFC should be obtained by collecting data of operating parameters, current density and cell voltage through experiments, and calculating these coefficient values through numerical data fitting.

3.4 Experiments

3.4.1 The Direct Methanol Fuel Cell (DMFC) – TekStak^{TM}

A DMFC kit, TekStak^{TM}, manufactured by Parker Hannifin Energy Systems was used to determine the values of the coefficients in the semi-empirical model (Parker, 2006). The DMFC stack is composed of a single cell with components of an MEA, two graphite end plates with

channels for the anode and cathode, and two plastic end plates. Components of the kit are shown in Figure 3.2.

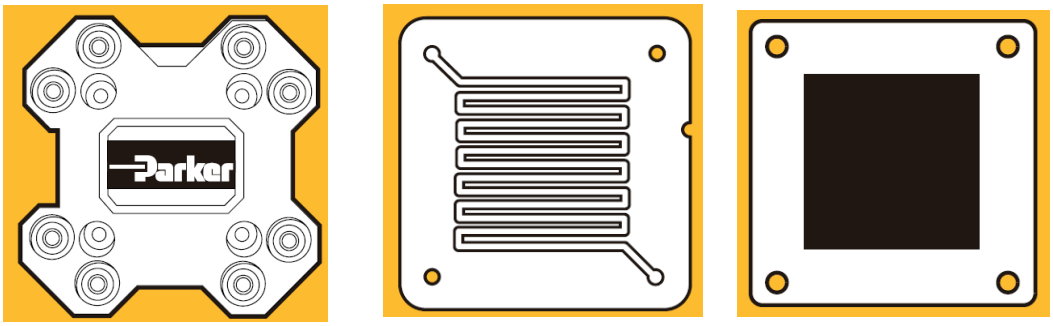

(a). Plastic end plate. (b). Electrode end plate. (c). MEA.

Figure 3.2. Components of the TekStak™ DMFC stack (Parker 2006).

The MEA is composed of a Nafion 117 membrane, an anode with catalyst of Pt-Ru, and a cathode with catalyst of Pt. The total electrode active area, *A*, is 10 cm^2 with a serpentine channel of 13 passes on one side of the anode or cathode as shown in Figure 3.2(b). Each of the passes is 30.90 mm long, 1.27 mm wide, and 0.5 mm high. The rib between two passes is 1.07 mm in width.

3.4.2 Experiment Setting

Figure 3.3 shows the schematic diagram of the experimental set-up. Figure 3.4 shows a snapshot of the experimental set-up.

The methanol is mixed with deionized water and pumped into the DMFC at a controlled flow rate using a peristaltic pump (VWR 54856-070). The air is fed into the fuel cell at a controlled flow rate using an air compressor and regulated by a rotameter (Omega FL-3861SA 150 mm). The DMFC was redesigned to replace the two plastic end plates with two aluminum end plates electrically insulated from the fuel cell with Teflon spacers such that a rope heater (Omega HTC) could be wrapped to change the working temperature of the fuel cell through a controller (Omega CSC32). The temperature inside the fuel cell is measured by a thermocouple (Omega Type K), and the temperature reading is displayed by a data acquisition unit. The anode and cathode outlet materials are collected by an outlet tank. The methanol container, the air pump,

and the outlet tank are connected with the inlets and outlets of the anode and cathode of the DMFC stack using polypropylene tubes. An electronic load device (BK Precision 8540) is used to change the current density to different levels and measure the corresponding values of the voltage. In addition, a potentiostat (Gamry Reference 600) is used to measure the resistance of the fuel cell.

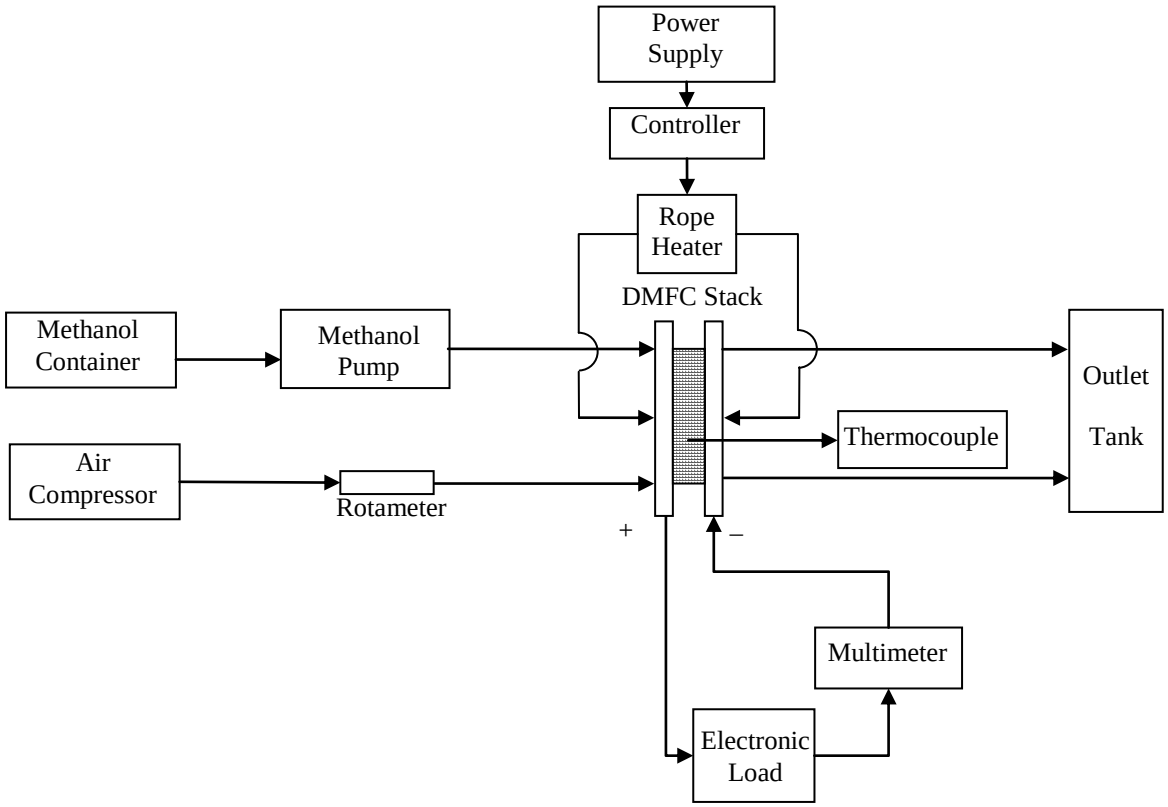

Figure 3.3. Schematic diagram for the direct methanol fuel cell testing system.

3.4.3 Design of Experiments

The coefficients in the semi-empirical model were obtained by changing the operating parameters, measuring the output parameters, and calculating the values of the coefficients through a numerical data fitting technique. The operating parameters, measurement parameters, and the coefficients to be fitted are shown in Table 3.1.

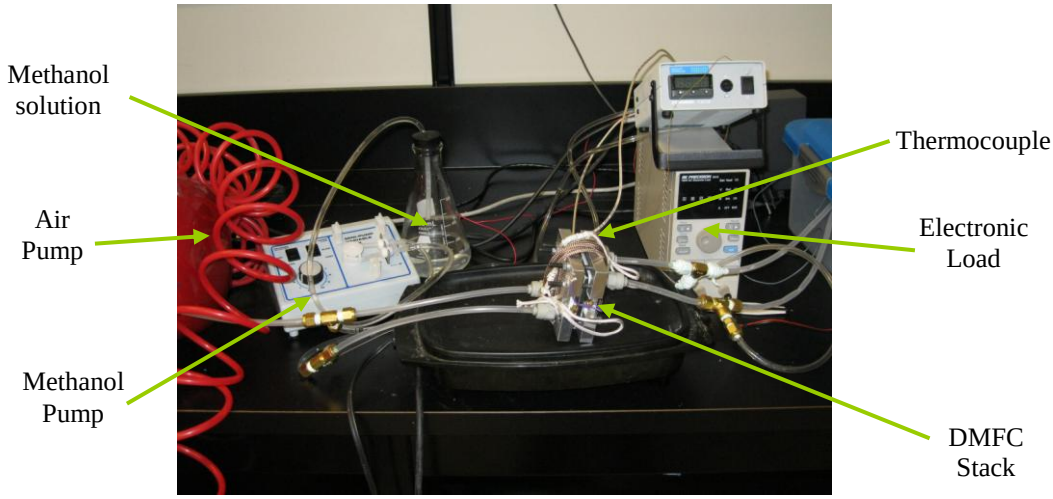

Figure 3.4. A snapshot of the direct methanol fuel cell testing system.

Table 3.1. Operating parameters, measurement parameters, and coefficients for the semi-empirical model.

Sub-model	Operating Parameters	Measurement Parameters	Coefficients
Resistance Sub-model	T: Temperature (K)	R_e: Area-Specific Resistance (Ω cm^{-2})	$a_1,...,a_3$
Open Circuit Sub-model	T: Temperature (K) C_{ME}: Methanol Concentration (M) F_{AIR}: Flow Rate of Air (ccm)	E_o: Open Circuit Voltage (V)	$b_1,...,b_4$
Closed Circuit Sub-model	T: Temperature (K) C_{ME}: Methanol Concentration (M) F_{ME}: Flow Rate of Methanol (ccm) F_{AIR}: Flow Rate of Air (ccm)	j: Current Density (A cm^{-2}) V_{cell}: Cell Voltage (V)	$c_1,...,c_{21}$

The coefficients for the resistance and the open circuit sub-models (Equations (3.11) and (3.12)) can be obtained directly using the operating and measurement parameters. For the closed circuit sub-model, first Equation (3.10) is transformed into:

$$\eta_{ac} = E_o - \eta_R - V_{cell} = E_o - R_e j - V_{cell} \tag{3.17}$$

to calculate the η_{ac}. In Equation (3.17), the E_o is calculated using Equation (3.12), R_e is calculated using Equation (3.11), and V_{cell} is measured through experimentation. The coefficients of the closed circuit sub-model in Equation (3.15) can then be calculated through numerical data fitting.

Four operating parameters, including temperature (T), methanol concentration (C_{ME}), flow rate of the methanol (F_{ME}), and flow rate of the air (F_{AIR}), are considered in this research. For each operating parameter, five different levels of values are selected. The values of the operating parameters, selected based on the literature review and our experimental practice, are summarized in Table 3.2.

Table 3.2. Operating parameters and five levels of these operating parameters.

Operating Parameter	**Level**				
	1	**2**	**3**	**4**	**5**
T: Temperature (K)	298	313	323	333	343
C_{ME}: Methanol Concentration (M)	0.25	0.5	1	1.5	2
F_{ME}: Flow Rate of Methanol (ccm)	3.5	4	4.5	5	5.5
F_{AIR}: Flow Rate of Air (ccm)	81.2	93.6	108.7	125.2	140.8

For the resistance sub-model, only the temperature is selected as the operating parameter. Since five levels of this operating parameter are considered, five test cases were conducted to obtain the coefficients in the resistance sub-model at the same temperature levels shown in Table 3.2.

Table 3.3. Forty-five test cases for the open circuit and closed circuit sub-models.

Test Case No.	**Levels of Operating Parameters**				**Testing Case No.**	**Levels of Operating Parameters**				**Testing Case No.**	**Levels of Operating Parameters**			
	T	**C_{ME}**	**F_{ME}**	**F_{AIR}**		**T**	**C_{ME}**	**F_{ME}**	**F_{AIR}**		**T**	**C_{ME}**	**F_{ME}**	**F_{AIR}**
1	1	3	5	2	**16**	3	1	5	2	**31**	5	1	4	5
2	4	3	3	4	**17**	2	5	3	5	**32**	4	5	2	5
3	3	5	2	1	**18**	4	4	1	3	**33**	5	2	1	5
4	4	1	1	1	**19**	2	3	1	1	**34**	4	1	3	2
5	3	4	4	2	**20**	3	4	1	5	**35**	5	4	4	3
6	1	4	2	1	**21**	2	5	5	1	**36**	1	1	4	1
7	3	2	2	4	**22**	1	2	1	2	**37**	3	3	2	2
8	3	2	3	4	**23**	2	1	1	3	**38**	4	5	3	2
9	5	5	1	2	**24**	1	4	5	5	**39**	1	1	2	5
10	2	3	2	3	**25**	1	5	1	4	**40**	5	1	2	3
11	1	2	3	4	**26**	2	1	5	4	**41**	5	5	5	4
12	5	4	3	1	**27**	4	3	4	1	**42**	2	3	4	5
13	4	2	5	3	**28**	2	2	3	2	**43**	1	5	4	3
14	2	4	3	3	**29**	5	2	5	1	**44**	3	2	4	3
15	3	4	4	4	**30**	4	3	5	5	**45**	5	3	2	4

The test cases of Table 3.2 can be used to obtain the coefficients in both the open circuit sub-model and the closed circuit sub-model. The open circuit voltage is measured when the external

resistance circuit is disconnected. Since four operating parameters and five levels are considered, the complete testing requires 5^4 = 625 cases. To reduce the testing effort, design of experiment methodology is employed in this research to reduce the number of test cases. In this research, a uniform design (UD) methodology (Fang et al., 2000) was used to determine design points that are uniformly scattered in the design space. A uniform experimental design considering four factors at five levels gives case tables for 5, 10, 15, 20, 25, 30, 35, 40, 45, 50, and 55 tests. We selected the table with 45 cases considering fuel cell test efficiency and quality of numerical data fitting. These 45 test cases are shown in Table 3.3.

3.4.4 Experimental Data Collection

The area-specific resistance measures of the fuel cell at different temperatures were obtained as shown in Table 3.4 using the potentiostat.

Table 3.4. Five test cases for the resistance sub-model.

Temperature (K)	Area-Specific Resistance (Ω cm^2)
298	1.42
313	1.39
323	1.11
333	1.02
343	0.98

In these tests, the other operating parameters were selected as:

C_{ME} = 0.5 M

F_{ME} = 3.5 ccm

F_{AIR} = 81.2 ccm

Different values of these three operating parameters have also been used to test the area-specific resistance measures. It was found that the influences of methanol concentration, flow rate of the methanol and flow rate of the air on the area-specific resistance were insignificant. The experimental results match with the assumptions for the semi-empirical model.

For each of the 45 test cases, the voltage at different current densities was measured as shown in Figure 3.5. The voltage at j = 0 is the open circuit voltage E_o. By reducing the electronic load, the

current density is increased and the cell voltage is decreased. For each test case, 15 or more data points were collected.

Multiple tests were conducted for some of the test cases. Three additional test cases with methanol concentration levels of 0.25 M, 0.5 M and 1 M were added because when the methanol concentration is increased, the cell voltage increases at low methanol concentration (around 0.25 M), while the cell voltage decreases at high methanol concentration (around 1 M). Other operating parameters for these three test cases were selected as T = 323 K, F_{ME} = 4.5 ccm, and F_{AIR} = 186 ccm. In total, 65 tests were conducted for the 48 test cases.

During the data collection process, degradation of fuel cell performance was observed for test cases repeated at different time points. In this work, a simple linear regression method was utilized to compensate the data considering this degradation. In this compensation method, a time parameter, in addition to the four operating parameters, was introduced to model the fuel cell performance. The collected data at different time points were used to obtain the coefficients in the linear regression model. The system performance measures for all test cases representing behavior at one point in time were selected to develop the semi-empirical model.

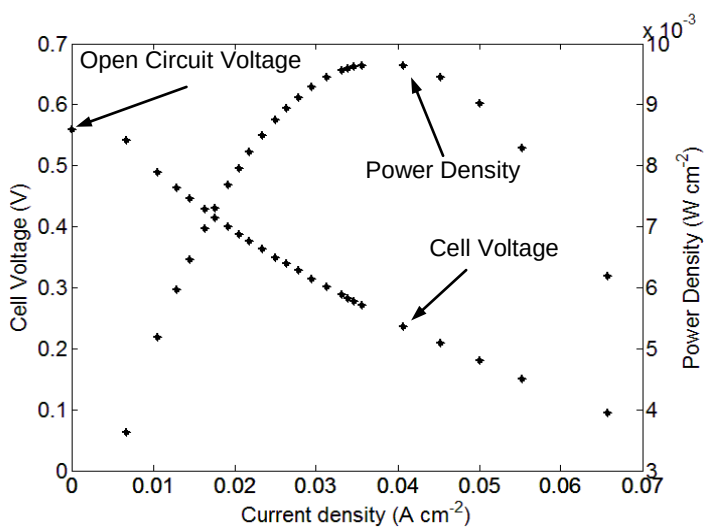

T = 313 K, C_{ME} = 0.5 M, F_{ME} = 5.5 ccm, F_{AIR} = 125.2 ccm

Figure 3.5. Data obtained in a test case for the open and closed circuit sub-models.

For the test cases with multiple tests, an error analysis has been conducted to study the variations of the performance measures. In this work, the error bars with 95% of the confidence intervals

were selected for the error analysis. The error bars for the performance measures in test case No. 2 are plotted in Figure 3.6. For this test case, three tests at identical conditions were carried out to collect 68 data points at three different time points. To better show the range of error, these 68 data points were divided into 9 groups according to their current density values. The standard deviation, σ, for the data in each group was first calculated. The -1.96σ and $+1.96\sigma$ boundaries, corresponding to 95% of the confidence interval, were then used to plot the error bar for the selected data point group.

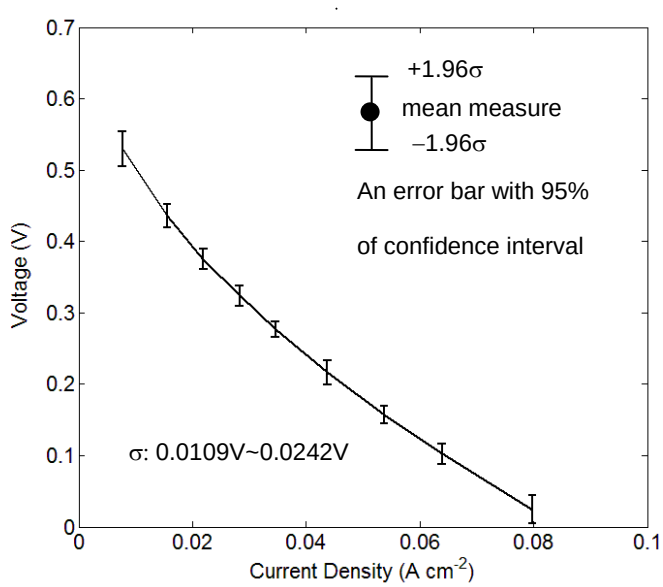

Figure 3.6. Error bars for the three tests in test case No. 2.

3.5 Results and Analysis

The coefficients for the semi-empirical model were obtained based on numerical fitting of the data collected in the experiments. In addition, the accuracy of the semi-empirical model and the significance of the coefficients in this semi-empirical model have also been analyzed.

3.5.1 Results

Resistance sub-model

Using the five test points given in Table 3.4, the coefficients in Equation (3.11) were obtained through nonlinear numerical data fitting using Matlab™ toolbox:

$a_1 = 6.9897$, $a_2 = 916.91$, $a_3 = 4.6392$

Substituting these coefficients into Equation (3.11), we can get:

$$R_e = 6.9897e^{(\frac{91691}{T} - 4.6392)} \tag{3.18}$$

The data and Equation (3.18) are shown in Figure 3.7.

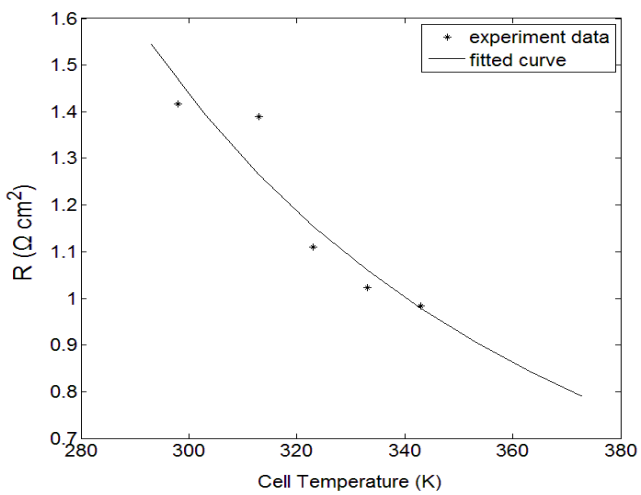

Figure 3.7. Influence of temperature on area-specific resistance.

<u>*Open circuit sub-model*</u>

For the open circuit sub-model, the data collected from the tests by changing the operating parameters of the temperature, methanol concentration, and air flow rate were used to obtain the coefficients in Equation (3.12) through nonlinear data fitting with Matlab™. In this work, the data collected in the 42 test cases were used to obtain the coefficients, and the data collected in the remaining three test cases were used to evaluate the modeling accuracy. For each of the 45 test cases, the test point at $j=0$ corresponding to the open circuit voltage was selected. When multiple tests were conducted for a test case, the average open circuit voltage was used. Therefore a total of 45 data points were used to calculate the coefficients. The obtained coefficients are:

$$b_1 = -3.7534\times10^{-5},\ b_2 = -3.1534\times10^{-4},\ b_3 = 6.6200\times10^{-5},\ b_4 = -0.74990$$

Substituting these coefficient values and Equation (3.13) into Equation (3.12), an expression for

the open circuit voltage is obtained:

$$E_o = 1.21 - 3.7534\times10^{-5}T - 3.1534\times10^{-4}T\ln C_{ME} + 6.6200\times10^{-5}T\ln(F_{AIR}) - 0.74990 \qquad (3.19)$$

<u>*Closed circuit sub-model*</u>

For the closed circuit sub-model, first the total overpotential value, η_{ac}, for each test case was calculated using Equation (3.17). In Equation (3.17), E_o is calculated using Equation (3.19) and R_e is calculated using Equation (3.18), while V_{cell} is measured through experimentation. The calculated η_{ac}, the measured current density j, and the measured cell voltage V_{cell} at the different operating parameter test cases were used to obtain the coefficients in Equation (3.15) through nonlinear numerical data fitting with Matlab™. In this work, the 62 tests including repeated test cases provided ~1,200 test points used to calculate the coefficients. The obtained coefficients are:

$c_1 = 1.2658\times10^5$, $c_2 = 46196$, $c_3 = -4281.0$ $c_4 = -0.40290$ $c_5 = -18.809$, $c_6 = 18.809$,

$c_7 = 10.496$, $c_8 = -3.9056$, $c_9 = -2.9582\times10^{-4}$, $c_{10} = 5.3466\times10^7$, $c_{11} = 5182.4$,

$c_{12} = -1.2687\times10^5$, $c_{13} = -46221$, $c_{14} = 4283.6$, $c_{15} = 0.40330$, $c_{16} = 18.818$,

$c_{17} = -18.818$, $c_{18} = -10.572$, $c_{19} = -3.8959$, $c_{20} = 8.2402\times10^{-4}$, $c_{21} = 31.583$

Substituting these coefficients into Equation (3.15), an expression for the total overpotential is obtained:

$$\begin{aligned}\eta_{ac} = {} & \left[1.2658\times10^5 j^3 + 46196 j^2 - 4281.0 j - 0.40290T - 18.8094C_{ME}^2 + 18.8094C_{ME} + 10.496\right] \\ & \times\left[\ln j - 3.9056 + 2.9582\times10^{-4}\left(\ln(C_{ME}) + \ln(1 - \frac{1}{5.3466\times10^7 e^{(-51824/T)}C_{ME}^2} j)\right)\right] \\ & + \left[-1.2687\times10^5 j^3 - 46221 j^2 + 4283.6 j + 0.40330T + 18.818C_{ME}^2 - 18.818C_{ME} - 10.572\right] \\ & \times\left[\ln j - 3.8959 - 8.2402\times10^{-4}\ln(F_{AIR})\right] - 31.583 j^2 \ln(F_{ME})\end{aligned} \qquad (3.20)$$

(4) The overall semi-empirical model

Integrating Equations (3.3), (3.10), (3.18), (3.19) and (3.20), the cell voltage can be calculated from the following expression:

$$
\begin{aligned}
V_{cell} &= 1.21 - 3.7534\times10^{-5}T - 3.1534\times10^{-4}T\ln C_{ME} + 6.6200\times10^{-5}T\ln(F_{AIR}) - 0.74990 \\
&- 6.9897e^{(\frac{91691}{T}-4.6392)}j \\
&- \left[1.2658\times10^{5}j^{3} + 46196j^{2} - 4281.0j - 0.40290T - 18.8094C_{ME}^{2} + 18.8094C_{ME} + 10.496\right] \\
&\times\left[\ln j - 3.9056 + 2.9582\times10^{-4}\left(\ln(C_{ME}) + \ln(1 - \frac{1}{5.3466\times10^{7}e^{(-51824/T)}C_{ME}^{2}}j)\right)\right] \\
&- \left[-1.2687\times10^{5}j^{3} - 46221j^{2} + 4283.6j + 0.40330T + 18.818C_{ME}^{2} - 18.818C_{ME} - 10.572\right] \\
&\times\left[\ln j - 3.8959 - 8.2402\times10^{-4}\ln(F_{AIR})\right] + 31.583j^{2}\ln(F_{ME})
\end{aligned}
\tag{3.21}
$$

The effectiveness of the semi-empirical model in predicting the DMFC performance based on operating parameters will be explained in Section 3.5.2 through accuracy analysis. Discussion of the influences of individual coefficients on the accuracy of the semi-empirical model will be provided in Section 3.5.3 through sensitivity analysis.

3.5.2 Verification and Accuracy Analysis

In this research, the data from 62 tests were used as the training tests to obtain the coefficients, and the data from three tests were reserved to validate the semi-empirical model and test its accuracy. Figure 3.8 shows the measured and predicted data for the operating conditions given in Table 3.5 in the three evaluation tests.

Table 3.5. Three test cases to analyze the accuracy of the semi-empirical model.

Test Case No.	T (K)	C_{ME} (M)	F_{ME} (ccm)	F_{AIR} (ccm)	n	σ (V)	δ (V)	δ_{max} (V)
1	323	0.25	4	81.2	22	0.0106	0.0082	0.0277
2	298	1	4.5	125.2	16	0.0236	0.0206	0.0312
3	343	0.5	5	140.8	15	0.0137	0.0116	0.0183
Total					53	0.0160	0.0129	0.0312

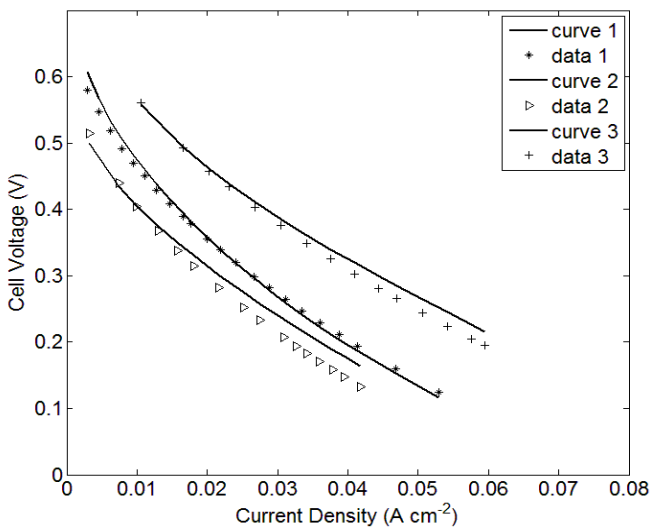

Figure 3.8. Collected data through experiments and predicted curves using the semi-empirical model.

In this research, three measures, the standard deviation σ, the average absolute error δ, and the maximum absolute error δ_{max}, are used to evaluate the accuracy of the semi-empirical model.

The standard deviation σ shown in Table 3.5 is defined by:

$$\sigma = \sqrt{\frac{\sum_{i=1}^{n}(U_i - \overline{U_i})^2}{n-1}} \tag{3.22}$$

where U_i is the predicted cell voltage using the semi-empirical model, $\overline{U_i}$ is the measured cell voltage from experiment, and n is the number of points in the test case.

The average absolute error δ shown in Table 3.5 is defined by:

$$\delta = \frac{1}{n}\sum_{i=1}^{n}\delta_i = \frac{1}{n}\sum_{i=1}^{n}\left|U_i - \overline{U_i}\right| \tag{3.23}$$

where the δ_i is the absolute error for the i-th data point.

The maximum absolute error δ_{max} shown in Table 3.5 for each test case is defined by:

$$\delta_{\max} = \max\{\delta_1, \delta_2, \delta_3, ..., \delta_n\} \tag{3.24}$$

The absolute error at each experimental data point between the predicted and measured voltages was analyzed to determine if there was any systematic error pattern relative to each operating parameter. Each parameter (i.e., temperature, methanol concentration, and methanol and air flow rates) was evaluated in a generalized linear model using Minitab™ against the absolute error as the outcome variable. The current density was included as a covariate. All factors were determined to be significant in contributing to the absolute error at p-values of less than 0.01. Figure 3.9 shows the mean absolute error of cell voltage for each level of the experimental tests. From this analysis, it was concluded that the model error is relatively insensitive to changes in temperature and methanol concentration (average error within ~0.005 V), but has a systematic trend for the methanol and air flows, with the error trending largest at the extremes of the flow ranges. The largest absolute errors are generally found in the model to occur in general at the extreme ranges of the parameters. The largest relative errors were generally found to occur at the highest methanol concentrations.

The accuracy analysis for the 62 training tests whose data were used to obtain the coefficients of the semi-empirical model is summarized in Table 3.6. The errors for the training tests are comparable with the errors for the evaluation tests. In general, the model predicted the experimental data points voltage within an accuracy of ±0.050 V approximately 90% of the time, and ±0.030 V approximately 70% of the time. On a relative basis, the model was determined to match the experimental data within a relative accuracy of ±25% approximately 90% of the time, and ±10% approximately 50% of the time. It should be noted that as a non-linear regression model, some combinations of parameters will lead to estimation with a negative voltage, especially when these parameters are at the limits of their regression ranges. While these operating points generally would have very low voltage, nonetheless they should be treated with caution. In summary, given the experimental error, it is therefore concluded the developed semi-empirical model is effective for predicting DMFC performance based on the operating parameters.

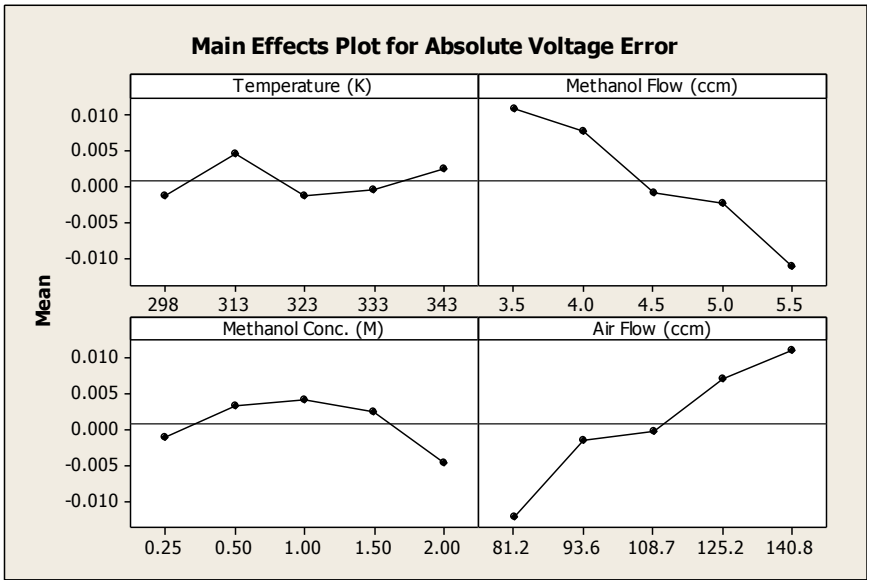

Figure 3.9. Contribution of operating parameters to absolute error.

Table 3.6. Comparison between the errors for the evaluation tests and the training tests.

Test Cases	**n**	**σ (V)**	**δ (V)**	**δ_{max} (V)**
Evaluation Tests	53	0.0160	0.0129	0.0312
Training Tests	1160	0.0224	0.0114	0.0568

3.5.3 Sensitivity Analysis

The semi-empirical model has 28 coefficients in its three sub-models: three in the resistance sub-model (Equation (3.11)), four in the open circuit sub-model (Equation (3.12)), and 21 in the closed circuit sub-model (Equation (3.15)). The scientific method requires that the model should be parsimonious, and therefore the number of coefficients should be reduced to simplify the complexity of the semi-empirical model if the quality of the model can be maintained. In this research, a sensitivity analysis considering the 21 coefficients of the closed circuit sub-model given by Equation (3.15) has been conducted.

An analysis of variance (ANOVA) (Shasha and Wilson, 2008) is employed to study the contribution of each of these coefficients. First a designed experiment is used to create test cases considering the relevant coefficients. In each test case, a coefficient is increased or decreased by 5%, and the change in the performance measure is observed. Then a Matlab™ n-way analysis of

variance (i.e., anovan) function is used to analyze the significance through the coefficient's p-value. A coefficient with a p-value less than or equal to 0.05 was considered significant, contributing to variance in the model's predicted values. If a p-value is larger than 0.05, the coefficient could be considered for removal from the semi-empirical model.

Among the 21 coefficients in the closed circuit sub-model given in Equation (3.15), five coefficients are considered as candidates for removal due to their large p-values given in Table 3.7.

Table 3.7. p-values considering the significance of the five coefficients.

Coefficient	p-value
c_1	0.1084
c_3	0.6662
c_{12}	0.4931
c_{13}	0.7484
c_{18}	0.3681

Removing these five coefficients from Equation (3.15), the modified closed circuit sub-model can now be described by:

$$\begin{aligned}\eta_{ac} = &\left[c_2 j^2 + c_4 T + c_5 C_{ME}^2 + c_6 C_{ME} + c_7\right] \\ &\times\left[\ln j + c_8 - c_9\left(\ln(C_{ME}) + \ln\left(1 - \frac{1}{c_{10} e^{(-c_{11}/T)} C_{ME}^2} j\right)\right)\right] \\ &+\left[c_{14} j + c_{15} T + c_{16} C_{ME}^2 + c_{17} C_{ME}\right] \\ &\times\left[\ln j + c_{19} - c_{20}\ln(F_{AIR})\right] - c_{21} j^2 \ln(F_{ME})\end{aligned} \tag{3.25}$$

The original semi-empirical model and the simplified semi-empirical model were evaluated using the three evaluation test cases. A comparison of the results shown in Table 3.8 finds that both semi-empirical models are acceptable to predict the DMFC performance based on the four operating parameters.

Table 3.8. Comparison between the original and the simplified semi-empirical models.

Semi-empirical Model	σ (V)	δ (V)	δ_{max} (V)
The original model with 28 coefficients	0.0160	0.0129	0.0312
The simplified model with 23 coefficients	0.0126	0.0098	0.0220

3.6 Applications of the Semi-empirical Fuel Cell Model

The semi-empirical fuel cell model can be used to analyze the influences of the operating parameters on the performance of the DMFC. The semi-empirical model can also be used to identify the optimal operating parameters based on the performance requirement through optimization.

3.6.1 The Influences of Operating Parameters on DMFC Performance

The semi-empirical model can be used to study the influences of the operating parameters on DMFC performance by changing only one of the operating parameters each time, and creating a curve of the relationship between the current density and cell voltage, as shown in Figure 3.10.

The influences of the four operating parameters are summarized as follows.

Influence of temperature (T)

When the temperature is increased, the cell voltage will increase at different current densities as shown in Figure 3.10(a). For example, consider the current density at j = 0.045 A cm^{-2}. When the temperature is increased from 298 K to 343 K, the cell voltage increases from 0.098 V to 0.179 V, an 82.6% increase in the cell voltage. Therefore high cell temperature is expected to improve the DMFC performance.

Influence of methanol concentration (C_{ME})

When the methanol concentration is increased, the cell voltage is increased at low methanol concentration, and cell voltage is decreased at high methanol concentration as shown in Figure 3.10(b). For example, consider again the current density at j = 0.045 A cm^{-2}. When the methanol concentration is increased from 0.25 M to 0.5 M, the cell voltage increases from 0.201 V to 0.209 V, a 3.9% increase in the cell voltage. When the methanol concentration is increased from 0.5 M to 1 M, the cell voltage decreases from 0.209 V to 0.177 V, a 15.2% decrease in the cell voltage. Therefore an optimal methanol concentration is expected to improve the DMFC performance.

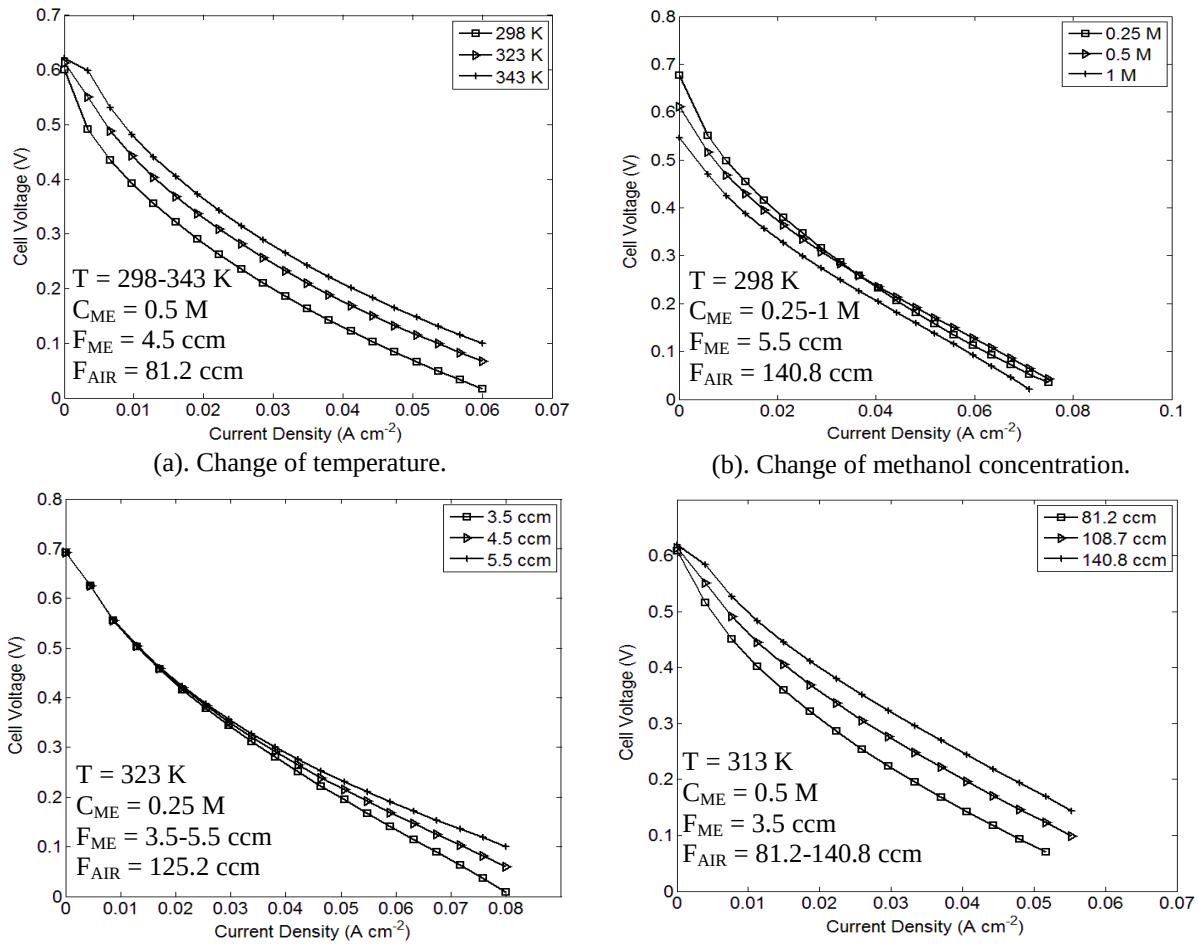

(a). Change of temperature.

(b). Change of methanol concentration.

(c). Change of methanol flow rate.

(d). Change of air flow rate.

Figure 3.10. Influence of the four operating parameters on DMFC performance.

Influence of methanol flow rate (F_{ME})

When the methanol flow rate is increased, the cell voltage in general will increase, especially when the current density level is high as shown in Figure 3.10(c). For example, consider again the current density at j = 0.045 A cm^{-2}. When the methanol flow rate is increased from 3.5 ccm to 5.5 ccm, the cell voltage will increase from 0.232 V to 0.260 V, a 12.5% increase in the cell voltage. Therefore high methanol flow rate is expected to improve the DMFC performance.

Influence of air flow rate (F_{AIR})

When the air flow rate is increased, the cell voltage in general will increase as shown in Figure 3.10(d). For example, at current density j = 0.045 A cm^{-2}, when the air flow rate increases from

81.2 ccm to 140.8 ccm, the cell voltage increases from 0.113V to 0.214 V, a 90.1% increase in the cell voltage. Therefore high air flow rate is expected to improve the DMFC performance.

3.6.2 Optimal Control of the Operating Parameters

The quantitative relationships between operating parameters and fuel cell performance measures in the semi-empirical model can be used to identify the optimal operating parameters based on a given requirement.

In DMFC applications, a number of fuel cells are usually connected in series to form a stack. A number of stacks are connected to provide the required power in a DMFC system. In addition to fuel cells, other modules such as methanol container, pumps, tubes, controllers, etc. are also needed for the fuel cell system. The operating parameters can be controlled by the controllers based on the power requirements. Therefore optimization of the operating parameters should be conducted considering the whole DMFC system.

First the semi-empirical model given by Equation (3.16) is used to define the cell voltage as a function of the operating parameters and the current density. Suppose this function is described as:

$$V_{cell} = f(T, C_{ME}, F_{ME}, F_{AIR}, j) \tag{3.26}$$

where V_{cell} is the cell voltage (V), T is the temperature (K), C_{ME} is the methanol concentration (K), F_{ME} is the methanol flow rate (ccm), F_{AIR} is the air flow rate (ccm), and j is the current density (A cm^{-2}). When n_{cell} cells are used in the stack, the stack voltage is then defined by:

$$V_{stack} = n_{cell} V_{cell} = n_{cell} f(T, C_{ME}, F_{ME}, F_{AIR}, j) \tag{3.27}$$

A DMFC system can be composed of a number of stacks. Suppose if m stacks are connected in series in a DMFC system, the system voltage can be described by:

$$V_{system} = m V_{stack} = m n_{cell} f(T, C_{ME}, F_{ME}, F_{AIR}, j) \tag{3.28}$$

The total power of the DMFC system can be obtained by:

$$P_{system\_total} = A V_{system}\, j = A m n_{cell} f(T, C_{ME}, F_{ME}, F_{AIR}, j) j \tag{3.29}$$

where A is the active area of the fuel cell. Suppose the power used by the supporting components

of the DMFC system is described by

$$P_{system\_con} = g(T,C_{ME},F_{ME},F_{AIR},j) \tag{3.30}$$

The net system power output can be calculated by:

$$P_{system\_net} = P_{system\_total} - P_{system\_con} = Amn_{cell}f(T,C_{ME},F_{ME},F_{AIR},j)j - g(T,C_{ME},F_{ME},F_{AIR},j) \tag{3.31}$$

Optimization can be employed to identify the optimal operating parameters based on the power requirements. The different power requirements and optimization models that can be used to optimize the system performance are listed in Table 3.9.

Table 3.9. Different optimization models to satisfy different power requirements.

Power Requirement	Optimization Model
Maximum Power Output	$\max P_{system\_net},\ j_{\min} \le j \le j_{\max}$
Overall Power Output	$\max \int_{j_{\min}}^{j_{\max}} P_{system\_net} dj$
Overall Power Efficiency	$\max \int_{j_{\min}}^{j_{\max}} \frac{P_{system\_net}}{P_{system\_total}} dj$

3.7 Summary

A systematic approach to model the relationships between the operating parameters and the direct methanol fuel cell performance was introduced in this chapter. Four operating parameters, including temperature, methanol concentration, and flow rates of methanol and air, are considered. A semi-empirical model was developed to describe the relationships. Experiments were designed and conducted to obtain the coefficients in the semi-empirical model. The accuracy of this semi-empirical model was also analyzed. In addition, the influences of the operating parameters and possible applications of the semi-empirical model were also discussed.

Characteristics of this research are summarized as follows.

(1) The semi-empirical model is effective to describe the relationships between the operating parameters and the direct methanol fuel cell performance. Compared with the theoretical models that require complicated processes to obtain the physical/chemical parameters, the

coefficients in our semi-empirical model can be obtained easily through numerical data fitting using data collected from experiments.

(2) Through an analysis of the influences of operating parameters on the DMFC performance based on the semi-empirical model, a better understanding of the DMFC behaviors was achieved. Furthermore, the influences of the four operating parameters on the open circuit voltage, resistance polarization, activation polarization and concentration polarization were also investigated.

(3) Based on the modeling of the relationships between the operating parameters and the DMFC performance measures, the optimal operating parameters of the DMFC system can be indentified according to different power requirements.

CHAPTER 4 A CFD MODEL WITH SEMI-EMPIRICAL ELECTROCHEMICAL RELATIONSHIPS TO STUDY THE INFLUENCES OF GEOMETRIC AND OPERATING PARAMETERS ON DMFC PERFORMANCE

4.1 Overview

The semi-empirical model for building the relationship between all the major operating parameters and direct methanol fuel cell performance has already been given in Chapter 3. In order to study the influences of both geometric parameters and operating parameters on the performance of DMFC system, a three-dimensional computational fluid dynamics (CFD) model with semi-empirical electrochemical relationships has been developed (Yu et al., 2013). The CFD modeling part of this research was conducted by Biao Yu, a visiting Ph.D. student at University of Calgary. Modeling of the semi-empirical electrochemical relationships is the main contribution of this thesis work.

In this research, semi-empirical relationships are introduced to describe the electrochemical behaviors required in the CFD governing equations. Coefficients in these semi-empirical relationships are fitted using experimental data. Two geometric configurations with serpentine channels at the anode and cathode are considered in this work. Temperature, methanol concentration, and methanol flow rate are selected as the operating parameters. Due to the computational effort of CFD, an adaptive metamodeling method is developed to reduce the number of data-fitting iterations for obtaining the coefficients in the semi-empirical relationships. The effectiveness of the method is demonstrated by fitting the model using the experimental data collected from the first geometric configuration of the DMFC and comparing the predicted performance of the second configuration with its experimental performance.

4.2 CFD Modeling of A DMFC with Semi-empirical Electrochemical Relationships

In this work, CFD is employed to model the relationships between geometric/operating parameters and DMFC performance. In the CFD model, the electrochemical behavior near the membrane is described by semi-empirical relationships. Coefficients in these semi-empirical relationships are fitted using experimental data. An adaptive metamodeling method is developed

to improve the efficiency for obtaining the values of coefficients in the semi-empirical relationships.

4.2.1 Physical Domains and Assumptions for CFD Modeling

In this CFD model, only the anode side is considered because a satisfactorily high air flow rate is assumed to be provided to the cathode side to guarantee a constant oxygen concentration in the simulation and thereby to simplify the computation. The physical domains in the CFD model include three fluid zones: the anode flow channel, the anode diffusion layer, and the anode catalyst layer. The anode catalyst layer is simplified as a thin interface with only one layer of mesh. Figure 4.1 shows the detailed structure of the three physical domains. The electrochemical kinetics in the cathode side is derived from the behaviors at the anode side. The CFD model is developed based on the following assumptions:

(1) All fluid flows are laminar;

(2) All fluids are incompressible;

(3) The DMFC is operating at steady state under isothermal condition;

(4) The carbon dioxide generated by the methanol oxidation is dissolved in the water completely, so only liquid phase exists in the anode side;

(5) All porous media (i.e., diffusion layers, membrane and catalyst layers) are isotropic materials;

(6) The membrane is operating at a fully hydrated state;

(7) The oxygen is sufficient for all conditions, so the concentration of oxygen is assumed as a constant.

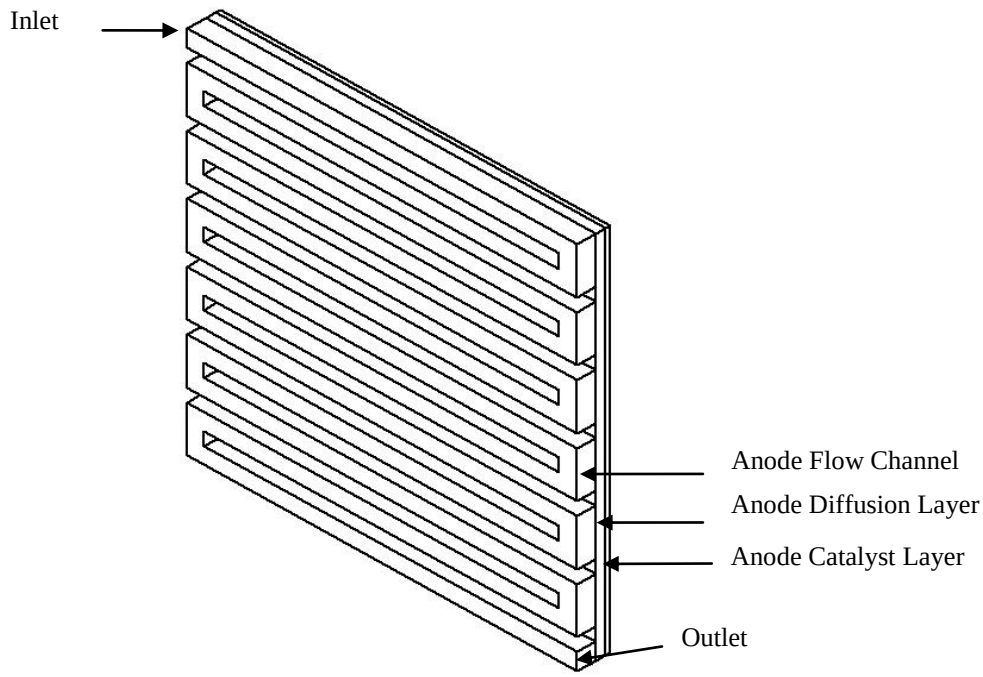

Figure 4.1. Three physical domains in the CFD model.

4.2.2 Theoretical Models

The CFD model is developed using three types of governing equations: continuity equations, momentum equations, and species equations. In this work, the crossovers of water and methanol from the anode to the cathode side through the membrane are treated as source terms of the continuity and species equations in the CFD model to simplify the modeling process.

Governing equations for CFD

The governing equations are applied to all physical domains. These equations are different in the different zones due to their different physical and chemical characteristics, such as material properties and chemical reactions. The continuity equation is used to ensure that the rate at which mass enters a system is equal to the rate at which mass leaves the system when the system is a steady state process. The continuity equation is given as (He et al., 2009):

$$\nabla \cdot (\varepsilon \rho \vec{v}) = S_m \tag{4.1}$$

where ε is the porosity of the physical domain (ε = 1 at the channel, ε = 0.6 at the diffusion layer, and ε = 0.4 at the catalyst layer), ρ is the mixture density (kg m^{-3}), $\vec{v}$ is the velocity vector of mixture (m s^{-1}), and S_m is the mass source term (kg m^{-3} s^{-1}) caused by reaction and crossover. The mass source terms in the channel and diffusion layer are zeros, while the mass source term in the catalyst layer is calculated by:

$$S_m = S_{CH_3OH} + S_{H_2O} + S_{CO_2} \tag{4.2}$$

where S_{CH_3OH}, S_{H_2O} and S_{CO_2} are the species source terms for CH_3OH, H_2O, and CO_2 in the anode catalyst layer, respectively. The detailed descriptions of these source terms are given in Equations (4.7), (4.8), and (4.9). The momentum equation is defined by (He et al., 2009):

$$\nabla \cdot (\varepsilon \rho \vec{v}\vec{v}) = -\nabla(\varepsilon P) + \nabla \cdot (\varepsilon \mu \nabla \vec{v}) + S_{mom} \tag{4.3}$$

where P is pressure (Pa), μ is mixture viscosity (kg m^{-1}s^{-1})), and S_{mom} is momentum source term (N m^{-3}) which is caused by porous media and is zero in the channel. S_{mom} is defined by (He et al., 2009; Le and Zhou, 2008):

$$S_{mom} = -\varepsilon^2 \frac{\mu}{K} \vec{v} \tag{4.4}$$

where K is the permeability of porous media (m^2). The species equations are defined as (Sivertsen and Djilali, 2005):

$$\nabla \cdot (\varepsilon \rho \vec{v} Y_k) = \nabla \cdot (\varepsilon \rho D_k^{eff} \nabla Y_k) + S_k \tag{4.5}$$

where Y_k is the mass fraction of species k, and S_k is the source term that is caused by reaction and crossover (kg m^{-3}s^{-1}). The different source terms are given in Equations (4.7), (4.8), and (4.9). The source terms are zeros in the channel and the diffusion layer. D_k^{eff} is the effective diffusion coefficient of species k (m^{2}s^{-1}), and is defined as (Ge and Liu, 2006):

$$D_k^{eff} = \begin{cases} D_k, & \text{In the channel} \\ \varepsilon^{1.5} D_k, & \text{In other zones} \end{cases} \tag{4.6}$$

where D_k is the diffusion coefficient in the channel. As noted before, because the CFD model just considers the anode side, the only species in the model are CH_3OH, H_2O, and CO_2.

Crossover of methanol and water

At the anode side, methanol and water are consumed and carbon dioxide is produced because of the methanol oxidation reaction. At the same time, methanol and water can migrate through the membrane to the cathode side, leading to crossover. Penetration of carbon dioxide through the membrane is prevented by its macromolecule structure. To reduce the computing complexity and simplify the model domain, crossovers of methanol and water are treated as source terms in the species equations. The source term S_k in the species equation due to the chemical reaction and physical crossover through the membrane is defined as:

$$S_k = S_{k,reaction} + S_{k,crossover} \tag{4.7}$$

The first term on the right side of Equation (4.7), $S_{k,reaction}$, is the source term caused by the electrochemical reaction, and the second term, $S_{k,crossover,}$ is caused by the crossover. The reaction source terms are given by:

$$S_{k,reaction} = \begin{cases} \dfrac{-M_{CH_3OH}}{6F} j_a, & \mathrm{k = CH_3OH} \\ \dfrac{-M_{H_2O}}{6F} j_a, & \mathrm{k = H_2O} \\ \dfrac{M_{CO_2}}{6F} j_a, & \mathrm{k = CO_2} \end{cases} \tag{4.8}$$

where M_k (kg kmol^{-1}) is the molecular weight of species k, F is the Faraday constant (9.6485 × 10^7 C kmol^{-1}), and j_a is the local volumetric current density (A m^{-3}) at the anode defined by Equation (4.25). The crossover terms are given by:

$$S_{k,crossover} = \begin{cases} M_{CH_3OH} N_{CH_3OH}, & \mathrm{k = CH_3OH} \\ M_{H_2O} N_{H_2O}, & \mathrm{k = H_2O} \\ 0, & \mathrm{k = CO_2} \end{cases} \tag{4.9}$$

where N_{CH_3OH} and N_{H_2O} are the local volumetric crossover rates for methanol and water through the membrane, respectively (kmol m^{-3}s^{-1}). Because the CO_2 cannot migrate to the cathode side, its crossover rate is zero. The methanol crossover rate through the membrane is defined by (Vera, 2007):

$$N_{CH_3OH} = \frac{n_{CH_3OH}\, j_a}{F} - D^{eff}_{CH_3OH,m} \frac{dC^m_{CH_3OH}}{dz} \frac{1}{t_{acl}} = \frac{n_{CH_3OH}\, j_a}{F} + D^{eff}_{CH_3OH,m} \frac{C^{\text{int}}_{CH_3OH}}{t_{mem} t_{acl}} \tag{4.10}$$

The water crossover rate through the membrane is given by (Jeng and Chen, 2002):

$$N_{H_2O} = \frac{n_{H_2O}\, j_a}{F} - D^{eff}_{H_2O,m} \frac{dC^m_{H_2O}}{dz} \frac{1}{t_{acl}} \approx \frac{n_{H_2O}\, j_a}{F} \tag{4.11}$$

where n_{CH_3OH} and n_{H_2O} are electro-osmotic drag coefficients for CH_3OH and H_2O, respectively, $D^{eff}_{CH_3OH,m}$ and $D^{eff}_{H_2O}$ are effective diffusion coefficients ($m^2\ s^{-1}$) in the membrane for CH_3OH and H_2O, respectively, $C^{\text{int}}_{CH_3OH}$ is the local methanol concentration at the interface between anode catalyst layer and membrane (kmol m^{-3}), and z is the direction perpendicular to the plane of the membrane. Because the membrane is assumed to be fully hydrated, the second term in Equation (4.11) can be deleted. Thicknesses t_{mem} and t_{acl} (m) are for the membrane and anode catalyst layer, respectively. The electro-osmotic drag coefficient n_{CH_3OH} is given by (Ge and Liu, 2006):

$$n_{CH_3OH} = n_{H_2O} X^{\text{int}}_{CH_3OH} \tag{4.12}$$

where $X^{\text{int}}_{CH_3OH}$ is methanol mole fraction at the interface between anode catalyst layer and membrane. Mole fraction $X^{\text{int}}_{CH_3OH}$ is calculated by:

$$X^{\text{int}}_{CH_3OH} = Y^{\text{int}}_{CH_3OH} \frac{M}{M_{CH_3OH}} \tag{4.13}$$

where $Y^{\text{int}}_{CH_3OH}$ is methanol mass fraction at the interface between anode catalyst layer and membrane, and M (kg $kmol^{-1}$) is molecular weight of the mixture and is calculated by (Lum and McGuirk, 2005):

$$M = \frac{1}{\sum_k \left(\frac{Y_k}{M_k} \right)}, \quad k = CH_3OH, H_2O, CO_2 \tag{4.14}$$

The electro-osmotic drag coefficient n_{H_2O} is defined by (Guo and Ma, 2004):

$$n_{H_2O} = 2.9\exp\left(\frac{1}{333} - \frac{1}{T}\right) \tag{4.15}$$

The effective diffusion coefficient $D^{eff}_{CH_3OH,m}$ is calculated by (Vera, 2007):

$$D^{eff}_{CH_3OH,m} = D_{CH_3OH,m}\varepsilon^{1.5} = 4.9\times10^{-10}\exp\left[2436\left(\frac{1}{333} - \frac{1}{T}\right)\right]\varepsilon^{1.5} \tag{4.16}$$

where ε is the porosity of membrane. The overall methanol crossover $N_{CH_3OH,ALL}$ (kmol s^{-1}) through the membrane can be determined by:

$$N_{CH_3OH,ALL} = \iiint_V N_{CH_3OH}\,dV \tag{4.17}$$

where N_{CH_3OH} is local methanol crossover rate given by Equation (4.10), and V is the volume space of the whole anode catalyst layer (m^3).

<u>*Electrochemical kinetics in the catalyst layers*</u>

The electrochemical kinetics in the two catalyst layers are governed by the Tafel equations (Ge and Liu, 2006):

$$\eta_a = \frac{RT}{\alpha_a F}\ln\left(\frac{j_a C^{ref}_{CH_3OH}}{a_{i_{0a}} C_{CH_3OH}}\right) \tag{4.18}$$

$$\eta_c = \frac{RT}{\alpha_c F}\ln\left(\frac{j_c C^{ref}_{O_2}}{a_{i_{0c}} C_{O_2}}\right) \tag{4.19}$$

where η_a and η_c are the overpotential values at the anode and cathode sides, respectively. The local current density at cathode catalyst layer, j_c (A m^{-3}), is defined by Equation (4.27), while a_{i0a} and a_{i0c} are the reference volumetric transfer current densities (A m^{-3}) at the anode and the cathode sides, respectively, α_a and α_c are the charge transfer coefficients at anode and cathode, respectively, R is the gas constant (8.314 J mol^{-1}), C_{CH3OH} is the local methanol concentration (kmol m^{-3}), $C^{ref}_{CH_3OH}$ is the reference methanol concentration (kmol m^{-3}), C_{O2} is the local oxygen

concentration (kmol m^{-3}), and $C_{O_2}^{ref}$ is the reference oxygen concentration (kmol m^{-3}). C_k is calculated by:

$$C_k = Y_k \frac{\rho}{M_k} \tag{4.20}$$

The reference volumetric transfer current densities a_{i_0a} and a_{i_0c} are calculated by (He et al., 2009):

$$a_{i_0a} = a_{ia}^{ref} \exp\left[\frac{35570}{R}\left(\frac{1}{353} - \frac{1}{T}\right)\right] \tag{4.21}$$

$$a_{i_0c} = a_{ic}^{ref} \exp\left[\frac{73200}{R}\left(\frac{1}{353} - \frac{1}{T}\right)\right] \tag{4.22}$$

where a_{ia}^{ref} and a_{ic}^{ref} are the reference volumetric current densities (A m^{-3}) at 353 K, and T is the temperature (K) .

It should be noted that since only one layer of mesh is used in the CFD model for the anode catalyst layer, the local methanol concentration C_{CH_3OH} and the anode overpotential η_a are constant through the thickness of the anode catalyst layer. The C_{O2} and η_a are also constant through the thickness of the cathode catalyst layer.

Cell potential and current density

The cell potential is defined by:

$$E_{cell} = E_0 - \eta_a - \eta_c - \eta_{mem} \tag{4.23}$$

where E_{cell} (V) is the cell potential, η_{mem} (V) is the potential loss due to the membrane resistance, and E_0 (V) is the open circuit voltage influenced by temperature, methanol concentration and air flow rate. In the research, a semi-empirical equation is developed based on Equations (3.12) and (3.13):

$$E_0 = 1.21 + k_1 T + k_2 T \ln(C_{CH_3OH}) + k_3 T \ln(F_{AIR}) + k_4 \tag{4.24}$$

where k_1-k_4 are coefficients, and F_{AIR} is the air flow rate (ccm).

In this model, E_{cell} is provided from experiment data, and η_a and η_c are calculated by Equations (4.18) and (4.19). The anode local current density of cell, j_a, is calculated by:

$$j_a = \frac{\eta_{mem}}{t_{acl} R_{mem}} \tag{4.25}$$

where R_{men} is the area specific resistance of the membrane (Ω m^2) calculated by (Yang et al., 2011):

$$R_{mem} = b_1 \exp(\frac{b_2}{T} + b_3) \tag{4.26}$$

where b_1-b_3 are coefficients. The coefficient values in Equations (4.24) and (4.26) can be found from Chapter 3. Cathode local current density is calculated by:

$$j_c = j_a + j_{crossover} \tag{4.27}$$

where $j_{crossover}$ (A m^{-3}) is the local crossover current density caused by methanol crossover. The local crossover current density is calculated by:

$$j_{crossover} = 6FN_{CH_3OH} \tag{4.28}$$

where N_{CH_3OH} is the local volumetric crossover rate of methanol calculated using Equation (4.10). Cell total current I (A) is calculated by:

$$I = \iiint_V j_a dV \tag{4.29}$$

Although the mechanistic models introduced in this section are effective for describing DMFC behavior, some parameters for modeling the electrochemical relationships are extremely difficult to obtain. In this research, semi-empirical models are developed to approximate these relationships.

4.2.3 Approximation of Electrochemical Kinetics by Semi-empirical Relationships

Many of the parameters presented in the CFD model cannot be obtained due to limitations in collecting data in this research. From the literature on CFD-based DMFC modeling, some parameters in these models have to be calibrated manually without good justification due to the

difficulty in obtaining the true values of these parameters. To simplify the CFD models, as well as to develop a generic CFD model that can be applied to the DMFCs with different geometric shapes, semi-empirical approximations of electrochemical kinetic relationships have been carried out to replace the theoretical Equations (4.18), (4.19), (4.21), and (4.22). These are the equations used to describe the relationships between the operating parameters near the membrane in the catalyst layers and the overpotential at the anode and cathode due to activation and concentration. The simplified semi-empirical relationships based on these equations are defined by:

$$\eta_a = c_1 T \ln\left(\frac{c_2}{\exp(\frac{c_3}{T} + c_4)} \cdot \frac{j_a}{C_{CH_3OH}} \right) \tag{4.30}$$

$$\eta_c = c_5 T \ln\left(\frac{c_6}{\exp(\frac{c_7}{T} + c_8)} \cdot \frac{j_c}{C_{O_2}} \right) \tag{4.31}$$

where c_1 to c_8 are coefficients determined using the collected experimental data.

4.2.4 Boundary Conditions and Numerical Methods for CFD-based DMFC Modeling

The CFD and semi-empirical electrochemical relationships were modeled using a commercially CFD system, Fluent 12.0, in this work. All source terms are defined with User Defined Functions (UDFs) using C++ and embedded in the Fluent for the simulation. For the physical domain inlet, velocity is used as the boundary condition. For the physical domain outlet, pressure is used as the boundary condition. No-slip boundaries are employed for all walls. Other operating parameters, such as methanol concentration and temperature, are also used as boundary conditions for both the inlet and outlet. Because the η_{mem} in Equation (4.25) is also a function of j_a, the value of j_a cannot be solved directly by Fluent. A numerical method is developed in this work to solve this problem. First, by substituting Equations (4.23), (4.30), and (4.31) into Equation (4.25), j_a can be rewritten as:

$$j_a = \frac{1}{t_{acl} R_{mem}} \left\{ E_0 - E_{cell} - c_1 T \ln\left(\frac{c_2}{\exp\left(\frac{c_3}{T} + c_4\right)} \cdot \frac{j_a}{C_{CH_3OH}} \right) - c_5 T \ln\left(\frac{c_6}{\exp\left(\frac{c_7}{T} + c_8\right)} \cdot \frac{j_c}{C_{O_2}} \right) \right\} \tag{4.32}$$

By substituting Equations (4.27), (4.28), and (4.10) into Equation (4.32), we get:

$$j_a = \frac{1}{t_{acl} R_{mem}} \left\{ E_0 - E_{cell} - c_1 T \ln\left(\frac{c_2}{\exp\left(\frac{c_3}{T} + c_4\right)} \cdot \frac{j_a}{C_{CH_3OH}} \right) - c_5 T \ln\left(\frac{c_6}{\exp\left(\frac{c_7}{T} + c_8\right)} \cdot \frac{(1 + 6n_{CH_3OH}) j_a + \frac{6F}{t_{acl} t_m} D^{eff}_{CH_3OH,m} C^{\text{int}}_{CH_3OH}}{C_{O_2}} \right) \right\} \tag{4.33}$$

Equation (4.33) is an implicit function and cannot be solved directly. By defining $f(j_a)$ as a function of j_a and then moving the j_a in Equation (4.33) from the left side to the right side, we get:

$$f(j_a) = \frac{1}{t_{acl} R_{mem}} \left\{ E_0 - E_{cell} - c_1 T \ln\left(\frac{c_2}{\exp\left(\frac{c_3}{T} + c_4\right)} \cdot \frac{j_a}{C_{CH_3OH}} \right) - c_5 T \ln\left(\frac{c_6}{\exp\left(\frac{c_7}{T} + c_8\right)} \cdot \frac{(1 + 6n_{CH_3OH}) j_a + \frac{6F}{t_{acl} t_m} D^{eff}_{CH_3OH,m} C^{\text{int}}_{CH_3OH}}{C_{O_2}} \right) \right\} - j_a = 0 \tag{4.34}$$

In Equation (4.34), the c_1-c_8 are the eight coefficients of the semi-empirical model. These coefficients are assigned with best guess initial values, and refined using optimization techniques

and the experimental data to minimize current density fit error. The volumetric current densities at different locations can be obtained iteratively by solving Equation (4.34) using the secant method. The secant method is a root-finding algorithm that uses a succession of roots of secant lines to approximate the root of a function. The secant method can be considered as a finite difference approximation of Newton's method. The secant method is defined by a recurrence relation:

$$X_{n+1} = X_n - f(X_n)\frac{X_n - X_{n-1}}{f(X_n) - f(X_{n-1})} \tag{4.35}$$

The first two initial values are assigned to X_0 and X_1, and a convergence stopping condition is specified. Through sufficient iterations, a stable result can be obtained as the root value of Equation (4.34). The secant method was implemented as a UDF using C++.

4.2.5 Identification of Semi-empirical Relationship Coefficients through Adaptive Metamodeling

In the CFD simulation, proper values of the eight coefficients in the semi-empirical relationships are required. When these coefficients are incorrect, the simulation results are different from the experimental results. Identification of the coefficient values, however, is a nontrivial task. In this study, an optimization-based adaptive metamodeling method (Liu et al., 2011) has been employed to obtain the values of these eight coefficients.

Metamodeling is an approach to identify the approximation relationships between input and output parameters using experimental input and output data (Liu et al., 2011). This method is effective when analytical relationships cannot be directly described. In this work, the approximation relationship developed is a function describing the difference between the CFD simulation and the experimental results in terms of the semi-empirical coefficients. Different mathematical functions or schemes, such as polynomials and neural networks, can be used to describe this coefficient/error relationship. The kriging method (Jeong et al., 2005) was chosen to build the metamodel in this research.

The input parameters of the metamodel are the eight coefficients c_1 to c_8, and the output parameter is the mean fuel cell current density error between the experimental and simulation data for a given set of values for the eight coefficients at different voltages and operating

conditions. This error is calculated for a number of coefficient sets such that a function can be fit predicting the error from the coefficients. These coefficient sets can be initially specified randomly, but are better set as a best guess based on simulation experience. Thus, the metamodel defines the mean simulation error as the output and the eight coefficients as the input. Adaptive metamodeling for optimization is used to find the values of the eight coefficients to minimize the simulation error. The algorithm for adaptive metamodeling for optimization will be further discussed in Section 5.2.1. The physical parameters used for the CFD simulation with adaptive metamodeling are given in Table 4.1.

Table 4.1. Physical parameters for the CFD simulation.

Parameter	**Value**	**Reference**
Water density ρ_{H_2O}	1,000 kg m^{-3}	
Water viscosity μ_{H_2O}	$0.458509-5.30474\times10^{-3}T+2.31231\times10^{-5}T^2-4.49161\times10^{-8}T^3+3.27681\times10^{-11}T^4$ kg $m^{-1}s^{-1}$	(Wang and Wang, 2003)
Air density ρ_{air}	1.29 kg m^{-3}	
Air viscosity μ_{air}	2.03×10^{-5} kg $m^{-1}s^{-1}$	(Wang and Wang, 2003)
Diffusion coefficient of methanol in water D_{CH_3OH}	$10^{-5.4163-(999.778/T)}$ m^2s^{-1}	(Wang and Wang, 2003)
Diffusion coefficient of carbon dioxide in water D_{CO_2}	1×10^{-10} m^2s^{-1}	(Wang and Wang, 2003)
Permeability of anode diffusion layer K_{adl}	1×10^{-11} m^2	Assumed
Permeability of anode catalyst layer K_{acl}	1×10^{-11} m^2	Assumed
Porosity of anode diffusion layer ε_{adl}	0.6	Assumed
Porosity of anode catalyst layer ε_{acl}	0.4	Assumed
Faraday constant F	9.6485×10^7 C $kmol^{-1}$	(Vera, 2007)
Gas constant R	8.31 J $mol^{-1}K^{-1}$	(Vera, 2007)
Molecular weight of methanol M_{CH_3OH}	0.032 kg mol^{-1}	(Vera, 2007)
Molecular weight of water M_{H_2O}	0.018 kg mol^{-1}	(Vera, 2007)
Molecular weight of carbon dioxide M_{CO_2}	0.044 kg mol^{-1}	(Divisek et al., 2003)
Molecular weight of oxygen M_{O_2}	0.032 kg mol^{-1}	(Divisek et al., 2003)
Molecular weight of nitrogen M_{N_2}	0.028 kg mol^{-1}	(Divisek et al., 2003)

4.3 Case Study

The CFD model introduced in Section 4.2 was tested through a case study to demonstrate its effectiveness for modeling the relationships between geometric/operating parameters and DMFC performance measures. In the case study, two DMFCs with different geometric shapes of the

channels were tested. The experiment data collected from the first geometric configuration was used to obtain the coefficients of the semi-empirical relationships in the CFD model. The fitted model was then used to predict the performance of the second configuration of the DMFC. The predicted performance measures were subsequently compared with the experimental performance data to validate the developed model.

4.3.1 Experiments and Data Collection

A DMFC kit, TekStak^{TM}, manufactured by Parker Hannifin Energy Systems was used for the experiments, which were introduced in Chapter 3. The DMFC is composed of an MEA, two graphite end plates with channels for the anode and cathode, and two aluminum end plates with Teflon^{TM} current isolators. The MEA is composed of a Nafion 117 membrane, an anode with catalyst of Pt-Ru, and a cathode with catalyst of Pt. Both anode and cathode are thick layers of carbon paper or cloth with catalysts deposited on them. The carbon paper or cloth of the anode and cathode also diffuses methanol and oxygen to the catalysts for reaction. The total electrode active area, A, is 10 cm^2 with a serpentine flow field.

The experiments were conducted by measuring the current density and cell output voltage when changing the external resistance load at different operating conditions. Three operating parameters considered in this work include temperature, methanol concentration, and methanol flow rate. Details of the experiment setup can be found in Section 3.4.2.

One research objective is to study the impact of geometric parameters on DMFC performance. To achieve this objective, two geometry configurations considering different channel shapes were manufactured as shown in Figure 4.2. Both configurations shown in Figure 4.2 have a single-path serpentine flow channel with approximately the same flow field open area. The open area of the flow field is defined as the area of the channel exposing the MEA to methanol fuel (Yang and Zhao, 2005). The major difference between these two configurations is the number of channel passes. The first configuration has 13 passes and the second one has 19 passes. The widths of channels for these two configurations were selected as 1.372 mm and 0.889 mm, respectively, as shown in Table 4.2.

Table 4.2. Geometry parameters for the two configurations.

Configuration No.	Number of Paths	Open Area (mm^2)	Channel Width (mm)	Channel Depth (mm)
1	13	558.1	1.372	0.5
2	19	512.7	0.889	0.5

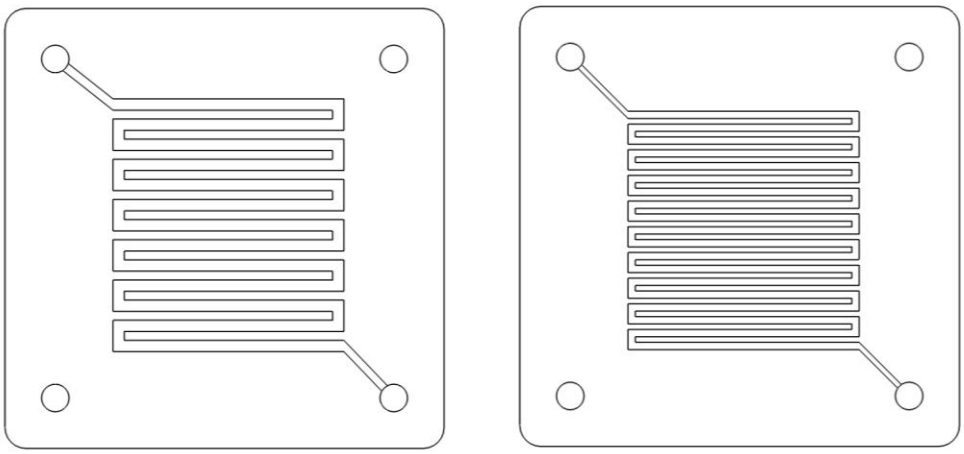

Configuration 1 Configuration 2

Figure 4.2. Two geometric configurations of graphite end plates.

Four tests were conducted for the two configurations. Three tests were conducted for the first configuration to obtain the coefficients of the semi-empirical relationships in the CFD model. One test was carried out for the second configuration to collect performance data and compare it with the data predicted using the fitted CFD model. Since the model was developed based on the assumption that the air flow rate at cathode side is sufficient large, this air flow rate was selected as 1,000 ccm for all the tests. Table 4.3 gives the operating parameters for the 4 tests.

After the experiments, four groups of performance data (i.e., I-V curves) were obtained. The 42 current-voltage data pairs from tests No. 1 to No. 3 were used to obtain the values of coefficients in the semi-empirical relationships. The 13 data pairs from test No. 4 were used to validate the developed DMFC model.

Table 4.3. Operating parameters for 4 designed tests.

Test No.	Methanol Flow Rate (ccm)	Methanol Concentration (M)	Temperature (K)	Geometric Configuration
1	3.06	0.5	343	1st
2	3.06	0.5	333	1st
3	2.27	0.5	343	1st
4	3.06	0.5	343	2nd

4.3.2 Fitting of Coefficient Values in the CFD Model

The adaptive metamodeling method given in Section 4.2.5 was employed to obtain the values of the eight coefficients in the semi-empirical relationships given in Equations (4.30) and (4.31). In this research, the experimental data collected from tests No. 1 to No. 3 were used to obtain these coefficients. Values of these fitted coefficients are shown in Table 4.4. Kriging metamodeling tool, DACE, developed by Lophaven et al. (2002) was selected for implementing the adaptive metamodeling method.

Table 4.4. Values of model coefficients fitted using the experimental data.

Coefficient	Value	Coefficient	Value
c_1	9.9033×10^{-5}	c_5	1.5780×10^{-4}
c_2	5.2070×10^{-9}	c_6	8.5645×10^{-8}
c_3	-4.2782	c_7	-8.8041
c_4	1.21×10^{-2}	c_8	2.49×10^{-2}

4.3.3 Validation of the CFD Model

Using the CFD model with the fitted coefficients, the I-V curves considering the three operating conditions of the tests No. 1-3 are plotted as shown in Figure 4.3. Comparing the CFD model and the data from the three experimental tests, also shown in Figure 4.3, it can be seen that the CFD model effectively describes the relationships between current density and cell voltage at different operating conditions. Figure 4.4 shows the data plotted using the fitted CFD model and the data collected from test No. 4.

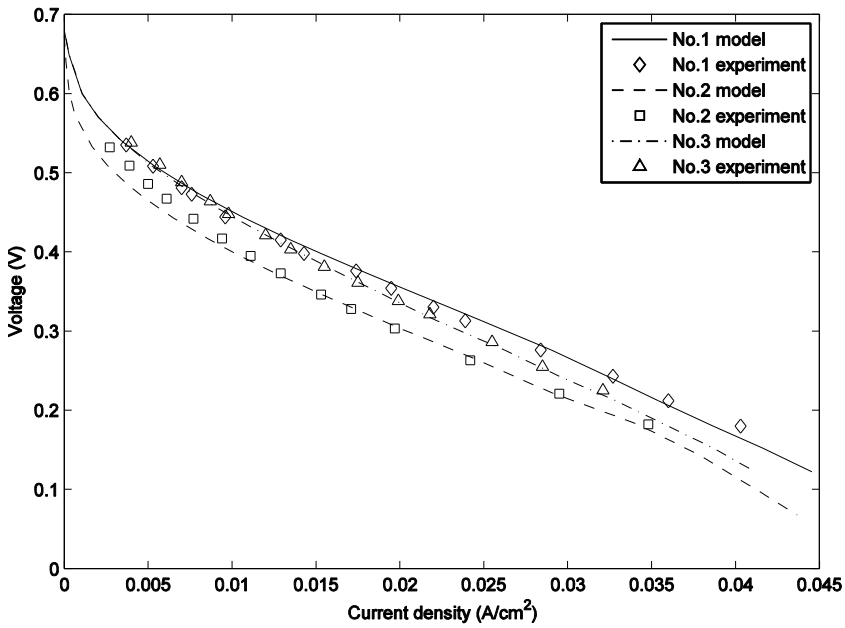

Figure 4.3. Simulation data and experimental data for the first geometric configuration with operating parameters given in Table 4.3.

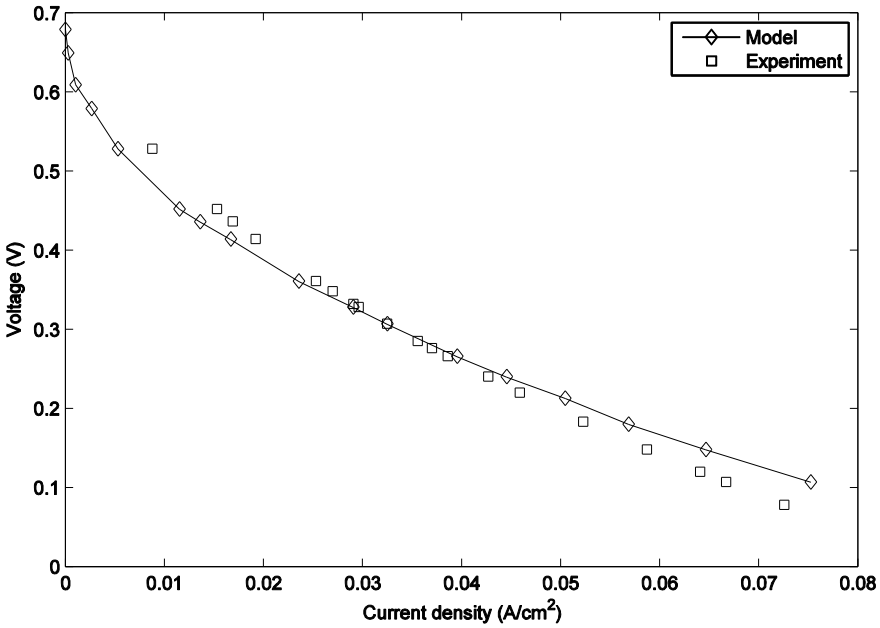

Figure 4.4. Simulation data and experimental data for second geometric configuration with operating parameters given in Table 4.3.

It should be noted that the coefficients used in the CFD model of this case study are accurate only around operating conditions similar to the operating parameters selected for the experiments. The three operating parameters for the second geometric configuration experiment were selected as the T = 343 K, C_{CH_3OH} = 0.5 M, and F_{CH_3OH} = 3.06 ccm, identical to test No. 1, and similar to the other test conditions listed in Table 4.3.

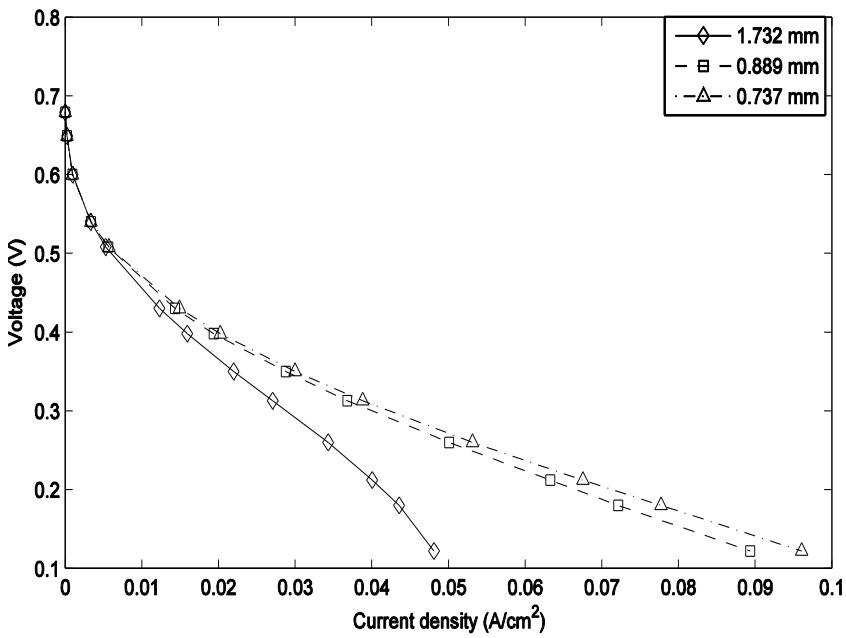

Figure 4.5. Simulation data to show influence of width of flow channel on DMFC performance.

4.4 Influences of Geometric and Operating Parameters on Performance

The fitted CFD model used in this research to study the influences of geometric parameters and operating parameters on DMFC performance measures will be discussed in the following sections.

4.4.1 Influences of Geometry Parameters on DMFC Performance

The channel width and height are selected to study the influences of geometric parameters on DMFC performance. Figures 4.5 and 4.6 show the influences of channel width and height on DMFC performance. The operating conditions for all simulations are the same: T = 343 K,

C_{CH_3OH} = 0.5 M, F_{CH_3OH} = 4.0 ccm, and F_{AIR} = 1,000 ccm. The open areas (i.e., the area of the channel exposing the MEA to methanol fuel) of these configurations are also very close. In Figure 4.5, the width of the flow channel was selected as 1.372 mm, 0.889 mm, and 0.737 mm, while the height was selected as 0.75 mm. In Figure 4.6, the height of the flow channel was selected as 0.5 mm, 0.75 mm and 1.0 mm, while the width was selected as 0.889 mm.

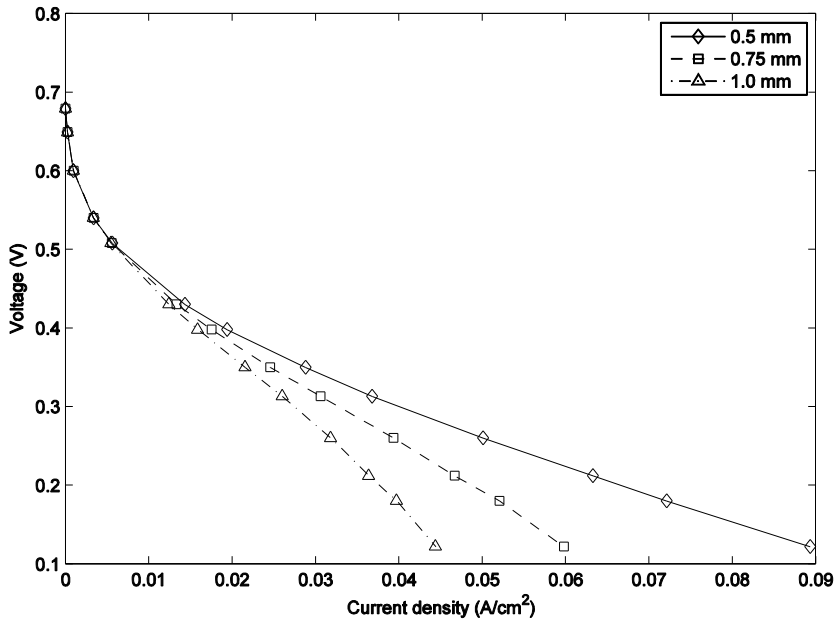

Figure 4.6. Simulation data to show influence of height of flow channel on DMFC performance.

It can be seen in Figure 4.5 that the DMFC performance increases as flow channel width decreases. One possible reason is that when the width of the flow channel is decreased, the total length of the flow channel is increased to maintain the open area of the flow field, therefore the pressure in the flow field also increases. High pressure can increase the velocity of methanol in the diffusion layer. In other words, high pressure can improve the mass transfer efficiency in DMFC and smaller channel width can provide better performance.

In Figure 4.5, it can be seen that at very low current density, the voltages of the three curves are similar, but at high current density, the voltages are different. This is because that at low current density, the methanol delivered into the flow field is sufficient due to its low reaction rate. At high current density, however, the methanol consumption rate is higher due to its high reaction

rate, leading to insufficient methanol for reaction. In this case, the high pressure with smaller channel width can improve the reaction rate of methanol.

From Figure 4.6, it can be seen that the DMFC performance increases with a decrease in flow channel height. The reason is similar to that for the change of width of the flow channel. When the height of the channel is decreased, pressure in the flow field is then increased, leading to improvement of mass transfer efficiency. It should be noted that the decrease of flow channel height may not always increase the cell performance, because carbon dioxide gas bubbles can block the flow channel when the height of the channel is very small.

The pressure distributions obtained through CFD simulation in the diffusion layers of the three bipolar plates are shown in Figure 4.7. The channel widths for designs A, B, C were specified as 1.372, 0.889, 0.737 mm. Through CFD simulation, the pressure drops corresponding to designs A, B and C were calculated as 0.48, 1.45 and 1.94 kPa.

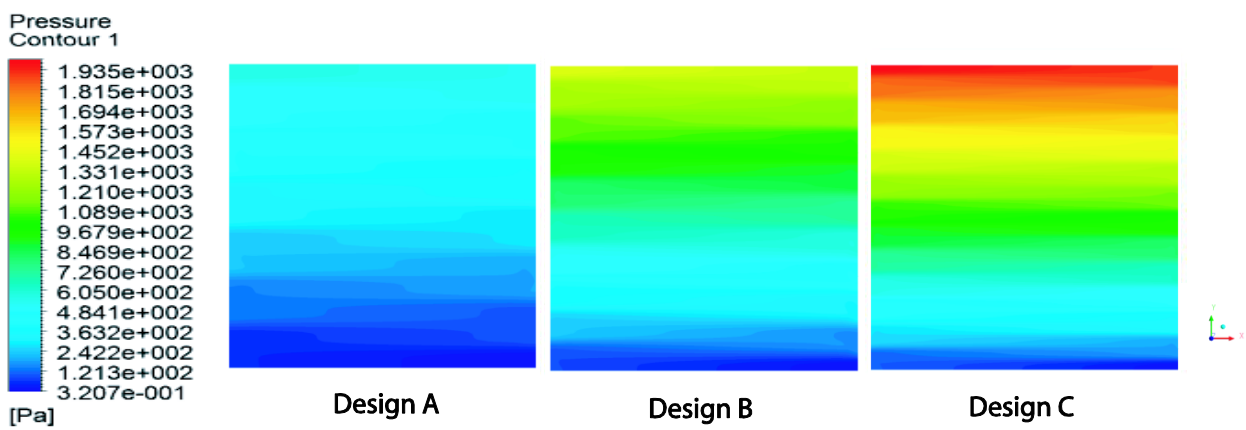

Figure 4.7. Pressure distributions obtained by CFD simulation in the diffusion layers of the three bipolar plates.

4.4.2 Influences of Operating Parameters on DMFC Performance

As noted before, the fitted CFD model in the case study is only effective near the operating condition of T = 343 K, C_{CH_3OH} = 0.5 M, and F_{CH_3OH} = 3.06 ccm. Therefore a discussion on the influences of operating parameters on DMFC performance is qualitative in nature.

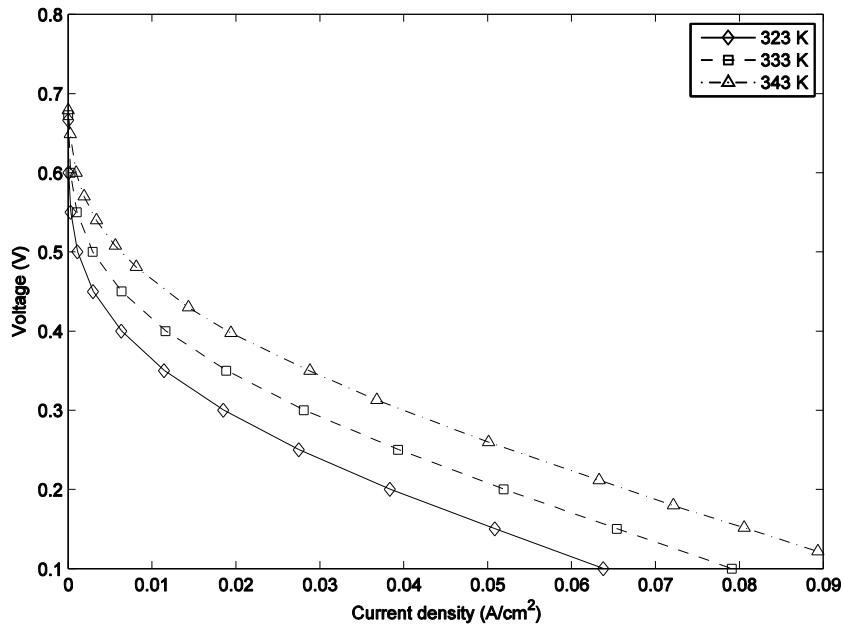

Figure 4.8. Simulation data to show influence of temperature on DMFC performance.

Figures 4.8, 4.9 and 4.10 show the influences of the three operating parameters, including temperature, methanol concentration, and methanol flow rate, on DMFC performance. In this study, the geometric parameter values are held constant to the second configuration of the DMFC. Figure 4.8 shows the influence of temperature on DMFC performance. Three temperature levels were selected as: T = 323 K, T = 333 K, and T = 343 K. The other operating conditions are: C_{CH_3OH} = 0.5 M, F_{CH_3OH} = 4.0 ccm, and F_{AIR} = 1,000 ccm. From Figure 4.8, it can be seen that the performance of the DMFC can be improved significantly when the temperature is increased. As is known, the chemical energy of molecules increases with increased temperature, generating more ions and electrons per Equations (3.2) and (3.3). The mass transfer efficiency can also be improved when temperature is increased. Figure 4.9 shows the influence of methanol concentration on performance of the DMFC under the operating conditions of T = 343 K, F_{CH_3OH} = 4.0 ccm, and F_{AIR} = 1,000 ccm. Three methanol concentration levels were selected as: C_{CH_3OH} = 0.25 M, C_{CH_3OH} = 0.5 M, and C_{CH_3OH} = 1.0 M. It can be seen from Figure 4.9 that when methanol concentration increases from 0.25 M to 1.0 M, the performance is decreased at low current density (≤ 0.03 A cm^{-2}). This is because some methanol molecules cannot be consumed completely in the reaction. A portion of methanol molecules penetrate

through the membrane to cathode side, leading to methanol crossover. A higher methanol concentration can lead to higher methanol crossover at low current density. At high current density (> 0.03 A cm^{-2}), when methanol concentration changes from 0.25 M to 0.5 M, the performance is increased since more methanol molecules are consumed at higher methanol concentration and the crossover is not as significant at high current density. When the methanol concentration is further increased from 0.5 M to 1.0 M, the contribution of methanol crossover again becomes significant, thus leading to a decrease in performance.

Figure 4.10 shows the influence of methanol flow rate on DMFC performance when T = 343 K, C_{CH_3OH} = 0.5 M, and F_{AIR} = 1,000 ccm. The three levels of methanol flow rate were selected as F_{CH_3OH} = 4.0 ccm, F_{CH_3OH} = 5.0 ccm, and F_{CH_3OH} = 6.0 ccm. From Figure 4.10, the DMFC performance is observed to increase only slightly with increased methanol flow rate. This can be explained by an improved mass transfer of methanol in the anode catalyst layer as the methanol flow rate increases. However when the methanol flow rate is sufficiently high, cell performance does not improve significantly. Overall, the influence of methanol flow rate is not as significant as the influences of temperature and methanol concentration. This result is also matched with the findings in Chapter 3.

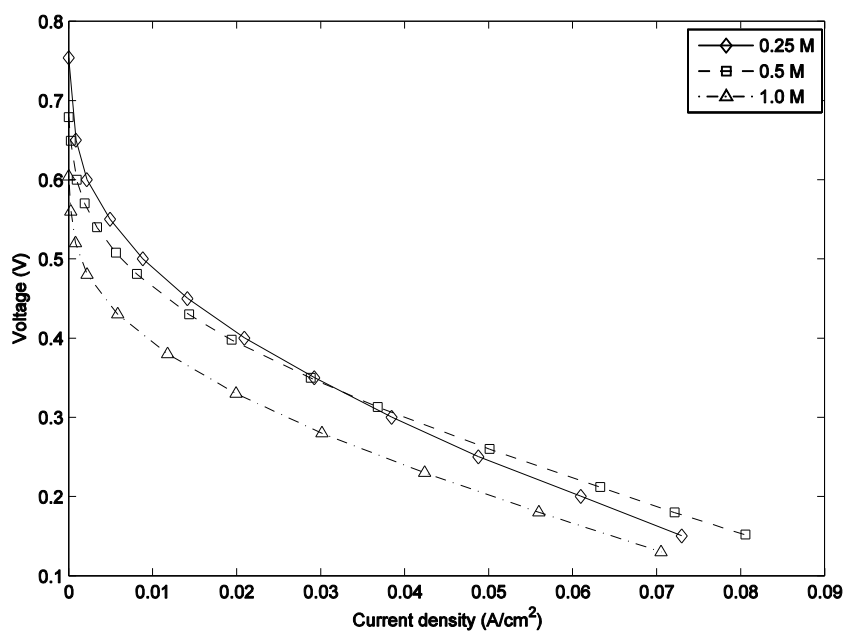

Figure 4.9. Simulation data to show influence of methanol concentration on DMFC performance.

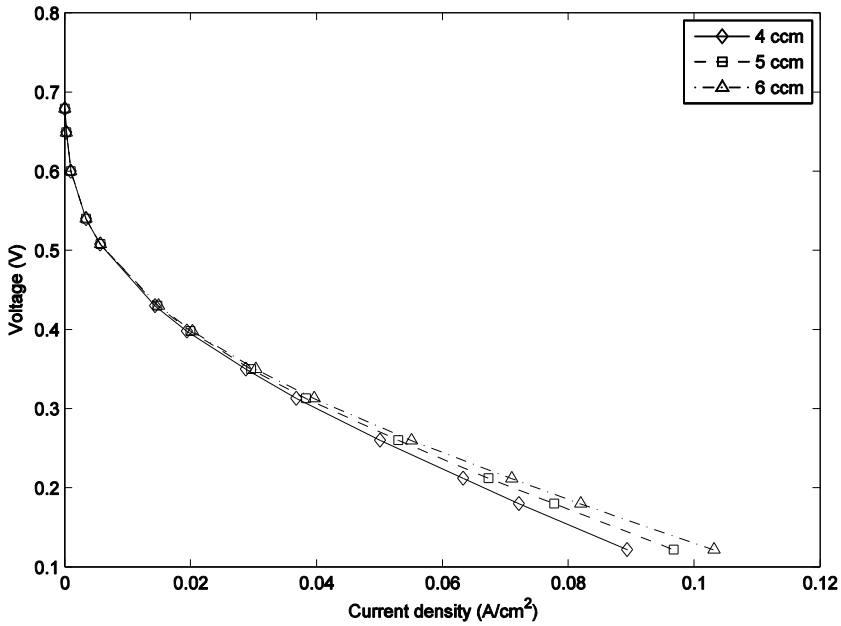

Figure 4.10. Simulation data to show influence of methanol flow rate on DMFC performance.

4.5 Summary

A three-dimensional computational fluid dynamics model has been developed in this research to study the influences of geometric and operating parameters on the performance of DMFC. In this model, the electrochemical behaviors are described by semi-empirical relationships. Coefficients for these semi-empirical relationships are obtained through adaptive metamodeling using data collected from experiments. The developed CFD model can be used to predict performance based on the geometric and operating parameters. The CFD model also provides a platform for the design and control of DMFC systems.

Compared with existing DMFC models, the CFD modeling approach developed in this research has two advantages:

(1) Sophisticated geometric shapes with serpentine channels, rather than simple geometric shapes in existing CFD models, are considered in this work. Therefore, the CFD model can be used not only to study the influences of geometric and operating parameters on DMFC performance, but also to carry out optimal design of geometric parameters and optimal control of operating parameters for developing DMFC systems.

(2) Based on CFD, a systematic approach to model the relationships between geometric/operating parameters and performance measures is introduced in this research. This characteristic makes our CFD model be different from existing ones, of which some physical/chemical parameter values must be calibrated manually based on experience or heuristics. In this CFD modeling approach, semi-empirical relationships are used to describe the electrochemical relationships. Adaptive metamodeling for optimization is used in fitting the data from experiments to obtain the coefficients in the semi-empirical relationships efficiently.

CHAPTER 5 COMPARATIVE STUDY ON INFLUENCING FACTORS IN ADAPTIVE METAMODELING

5.1 Overview

As introduced in Chapters 2 and 4, adaptive metamodeling is effective to describe the relations between input and output parameters when extensive effort is required to collect these input and output data through experiments or computer based simulation. In the CFD model introduced in Chapter 4, an adaptive metamodeling method is developed to reduce the number of data-fitting iterations for obtaining the coefficients in the semi-empirical relationships. The metamodels developed through adaptive metamodeling can also be used to describe the relationships between design/operating parameters and performance measures of direct methanol fuel cell (DMFC) systems. Compared with traditional metamodeling, adaptive metamodeling is of higher computation efficiency and accuracy.

The accuracy and efficiency of different adaptive metamodeling methods are influenced by many factors, such as the characteristics of the relationships to be modeled, the selected metamodeling scheme, sampling size and quality, and so on. For different engineering problems with different modeling requirements, different metamodeling methods need to be selected. In this research, influences of two factors in adaptive metamodeling, noise level of samples and initial size of samples, are investigated through comparative study, such that the appropriate adaptive metamodeling method can be selected to solve different DMFC problems. Two cases of adaptive metamodeling considering the best output point for optimization and the best fit in a specific output parameter space are considered. Three different metamodels, kriging, radial basis function and multivariate polynomial, are employed in this study. Various test functions are used to create the sample data and evaluate the accuracy and efficiency of the adaptive metamodeling methods considering influences of noise and initial size of samples. The results of this research provide guidelines for selecting appropriate adaptive metamodeling methods to solve various engineering problems. Effectiveness of the developed guidelines has been demonstrated through case study applications.

The issues addressed in this research are summarized as follows.

- Two types of adaptive metamodeling problems, adaptive metamodeling for optimization at a particular point and adaptive metamodeling for accurate approximation in a certain metamodeling space, are considered in this work. Since the quality of input data can be easily improved by uniform sampling in the input parameter space without using the metamodel, quality of the output data in terms of uniformity in a specific output space, which has to be achieved through adaptive metamodeling, is selected in this work.
- Three popular metamodels, kriging, radial basis function and multivariate polynomial, are selected in this research.
- Two factors in adaptive metamodeling, noise level of samples and initial size of samples, are investigated in this research. These two factors play important roles to influence the accuracy and efficiency of adaptive metamodeling.
- Computation accuracy and efficiency are selected in this work to evaluate the quality of an adaptive metamodeling method. When the total sample size is given, average error and average relative error of the metamodel are used to evaluate the computation accuracy. When the required accuracy is given, the total sample size is then used to evaluate the computation efficiency.
- Various test functions with different relationships between the input and output parameters are selected to create the sample data and to evaluate the adaptive metamodeling methods.

5.2 Adaptive Metamodeling

Metamodeling techniques were initiated from many different disciplines including statistics, computer science and engineering. The metamodels were developed as "surrogates" of the actual relationships that usually require expensive and extensive experiments or simulation to obtain (Wang and Shan, 2007).

In metamodeling, the relationship between a vector of input parameters, $\boldsymbol{x}$, and an output parameter, Y, can be formulated as:

$$Y = \hat{f}(\boldsymbol{x}) + \varepsilon_1 + \varepsilon_2 \tag{5.1}$$

where Y is a random output variable, $\hat{f}(\cdot)$ is the approximated relationship, ε_1 is the error of sample data due to the uncertainty in measurement, and ε_2 is the error of metamodel due to the uncertainty introduced by the metamodeling method. Many different metamodels, such as multivariate polynomial, radial basis function (RBF) and kriging, can be used to build the approximation relationship $\hat{f}(\cdot)$. In metamodeling, first m sample data ($\boldsymbol{x}_i$,y_i) (i=1,2,...,m) are collected to build the $\hat{f}(\cdot)$. When an input point $\boldsymbol{x}_0$ is given, the metamodel can then be used to predict the output Y_0 using:

$$Y_0 = \hat{f}(\boldsymbol{x}_0) \tag{5.2}$$

In non-adaptive metamodeling, the m sample data are collected first to build the metamodel. Effective sampling methods, such as the Latin hypercube sampling method (McKay et al., 1979), are often used to improve the quality of samples in the whole input parameter space.

When metamodeling is used for solving specific problems, collection of sample data in specific parameter space, rather than the whole parameter space, is then required to improve the accuracy and efficiency. This issue is critical when expensive or extensive experiments/simulations are required to collect the sample data. Since the relationship is unknown at beginning, initial samples are usually collected to build the initial metamodel. This currently developed metamodel is then used to identify the input parameters that have the best potential to lead to the expected output result. Due to the errors of the metamodel, the actual output obtained from experiment/simulation is usually different from the expected one. The previously obtained metamodel is subsequently updated to improve its quality using the new pair of input-output data. The method to iteratively modify the metamodel through an iterative sampling process is called adaptive metamodeling.

In this work, two types of adaptive metamodeling problems are considered: (1) adaptive metamodeling for optimization, and, (2) adaptive metamodeling for uniformity in specific output space.

5.2.1 Adaptive Metamodeling for Optimization

The presently developed adaptive metamodeling methods are primarily used for optimization. In these methods, design variables are modeled as input parameters and optimization objective function is modeled as the output parameter. The algorithm is composed of 4 steps as follows.

Step 1: The m initial samples with input parameters $\boldsymbol{x_i}$ (i=1,2,...,m) and output parameter Y_i (i=1,2,...,m) are collected to build the metamodel:

$$Y = f_m(\mathbf{x}) \tag{5.3}$$

Step 2: Based on the metamodel relationship f_m, we can identify the potential input parameters $\boldsymbol{x}^*$ that lead to the minimum output through optimization:

$$\min_{w.r.t.\mathbf{x}} f_m(\mathbf{x}) \tag{5.4}$$

Step 3: The optimization result of $\boldsymbol{x}^*$ is then selected as the vector of input parameters for the (m+1)-th sample $\boldsymbol{x_{m+1}}$. The output Y_{m+1} corresponding to the $\boldsymbol{x_{m+1}}$ is subsequently obtained through experiment or simulation.

Step 4: The new pair of data, ($\boldsymbol{x_{m+1}}$, Y_{m+1}), together with all the previously collected sample data are used to update the metamodel into a new relationship f_{m+1}:

$$Y = f_{m+1}(\boldsymbol{x}) \tag{5.5}$$

If the optimization criteria are satisfied, the process is stopped. If not, go to Step 2.

In this research, the simulated annealing function called `simulannealbnd()` in Matlab R2013a global optimization toolbox was selected for obtaining the potential input parameters based on Equation (5.4).

5.2.2 Adaptive Metamodeling for Uniformity in Specific Output Space

In this research, a new case of adaptive metamodeling for uniformity in specific output parameter space is introduced. The traditional sampling methods focus on achieving the uniformity in the input parameter space, as shown in Figure 5.1(a). This approach is effective to predict Y_0 based on the given $\boldsymbol{x_0}$ using the developed metamodel, since a metamodel developed

by sample data with good uniformity in the whole input parameter space is usually considered accurate and robust (Hickernell and Liu, 2002). In engineering design, however, the target value Y_0 sometimes is given first, and the design is to identify the $\boldsymbol{x_0}$ to achieve the target Y_0. In this case, uniformity of the output parameter space, as shown in Figure 5.1(b), has to be considered. Adaptive metamodeling is employed in this work to identify the sample points with the best uniformity in the output parameter space. For the design problem to obtain the input parameters $\boldsymbol{x_0}$ from a given target Y_0, only the uniformity in a specific output parameter space needs to be considered.

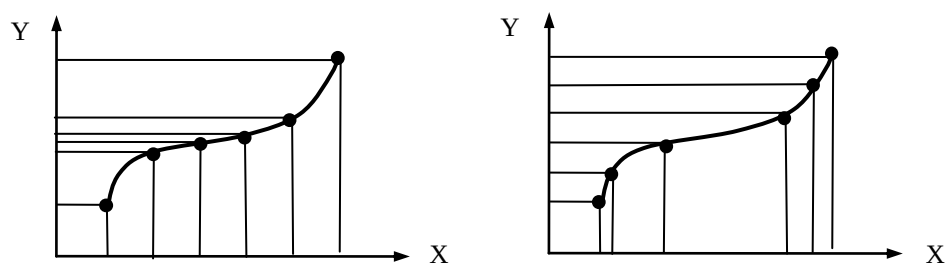

(a). Uniform input space. (b). Uniform output space.

Figure 5.1. Uniform input space and uniform output space.

The algorithm of adaptive metamodeling for uniformity in specific output space is composed of 4 steps.

Step 1: The m initial samples with input parameters $\boldsymbol{x_i}$ (i=1,2,...,m) from the whole design space and output parameter Y_i (i=1,2,...,m) from the whole output space are collected to build the metamodel:

$$Y = f_m(\mathbf{x}) \tag{5.6}$$

Step 2: Based on the metamodel relationship f_m, we can identify the potential input parameters $\boldsymbol{x}^*$ that lead to the best uniformity in specific output space through optimization:

$$\max_{w.r.t.\boldsymbol{x}} uniformity\{Y_1, Y_2, ..., Y_m, f_m(\boldsymbol{x})\} \tag{5.7}$$

where $Y_1, Y_2, ..., Y_m$ are the m output parameter values in the m samples, and f_m is the metamodel relationship obtained using the m samples.

Step 3: The optimization result of $\boldsymbol{x}^*$ is then selected as the vector of input parameters for the (m+1)-th sample $\boldsymbol{x}_{m+1}$. The output Y_{m+1} corresponding to the $\boldsymbol{x}_{m+1}$ is subsequently obtained through experiment or simulation.

Step 4: The new pair of data, ($\boldsymbol{x}_{m+1}$, Y_{m+1}), together with all the previously collected sample data are used to update the metamodel into a new relationship f_{m+1}:

$$Y = f_{m+1}(\boldsymbol{x}) \tag{5.8}$$

If the optimization criteria are satisfied, the process is stopped. If not, go to Step 2.

In this research, the simulated annealing function called `simulannealbnd()` in Matlab R2013a global optimization toolbox was selected for obtaining the potential input parameters based on Equation (5.7).

5.3 Scope of This Study

This research focuses on the study of influences of two factors, noise level of samples and initial size of samples, on accuracy and efficiency of different adaptive metamodeling methods.

5.3.1 Two Influencing Factors

Two influencing factors are considered in this research: (1) noise level of samples, and, (2) initial size of samples.

Noise level of samples

The various uncertainties, especially the uncertainties of the measurement devices and measurement processes, lead to the errors of the collected sample data that are used to train the metamodel. Different levels of noises have different impacts on the metamodels as shown in Figure 5.2. When the noise level is low as shown in Figure 5.2(a), the metamodel that can better interpolate the measurement points should be selected. When the noise level is high as shown in Figure 5.2(b), the metamodel with smoother change of the shape should be selected.

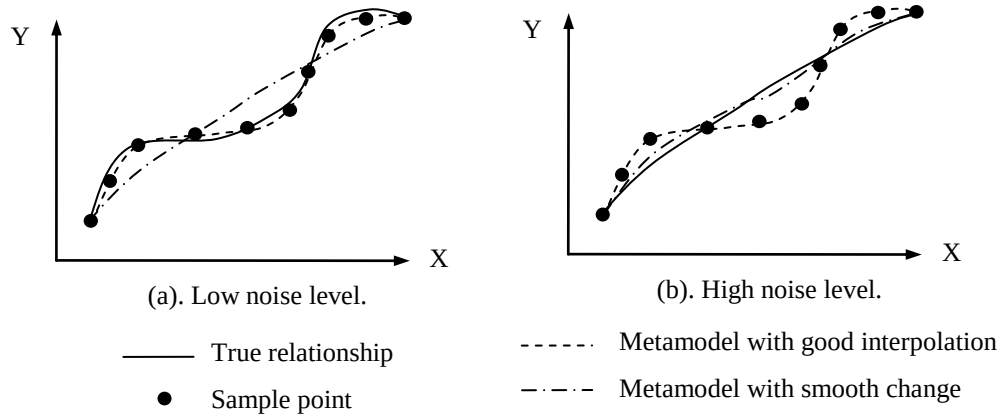

Figure 5.2. Influence of noise level in samples.

Initial size of samples

In adaptive metamodeling, initial samples are collected to build the initial metamodel. When the initial sample size is too small, new sample points at wrong locations are often identified based on the poorly developed metamodel, leading to slow progress and long training time as shown in Figure 5.3. Although the progress with large number of samples is significant, great effort has already been devoted for creating these initial samples at beginning. Therefore selection of appropriate initial sample size is expected to obtain good tradeoff between the effort to collect the initial samples and the training progress.

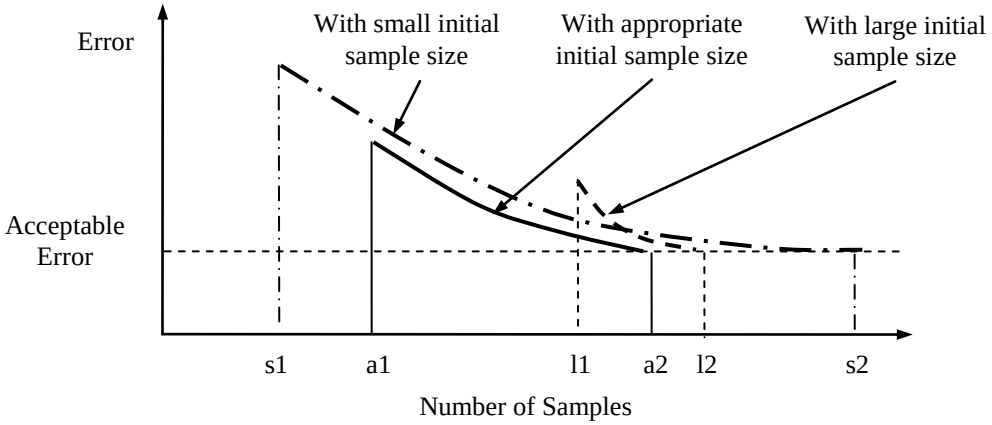

Figure 5.3. Influence of initial sample size.

5.3.2 Metamodels

Among various metamodels, kriging, radial basis function (RBF) and multivariate polynomial are the three most popular ones selected in metamodeling (Wang and Shan, 2007; Zhao and Xue, 2010). The kriging method, although complicated, can model the approximation relationship accurately with small number of data. The RBF is fairly easy to implement with reasonably good quality. The multivariate polynomials, especially the cubic polynomial, are often used in numerical method for data fitting due to their simplicity. In this research, these three metamodels are selected for the study.

Kriging method

Kriging method was originated from the geostatistics community (Matheron, 1963) and used by Sacks et al. (1989) to model computer experiment. Kriging method is based on the assumption that the true system response can be modeled by:

$$Y = \sum_{i=0}^{m} \beta_i f_i(\boldsymbol{x}) + Z(\boldsymbol{x}) \tag{5.9}$$

where $f_i(\cdot)$ is a regression function, β_i is the coefficient for $f_i(\cdot)$, m+1 is the number of regression functions, and $Z(\cdot)$ is the stochastic process with mean of zero and covariance defined by:

$$Cov\left(\mathrm{Z}(\boldsymbol{x}_j), \mathrm{Z}(\boldsymbol{x}_k)\right) = \sigma^2 R_{jk}\left(\boldsymbol{\theta}, \boldsymbol{x}_j, \boldsymbol{x}_k\right) \tag{5.10}$$

where σ^2 is the process variance, and $R_{jk}(\cdot)$ is the correlation function. The linear part of Equation (5.9) is usually assumed to be a constant (called *ordinary kriging*), whereas the correlation function $R_{jk}(\boldsymbol{\theta}, \boldsymbol{x}_j, \boldsymbol{x}_k)$ is generally formulated as:

$$R_{jk}\left(\boldsymbol{\theta}, \boldsymbol{x}_j, \boldsymbol{x}_k\right) = \prod_{i=1}^{p} Q\left(\theta_i, x_{ji}, x_{ki}\right) \tag{5.11}$$

where p is the dimension of $\boldsymbol{x}$, x_{ji} is the i-th component of $\boldsymbol{x}_j$, x_{ki} is the i-th component of $\boldsymbol{x}_k$, and $Q(\cdot)$ is usually assumed to be Gaussian as:

$$Q\left(\theta_i, x_{ji}, x_{ki}\right) = exp\left(-\theta_i d_i^2\right), \quad d_i = \left|x_{ji} - x_{ki}\right| \tag{5.12}$$

where θ_i is a coefficient to be determined.

The linear predictor of kriging method is formulated as:

$$\hat{g}(\boldsymbol{x}) = \boldsymbol{c}^T(\boldsymbol{x})\boldsymbol{y} \tag{5.13}$$

where $\boldsymbol{c}^T(\cdot)$ is the coefficient vector, and $\boldsymbol{y}$ is the vector of the observations at the sample sites $(\boldsymbol{x}_1,\ldots,\boldsymbol{x}_n)$:

$$\boldsymbol{y} = [y(\boldsymbol{x}_1) \quad \cdots \quad y(\boldsymbol{x}_n)]^T \tag{5.14}$$

By minimizing the prediction variance σ_t^2:

$$\sigma_t^2 = E\left[(\hat{g}(\boldsymbol{x}) - Y)^2\right] \tag{5.15}$$

with respect to the coefficient vector $\boldsymbol{c}^T(\boldsymbol{x})$, the best linear unbiased predictor (BLUP) is solved as (Lophaven et al., 2002):

$$\hat{g}(\boldsymbol{x}) = \boldsymbol{r}^T\boldsymbol{R}^{-1}\boldsymbol{y} - \left(\boldsymbol{F}^T\boldsymbol{R}^{-1}\boldsymbol{r} - \boldsymbol{f}\right)^T\left(\boldsymbol{F}^T\boldsymbol{R}^{-1}\boldsymbol{F}\right)^{-1}\left(\boldsymbol{F}^T\boldsymbol{R}^{-1}\boldsymbol{y}\right) \tag{5.16}$$

where

$$\boldsymbol{r} = [R(\boldsymbol{\theta}, \boldsymbol{x}_1, \boldsymbol{x}) \quad \cdots \quad R(\boldsymbol{\theta}, \boldsymbol{x}_n, \boldsymbol{x})]^T \tag{5.17}$$

$$\boldsymbol{R} = \begin{bmatrix} R(\boldsymbol{\theta}, \boldsymbol{x}_1, \boldsymbol{x}_1) & \cdots & R(\boldsymbol{\theta}, \boldsymbol{x}_1, \boldsymbol{x}_n) \\ \cdots & \cdots & \cdots \\ R(\boldsymbol{\theta}, \boldsymbol{x}_n, \boldsymbol{x}_1) & \cdots & R(\boldsymbol{\theta}, \boldsymbol{x}_n, \boldsymbol{x}_n) \end{bmatrix} \tag{5.18}$$

$$\boldsymbol{F} = \begin{bmatrix} f_0(\boldsymbol{x_1}) & \cdots & f_0(\boldsymbol{x_n}) \\ \cdots & \cdots & \cdots \\ f_m(\boldsymbol{x_1}) & \cdots & f_m(\boldsymbol{x_n}) \end{bmatrix}^T \tag{5.19}$$

$$\boldsymbol{f} = [f_0(\boldsymbol{x}) \quad \cdots \quad f_m(\boldsymbol{x})]^T \tag{5.20}$$

The coefficients $\boldsymbol{\theta}$ can be obtained by using maximum likelihood estimation as (Lophaven et al., 2002):

$$\min_{\boldsymbol{\theta}} \quad \psi(\boldsymbol{\theta}) = |\boldsymbol{R}|^{\frac{1}{n}}\sigma^2 \tag{5.21}$$

where $|\boldsymbol{R}|$ is the determinant of $\boldsymbol{R}$, and σ is obtained by generalized least squares fit as (Lophaven et al., 2002):

$$\hat{\sigma}^2 = \frac{1}{n-m-1}\left(\boldsymbol{y}-\boldsymbol{F}\boldsymbol{\beta}^*\right)^T \boldsymbol{R}^{-1}\left(\boldsymbol{y}-\boldsymbol{F}\boldsymbol{\beta}^*\right) \tag{5.22}$$

where β^* is the coefficients obtained from generalized least squares fit and is calculated by:

$$\boldsymbol{\beta}^* = \left(\boldsymbol{F}^T\boldsymbol{R}^{-1}\boldsymbol{F}\right)^{-1}\boldsymbol{F}^T\boldsymbol{R}^{-1}\boldsymbol{y} \tag{5.23}$$

The kriging metamodeling function in the DACE toolbox developed by Lophaven et al (2002) was used in this research.

Radial basis function (RBF) method

The radial basis function (RBF) model was first developed by Hardy (1971). An RBF model can be described by:

$$\hat{f}(\boldsymbol{x}) = \beta_0 + \sum_{i=1}^{m}\left[\beta_i b\left(\left\|\boldsymbol{x}-\boldsymbol{x}_i\right\|\right)\right] \tag{5.24}$$

where $\boldsymbol{x_i}$ is a center point selected from the training dataset, $b(\cdot)$ is the basis function, β_0 is a constant, β_i is the coefficient of a basis function, and m is the number of center points. Popular basis functions, including Gaussian, multiquadric and thin plate spline functions, are given in Equation (5.25).

$$b(r) = \begin{cases} e^{-\varepsilon r^2} \\ \sqrt{1+(\varepsilon r)^2} \\ r^2\ln(r) \end{cases} \tag{5.25}$$

where ε is a coefficient. In our research, Gaussian basis function is used for low dimensional problems and thin plate spline basis function is used for high dimensional problems.

Multivariate polynomial method

Multivariate polynomial method here refers to the polynomial used by response surface method (Myers and Montgomery, 1995). The general form of a multivariate polynomial model of degree d can be written as:

$$\hat{g}(\boldsymbol{x}) = \beta_0 + \sum_i \beta_i x_i + \sum_i \sum_{j>i} \beta_{ij} x_i x_j + \sum_i \beta_{ii} x_i^2 + \sum_i \sum_{j>i} \sum_{k>j} \beta_{ijk} x_i x_j x_k + \ldots + \sum_i \beta_{ii\ldots i} x_i^d \tag{5.26}$$

where x_i is a component of $\boldsymbol{x}$, and $\beta_0,\ldots,\beta_i,\ldots,\beta_{ij},\ldots,\beta_{ijk},\ldots$ are coefficients. Linear least squares estimation can be applied to this linear regression model (in terms of $\boldsymbol{\beta}$) to obtain the best fit to the data. The stepwise forward selection scheme based on mean squared error (Miller, 2002) can be used to reduce the number of terms in the polynomial.

5.3.3 Test Functions

Test functions are used to evaluate the adaptive metamodeling methods. In research on metamodeling, many test functions have been developed (Simpson et al., 2001). In this research, five test functions are selected. These test functions are classified into two categories: low-dimensional test functions with two input parameters and high-dimensional test function with six input parameters.

(1) Low-dimensional test functions

- Branin function

$$f(x_1, x_2) = [x_2 - 5.1\left(\frac{x_1}{2\pi}\right)^2 + \frac{5x_1}{\pi} - 6]^2 + 10\left(1 - \frac{1}{8\pi}\right)\cos(x_1) + 10, \quad x_1 \in [-5,10], x_2 \in [0,15] \tag{5.27}$$

- Six-hump camel back function

$$f(x_1, x_2) = (4 - 2.1x_1^2 + \frac{x^4}{3})x^2 + x_1 x_2 + (-4 + 4x_2^2)x_2^2, \;\; x_1 \in [-3,3], x_2 \in [-2,2] \tag{5.28}$$

- Booth function

$$f(x_1, x_2) = (x_1 + 2x_2 - 7)^2 + (2x_1 + x_2 - 5)^2, \;\; x_1 \in [-10,10], x_2 \in [-10,10] \tag{5.29}$$

- Beale function

$$f(x_1, x_2) = (1.5 - x_1 + x_1 x_2)^2 + (2.25 - x_1 + x_1 x_2^2)^2 + (2.625 - x_1 + x_1 x_2^3)^2, \quad x_1 \in [-4.5, 4.5], x_2 \in [-4.5, 4.5] \tag{5.30}$$

(2) High-dimensional test function

- Hartmann 6 function

$$f(x_1, x_2, x_3, x_4, x_5, x_6) = -\sum_{i=1}^{4} \left\{ c_i \exp[-\sum_{j=1}^{6} a_{ij}(x_j - p_{ij})^2] \right\}, \; x_j \in [0,1], \; j = 1,2,...,6 \tag{5.31}$$

where a_{ij}, c_i and p_{ij} (i=1,2,...,4; j=1,2,...,6) are defined by:

$$a = \begin{bmatrix} 10 & 3 & 17 & 3.5 & 1.7 & 8 \\ 0.05 & 10 & 17 & 0.1 & 8 & 14 \\ 3 & 3.5 & 1.7 & 10 & 17 & 8 \\ 17 & 8 & 0.05 & 10 & 0.1 & 14 \end{bmatrix} \tag{5.32}$$

$$c = [1 \quad 1.2 \quad 3 \quad 3.2] \tag{5.33}$$

$$p = \begin{bmatrix} 0.1312 & 0.1696 & 0.5569 & 0.0124 & 0.8283 & 0.5886 \\ 0.2329 & 0.4135 & 0.8307 & 0.3736 & 0.1004 & 0.9991 \\ 0.2348 & 0.1451 & 0.3522 & 0.2883 & 0.3047 & 0.6650 \\ 0.4047 & 0.8828 & 0.8732 & 0.5743 & 0.1091 & 0.0381 \end{bmatrix} \tag{5.34}$$

5.3.4 Data Sampling Methods

Data sampling methods in adaptive metamodeling are classified into two categories: initial data sampling and adaptive data sampling. Initial data sampling is used to build the initial metamodel considering the whole input space. The regular one-time sampling method, like random sampling, Latin hypercube sampling and uniform sampling, can all be used for initial sampling. Adaptive data sampling aims at creating new sample data only in the space we are interested in.

Latin hypercube design (McKay et al., 1979) is used in this work for initial sampling. The basic idea for the Latin hypercube sampling method is to divide the design space C_s into *n* strata with equal marginal probability 1/n and then sample once from each stratum (Fang et al., 2006). The

goal is to ensure that each input variable has all portions of its range represented (Sacks et al., 1989). The obvious advantages of Latin hypercube sampling method have been introduced in Section 2.3.1. The function called `lhsdesign()` in Matlab R2013a was selected for Latin hypercube design.

In adaptive sampling, when the adaptive metamodeling is used for optimization, the new sample should be created at or near the location with the minimum output. The input parameters of the new sample data are identified using Equation (5.4). When the adaptive metamodeling is used for achieving uniformity in a specific output space, the new sample should be identified at the location with the maximum uniformity of the output measures in this specific output space. In this work, several candidate points are created within the output space. For each of these candidate points, the modified L_2 discrepancy developed by Hickernell (1998a) is used to evaluate the uniformity of the output data. The candidate with the best uniformity in output space is selected as the expected output to identify its potential input parameters using Equation (5.7) for a new sample. For other discrepancy measures, such as maximin and minimax, they are not effective to create sufficient samples when only some of the input variables have significant contributions to the output (Morris and Mitchell, 1995).

The centered L_2 discrepancy is calculated by:

$$\begin{aligned}\left(CD\left(D_n\right)\right)^2 = &\left(\frac{13}{12}\right)^p - \frac{2}{n}\sum_{j=1}^{n}\prod_{i=1}^{p}\left[1+\frac{1}{2}\left|x_{ji}-0.5\right|-\frac{1}{2}\left|x_{ji}-0.5\right|^2\right] \\ &+\frac{1}{n^2}\sum_{k=1}^{n}\sum_{j=1}^{n}\prod_{i=1}^{p}\left[1+\frac{1}{2}\left|x_{ki}-0.5\right|+\frac{1}{2}\left|x_{ji}-0.5\right|-\frac{1}{2}\left|x_{ki}-x_{ji}\right|\right]\end{aligned} \tag{5.35}$$

where n is the number of points, p is the dimension of the output parameters, and x_{ji} is the value in the i-th dimension of the j-th point. Since only one output parameter is considered in metamodeling, p and i are selected as 1s. The value of centered L_2 discrepancy ranges from 0 to 1. The smaller the value of centered L_2 discrepancy is, the more uniform the samples are scattered in the space.

5.4 Study on Influence of Noise Level in Sample Data

The sample data with different levels of noises are obtained by adding artificial noises to the data created from the test functions. When the test function is defined by ***f(x)***, the sample data with artificial noises are created by:

$$Y = f(x) + \alpha Z \tag{5.36}$$

where $\alpha =$ 0-2 is a scaling factor, and Z is a random number sampled from the uniform distribution in the region (-1,1).

5.4.1 Adaptive Metamodeling without Influences of Noises

When α in Equation (5.36) is selected as 0, influences of noises are not considered in adaptive metamodeling. In this work, adaptive metamodeling is used for two cases: adaptive metamodeling for optimization and adaptive metamodeling for uniformity in specific output space.

Adaptive metamodeling for optimization without influences of noises

The low-dimensional Branin and six-hump camel back functions and the high-dimensional Hartmann 6 function are used for evaluating the efficiency of optimization methods based on non-adaptive metamodeling and adaptive metamodeling. The true minimum output measures for Branin function, six-hump camel back function and Hartmann 6 function are 0.397887, -1.03163 and -3.32237, respectively. The optimization process is stopped when the change of the objective function in five consecutive iterations is less than 0.05, or the maximum number of iterations is reached. The maximum iteration numbers for Branin, six-hump camel back and Hartmann 6 test functions in adaptive metamodeling are selected as 50, 50 and 125, respectively. The evaluation results are summarized in Table 5.1.

Table 5.1. Comparison for optimization without influence of noises.

Test function	Metamodel	Metamodeling method	Initial sample size	Total sample size	Minimum output
Branin	Kriging	Adaptive	9	23	0.3979
		Non-adaptive	50	50	0.4070
	RBF	Adaptive	9	40	0.4019
		Non-adaptive	50	50	0.4274
	Polynomial	Adaptive	9	35	3.1574
		Non-adaptive	50	50	16.0924
Six-hump camel back	Kriging	Adaptive	9	25	-1.0319
		Non-adaptive	50	50	-1.0312
	RBF	Adaptive	9	31	-1.0307
		Non-adaptive	50	50	-1.0192
	Polynomial	Adaptive	9	17	0.0011
		Non-adaptive	50	50	0.2015
Hartmann 6	Kriging	Adaptive	27	51	-3.3055
		Non-adaptive	125	125	-2.9820
	RBF	Adaptive	27	77	-3.2699
		Non-adaptive	125	125	-2.6163
	Polynomial	Adaptive	27	43	-0.0541
		Non-adaptive	125	125	-0.1686

From Table 5.1, we can see that for both the low-dimensional test functions and high-dimensional test function, adaptive metamodeling using kriging and RBF metamodels can improve the optimization efficiency and accuracy by using less numbers of sample data and modeling the relationships accurately in the regions with the optimal solutions. The multivariate polynomial metamodel is not effective for the three test functions due to the multi-optimum nature of the test function shapes. The kriging based adaptive metamodeling methods provide higher optimization efficiency and accuracy than the RBF based adaptive metamodeling methods when noises are not considered. In addition, the low-dimensional optimization problems need less numbers of iterations to obtain the optimal results than the high-dimensional optimization problems.

Adaptive metamodeling for uniformity in specific output space without influences of noises

Due to the large number of mapped regions in the input parameter space from the same output space in high-dimensional problems, study on adaptive metamodeling for uniformity in specific output space is limited to only low-dimensional test functions in this work. The four 2-D test

functions, their original output parameter spaces, and the selected specific output spaces for this study are summarized in Table 5.2.

Table 5.2. Whole output spaces and specific output spaces for different 2-D test functions.

Test function	Whole input space	Whole output space (approximation)	Specific output space selected for this study
Branin	$x_1 \in [-5,10]$, $x_2 \in [0,15]$	[0, 300]	[140, 150]
Six-hump camel back	$x_1 \in [-3,3]$, $x_2 \in [-2,2]$	[-1.0316, 160]	[100, 110]
Booth	$x_1 \in [-10,10]$, $x_2 \in [-10,10]$	[0, 2,600]	[200, 220]
Beale	$x_1 \in [-4.5,4.5]$, $x_2 \in [-4.5,4.5]$	[0, 177,000]	[50,000, 51,000]

For non-adaptive metamodeling, Latin hypercube sampling is used to get N sample points. For adaptive metamodeling, n_0 initial samples are used to build the initial metamodel, and the metamodel is updated with a total of N samples. The initial sample size, n_0, and the total sample size, N, are selected as n_0=60 and N=160. Quality of each metamodeling method is evaluated by n_t evaluation points. At each evaluation point, the vector with input parameter values is given as $\boldsymbol{x_i}$ (i=1,2,..., n_t), and the predicted output y_i' and the actual output y_i are compared to get the metamodeling error at this point, δ_i. The average error, $\bar{\delta}$, considering all evaluation points is calculated by:

$$\bar{\delta} = \frac{1}{n_t}\sum_{i=1}^{n_t}\delta_i = \frac{1}{n_t}\sum_{i=1}^{n_t}\left|y_i' - y_i\right| \tag{5.37}$$

The average relative error, $\bar{\lambda}$, considering all evaluation points is calculated by:

$$\bar{\lambda} = \frac{1}{n_t}\sum_{i=1}^{n_t}\lambda_i = \frac{1}{n_t}\sum_{i=1}^{n_t}\frac{\left|y_i' - y_i\right|}{y_i} \tag{5.38}$$

where λ_i is the relative metamodeling error at each evaluation point. In this research, the number of evaluation points, n_t, is selected as n_t=200.

The evaluation results are summarized in Table 5.3. From this table, we can see that adaptive metamodeling methods can improve the uniformity of the output samples considering the selected specific output space for all the cases compared with the non-adaptive metamodeling methods. The kriging method provides the best metamodeling quality in most cases. Multivariate

polynomial method is the best for both adaptive metamodeling and non-adaptive metamodeling when Booth test function is used, since the Booth test function itself is a polynomial function. For other three test functions, multivariate polynomial method is worse than the RBF method for both adaptive metamodeling and non-adaptive metamodeling.

Based on the comparisons in this section, we can see that adaptive metamodeling methods have demonstrated effectiveness to improve accuracy and efficiency of metamodeling compared with the non-adaptive metamodeling methods. In the rest of this chapter, only adaptive metamodeling methods will be discussed.

Table 5.3. Comparison for uniformity in specific output space without influence of noises.

Test functions	**Metamodel**	**Adaptive metamodeling**		**Non-adaptive metamodeling**	
		Average error $\bar{\delta}$	**Average relative error** $\bar{\lambda}$ (%)	**Average error** $\bar{\delta}$	**Average relative error** $\bar{\lambda}$ (%)
Branin	Kriging	1.5046×10^{-6}	1.0436×10^{-6}	0.0104	7.1293×10^{-3}
	RBF	0.0156	1.0811×10^{-2}	0.1833	0.13
	Polynomial	15.1430	10.41	37.0716	25.5000
Six-hump camel back	Kriging	0.0112	1.0621×10^{-4}	0.0331	3.1108×10^{-4}
	RBF	0.0304	2.8944×10^{-4}	0.1222	3.1108×10^{-4}
	Polynomial	35.1793	0.3349	46.6207	0.4434
Booth	Kriging	3.2646×10^{-5}	1.5573×10^{-5}	0.0013	6.1524×10^{-4}
	RBF	0.0150	7.1066×10^{-3}	2.3647	1.12
	Polynomial	4.7751×10^{-13}	2.2713×10^{-13}	1.4132×10^{-12}	6.7291×10^{-13}
Beale	Kriging	0.0479	9.5049×10^{-5}	16.9911	3.3643×10^{-2}
	RBF	0.7346	1.4534×10^{-3}	33.0104	6.5367×10^{-2}
	Polynomial	2.5600×10^{3}	5.07	1.5612×10^{4}	30.91

5.4.2 Adaptive Metamodeling with Influences of Noises

When α in Equation (5.36) is not selected as 0, influences of noises are considered in adaptive metamodeling. In this work, adaptive metamodeling considering influences of noises are used for two cases: adaptive metamodeling for optimization and adaptive metamodeling for uniformity in specific output space.

Adaptive metamodeling for optimization with influences of noises

The simulated samples with noises are created by generating samples using the given test functions and adding the noises based on Equation (5.36) considering different noise levels.

When the noise level α is selected as 0, the noises in samples are not considered (see the discussions in Section 5.4.1).

Two low-dimensional functions and one high-dimensional function are used for evaluating the efficiency and accuracy of optimization methods based on adaptive metamodeling considering influences of noises. The true minimum output measures for Branin function, six-hump camel back function and Hartmann 6 function are 0.397887, -1.03163 and -3.32237, respectively. The optimization process is stopped when the change of the objective function in five consecutive iterations is less than 0.05, or the maximum number of iterations is reached. The maximum iteration numbers for Branin, six-hump camel back, and Hartmann 6 test functions in adaptive metamodeling are selected as 100, 100, and 150, respectively. The evaluation results for the cases when noise level α is selected as 0.01 are summarized in Table 5.4.

From Table 5.4, we can see that kriging and RBF metamodels can be used for optimization considering both cases with noises and without noises. Multivariate polynomial metamodel may not be able to find the optimal solution when the maximum iteration number is reached (e.g., for the Branin test function) or find the wrong optimal solution (e.g., for the six-hump camel back test function). When noises are not considered, kriging is more efficient than RBF for both the low-dimensional Branin function and six-hump camel back function, and the high-dimensional Hartmann 6 function with smaller total sample sizes. When noises are considered, RBF is more efficient than kriging for both the low-dimensional functions and the high-dimensional function with smaller total sample sizes. These results match with the finding from the previous research by Zhao and Xue (2010) on comparison of non-adaptive metamodeling methods that kriging works better than RBF when noise level is low while RBF is more effective than kriging when noise level is high.

Table 5.4. Comparison for optimization considering influence of noises.

Test function	Metamodel	Without noise			With noise (α = 0.01)		
		Initial sample size	Total sample size	Minimum output	Initial sample size	Total sample size	Minimum output
Branin	Kriging	9	23	0.3979	9	58	0.3980
	RBF	9	40	0.4019	9	47	0.4097
	Polynomial	9	35	3.1574	9	100	8.4329
Six-hump camel back	Kriging	9	25	-1.0316	9	73	-1.0359
	RBF	9	31	-1.0307	9	51	-1.0293
	Polynomial	9	17	0.0010	9	24	-0.0029
Hartmann 6	Kriging	27	51	-3.3055	27	150	-3.1794
	RBF	27	77	-3.2699	27	89	-3.2547
	Polynomial	27	43	-0.0541	27	150	-2.6429

In this research, influences of different levels of noises on the efficiency of metamodeling based optimization methods have also been studied. The different levels of α are selected as 0.001, 0.002, 0.005 and 0.01. The samples without noises (i.e., α = 0) are also considered in the comparison. Since the multivariate polynomial method usually has difficulty to obtain the optimal solutions, only kriging and RBF are selected as the metamodels to be studied. The comparison results are shown in Table 5.5.

From Table 5.5, we can see that with the increase of the noise level, the total sample sizes in kriging based optimization methods are usually increased considerably while the total sample sizes in RBF based optimization methods usually remain minor variations. When noises are not considered (i.e., α = 0) or low, kriging is more efficient than RBF. When noises are high, RBF is more efficient than kriging.

Adaptive metamodeling for uniformity in specific output space with influences of noises

The conditions to evaluate the quality of adaptive metamodeling methods for uniformity in specific output space considering influences of noises are similar to those used to evaluate the quality of adaptive metamodeling methods without considering influences of noises. These conditions include:

- Only low-dimensional test functions are selected, since large number of mapped regions in the input parameter space can be identified from the same output space in high-dimensional problems.

Table 5.5. Comparison for optimization considering influence of different levels of noises.

Test functions	Noise level (α)	Metamodel	Initial sample size	Total sample size	Minimum Output
Branin	0	Kriging	9	23	0.3979
		RBF	9	40	0.4019
	0.001	Kriging	9	25	0.3980
		RBF	9	36	0.4000
	0.002	Kriging	9	50	0.3979
		RBF	9	41	0.4213
	0.005	Kriging	9	55	0.3980
		RBF	9	41	0.4164
	0.01	Kriging	9	58	0.3980
		RBF	9	47	0.4097
Six-hump camel back	0	Kriging	9	25	-1.0316
		RBF	9	31	-1.0307
	0.001	Kriging	9	27	-1.0326
		RBF	9	29	-0.9762
	0.002	Kriging	9	35	-1.0277
		RBF	9	44	-1.0325
	0.005	Kriging	9	60	-1.0365
		RBF	9	48	-1.0238
	0.01	Kriging	9	73	-1.0359
		RBF	9	51	-1.0293
Hartmann 6	0	Kriging	27	51	-3.3055
		RBF	27	77	-3.2699
	0.001	Kriging	27	47	-3.2625
		RBF	27	68	-3.2916
	0.002	Kriging	27	44	-3.2899
		RBF	27	77	-3.1751
	0.005	Kriging	27	54	-3.2814
		RBF	27	81	-3.1769
	0.01	Kriging	27	150	-3.1794
		RBF	27	89	-3.2547

- In adaptive metamodeling, n_0 initial samples are used to build the initial metamodel, and the metamodel is updated with a total of N samples.

- Quality of each metamodeling method is evaluated by average error, $\bar{\delta}$, and average relative error, $\bar{\lambda}$, for the n_t evaluation points.

Table 5.6. Comparison for uniformity in specific output space considering influence of noises.

Test functions	Metamodel	Without noise		With noise	
		Average error $\bar{\delta}$	Average relative error $\bar{\lambda}$ (%)	Average error $\bar{\delta}$	Average relative error $\bar{\lambda}$ (%)
Branin	Kriging	1.5046×10^{-6}	1.0436×10^{-6}	0.1983	0.1400
	RBF	0.0156	1.0811×10^{-2}	0.1483	0.1000
	Polynomial	15.1430	10.41	13.3713	9.4500
Six-hump camel back	Kriging	0.0112	1.0621×10^{-4}	0.2823	0.0027
	RBF	0.0304	2.8944×10^{-4}	0.2569	0.0025
	Polynomial	35.1793	0.3349	35.0729	0.3339
Booth	Kriging	2.1284×10^{-5}	1.0146×10^{-5}	1.8279	0.8700
	RBF	0.0294	1.3955×10^{-2}	0.2012	9.6098×10^{-2}
	Polynomial	2.2836×10^{-13}	1.0868×10^{-13}	0.1949	9.2900×10^{-2}
Beale	Kriging	0.0479	9.5049×10^{-5}	3.7352	7.3979×10^{-3}
	RBF	0.7346	1.4534×10^{-3}	0.3928	7.7669×10^{-4}
	Polynomial	2.5600×10^{3}	5.07	2.8910×10^{4}	57.25

In this work, the initial sample size, n_0, and the total sample size, N, are selected as n_0=60 and N=160. The number of evaluation points, n_t, is selected as 200. The noise levels for the samples to study Branin, six-hump camel back, Booth, and Beale functions are selected as $\alpha = 0.5$, 0.5, 0.5 and 2, respectively. The evaluation results are summarized in Table 5.6.

From this table, we can see that kriging and RBF metamodels can be used for achieving the uniformity in specific output space both considering noises and without considering noises for all four test functions. Multivariate polynomial is effective for only Booth function which is actually a polynomial. Multivariate polynomial cannot be used for the other three test functions. The kriging method provides better metamodeling quality than RBF when noises are not considered. The RBF is better than kriging when noises are considered.

5.5 Study on Influence of Initial Sample Size

Study on influence of initial sample size is based on the following two considerations:

- When the initial sample size is too small, wrong new sample points are often identified based on the poorly developed initial metamodel, leading to slow progress and long training time.
- When the initial sample size is large, although the training progress is significant, great effort has already been devoted for creating the initial samples at very beginning.

Therefore selection of appropriate initial sample size is expected to obtain good tradeoff between the effort to collect the initial samples and the effort in the training progress. In this research, influence of initial sample size on the accuracy and efficiency of adaptive metamodeling methods is also studied considering the two cases: adaptive metamodeling for optimization and adaptive metamodeling for uniformity in specific output space. Since noises are not considered in the study of initial sample size influence, only kriging metamodel is selected.

5.5.1 Influence of Initial Sample Size on Adaptive Metamodeling for Optimization

The low-dimensional Branin function and the high-dimensional Hartmann 6 function are used for evaluating the efficiency of adaptive metamodeling based optimization methods considering different initial sample sizes. The true minimum output measures for Branin function and Hartmann 6 function are 0.397887 and -3.32237, respectively. The optimization process is stopped when the change of the objective function in five consecutive iterations is less than 0.05, or the maximum number of iterations is reached. The maximum iteration numbers for Branin and Hartmann 6 test functions in adaptive metamodeling are selected as 50 and 125, respectively.

The influence of sample size on the efficiency of adaptive metamodeling considering both the low-dimensional test function and the high-dimensional test function are summarized in Table 5.7. During the study, differences in total sample sizes are observed when the different initial samples with the same sample size are used for adaptive metamodeling. To solve this problem, for one initial sample size, 25 different sample sets are created with the same sampling method. The average total number is used to evaluate the optimization efficiency. The average minimum output measures for different adaptive metamodeling methods are also provided in Table 5.7.

Table 5.7. Comparison for optimization with different initial sample sizes using kriging metamodel.

Test function	Initial sample size	Average total sample size for 25 sample sets	Average minimum output for 25 sample sets
Branin	2	19.08	0.3979
	4	18.72	0.3980
	9	20.08	0.3979
Hartmann 6	2	38.6000	-3.1924
	4	32.8636	-3.1974
	15	45.1667	-3.2139

From Table 5.7, we can see that the too small initial sample sizes can lead to slightly large numbers of optimization iterations due to the poor quality of the initial metamodels. When the initial sample size is increased, the total number of samples for optimization is decreased when the initial sample size is too small. When the initial sample size is large, the increase of the initial sample size, however, leads to the increase in the total number of the samples. This result matches with the assumptions given in Figure 5.3.

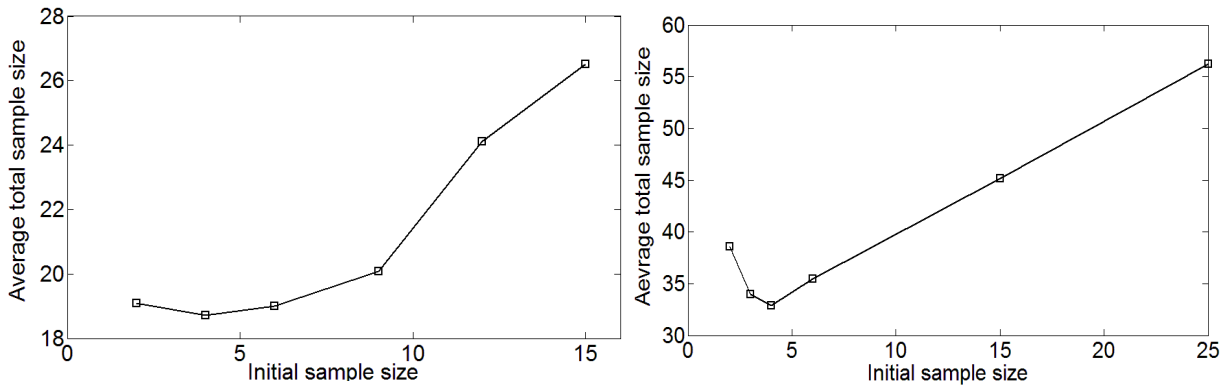

(a). Branin test function. (b). Hartmann 6 test function.

Figure 5.4. Influence of initial sample size for optimization using kriging metamodel.

Many initial sample sizes are selected to study the influence of initial sample size on efficiency of adaptive metamodeling based optimization methods using the low-dimensional Branin function and the high-dimensional Hartmann 6 function as shown in Figure 5.4.

5.5.2 Influence of Initial Sample Size on Adaptive Metamodeling for Uniformity in Specific Output Space

The conditions to evaluate the quality of adaptive metamodeling methods for uniformity in specific output space considering influence of initial sample size are similar to those used to evaluate quality of adaptive metamodeling methods for uniformity in specific output space considering influence of noise. These conditions include:

- Only low-dimensional test functions are selected, since large number of mapped regions in the input parameter space can be identified from the same output space in high-dimensional problems.

- Since noises are not considered in the study of the influence of initial sample size, only kriging metamodel is selected.
- For adaptive metamodeling, n_0 initial samples are used to build the initial metamodel, and the metamodel is updated with a total of N samples.
- Quality of each adaptive metamodeling method is evaluated by average error, $\bar{\delta}$, and average relative error, $\bar{\lambda}$, for the n_t evaluation points.
- Due to the uncertainty, different average errors and average relative errors are observed when different initial samples with the same sample size are used. To solve this problem, for one initial sample size, 25 different sample sets are created with the same sampling method. The statistical average errors and average relative errors considering 25 different tests are used to evaluate the adaptive metamodeling methods.

In this work, the total sample size, N, is selected as N=145. The number of evaluation points, n_t, is selected as 200. The evaluation results are summarized in Table 5.8.

Table 5.8. Comparison for uniformity in specific output space with different initial sample sizes using kriging metamodel.

Test function	**Initial sample size**	**Total sample size**	**Average error $\bar{\delta}$ for 25 sample sets**	**Average relative error $\bar{\lambda}$ (%) for 25 sample sets**
Branin	5	145	3.0692×10^{-6}	2.1332×10^{-8}
	10	145	2.9353×10^{-6}	2.0371×10^{-8}
	20	145	3.5358×10^{-6}	2.4554×10^{-8}
	40	145	4.1560×10^{-6}	2.8796×10^{-8}

From Table 5.8, we can see that the too small initial sample sizes can lead to slightly large average errors and average relative errors due to the poor quality of the initial metamodels. When the initial sample size is increased, the average error and average relative error are decreased when the initial sample size is too small. When the initial sample size is large, the increase of the initial sample size, however, leads to the large average error and average relative error due to the smaller number of remaining adaptive iterations in adaptive metamodeling. This result matches with the assumptions given in Figure 5.3.

Many initial sample sizes are selected to study the influence of initial sample size on quality measures, including the average error, $\bar{\delta}$, and average relative error, $\bar{\lambda}$, of adaptive metamodeling for uniformity in specific output space using the low-dimensional Branin function and the high- dimensional Hartmann function as shown in Figure 5.5.

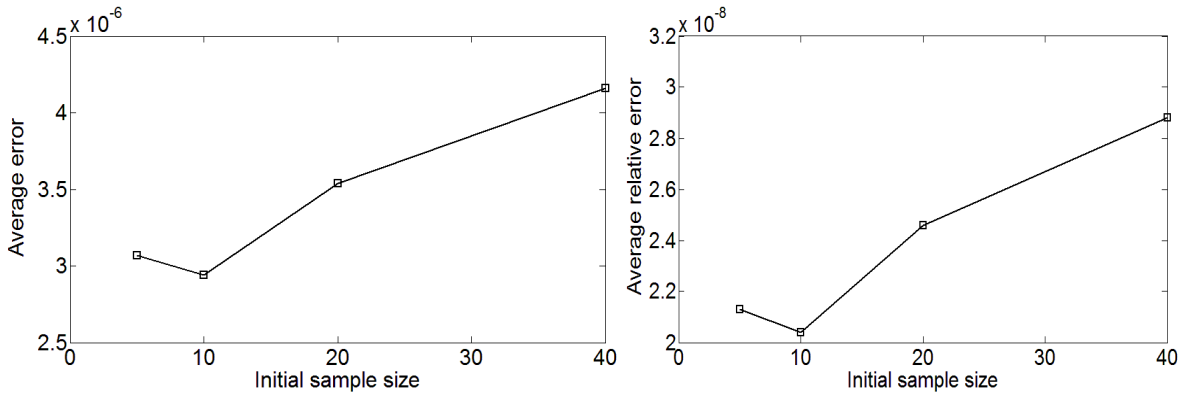

(a). Branin test function. (b). Branin test function.

Figure 5.5. Influence of initial sample size for uniformity in specific output space using kriging metamodel.

The iteration processes with different initial sample sizes and the average errors in these iterations for the low-dimensional Branin function are shown in Figure 5.6.

5.6 Applications in DMFC Modeling

In this research, adaptive metamodeling method is employed to solve engineering problems in the design of a direct methanol fuel cell (DMFC) system, which has been introduced in Chapter 3. The findings from this comparative study are used to select metamodel and initial sample size. Both the adaptive metamodeling for optimization and the adaptive metamodeling for uniformity in specific output space are considered in these case studies.

5.6.1 A Direct Methanol Fuel Cell System

As introduced in Chapter 2, the performance of a fuel cell is usually modeled by output voltage (V) measures at different current density (I) points as shown in Figure 5.7. The I-V curve for a particular fuel cell is influenced by operating parameters. In the research given in Chapter 3, four operating parameters, including temperature (T), methanol concentration (C_{ME}), methanol flow

rate (F_{ME}), and air flow rate (F_{AIR}), were considered (Yang et al., 2011). The relationship among output voltage, current density, and the four operating parameters can be defined by:

$$V = f\left(I, T, C_{ME}, F_{ME}, F_{AIR}\right) \tag{5.39}$$

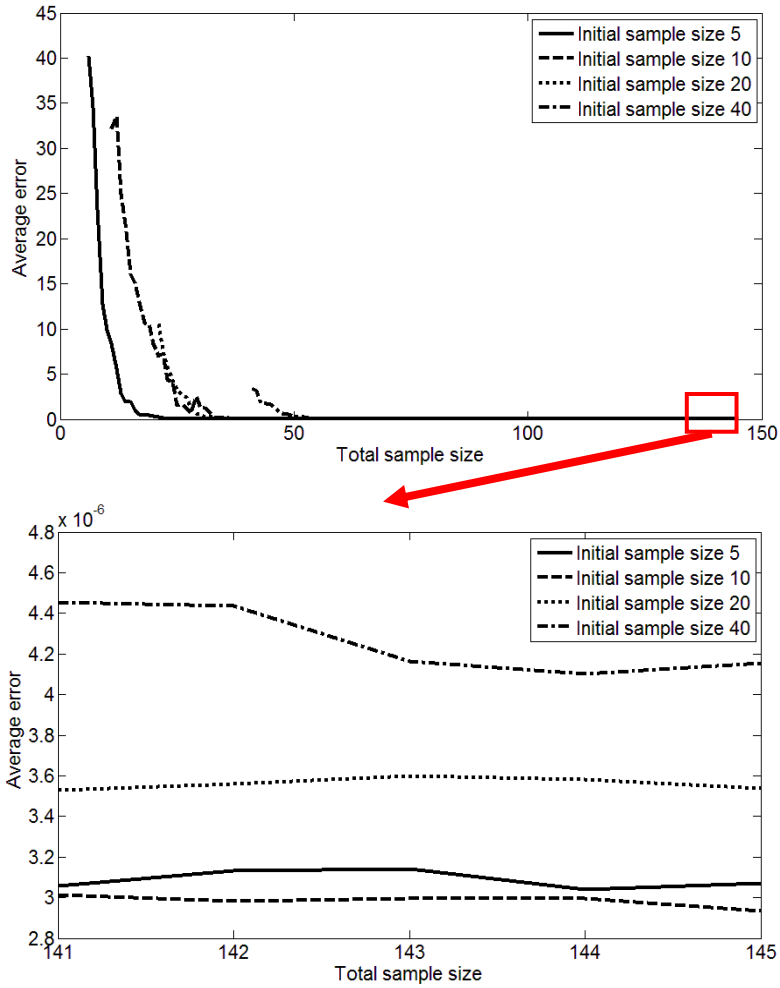

Figure 5.6. Improvement of quality of adaptive metamodeling during the iterations.

The power density, P, another important performance measure for a fuel cell, is calculated by:

$$P = VI = f\left(I, T, C_{ME}, F_{ME}, F_{AIR}\right)I \tag{5.40}$$

Modeling of the relationship in Equation (5.39), however, is a non-trivial task. Extensive experiments are usually conducted first to model the relationship among these parameters. In the research work given in Chapter 3, 45 experiments with different operating conditions were

conducted, and each experiment was used to collect around 15 voltage data at different current densities. A semi-empirical model was also developed to model the relationship (Yang et al., 2011). The samples used in the two case studies of this research are actually obtained from the semi-empirical model, rather than the experiments directly, to reduce the effort to implement these case studies. The semi-empirical model used in this work is given by:

$$
\begin{aligned}
V = {} & 1.21 - 3.7534\times10^{-5}T - 3.1534\times10^{-4}T\ln C_{ME} + 6.6200\times10^{-5}T\ln(F_{AIR}) - 0.74990 \\
& - 6.9897e^{(\frac{91691}{T}-4.6392)}I \\
& - \left[1.2658\times10^{5}I^{3} + 46196I^{2} - 4281.0I - 0.40290T - 18.8094C_{ME}^{2} + 18.8094C_{ME} + 10.496\right] \\
& \times\left[\ln I - 3.9056 + 2.9582\times10^{-4}\left(\ln(C_{ME}) + \ln(1 - \frac{1}{5.3466\times10^{7}e^{(-51824/T)}C_{ME}^{2}}I)\right)\right] \\
& - \left[-1.2687\times10^{5}I^{3} - 46221I^{2} + 4283.6I + 0.40330T + 18.818C_{ME}^{2} - 18.818C_{ME} - 10.572\right] \\
& \times\left[\ln I - 3.8959 - 8.2402\times10^{4}\ln(F_{AIR})\right] + 31.583I^{2}\ln(F_{ME})
\end{aligned}
\tag{5.41}
$$

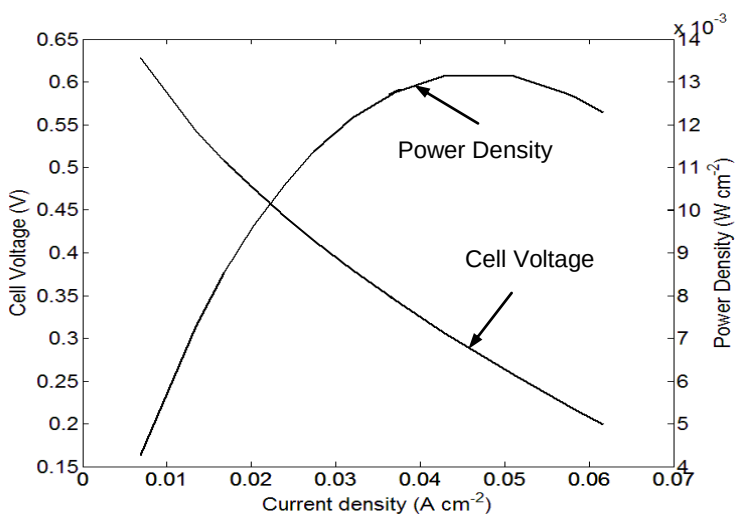

Figure 5.7. Curves to model fuel cell performances.

The five input parameters, including four operating parameters and current density, are summarized in Table 5.9.

Table 5.9. Input parameter space.

Input parameter	Symbol	Unit	Boundaries
Current density	I	A/cm^2	[0.0003, 0.08]
Temperature	T	K	[298, 343]
Methanol concentration	C_{ME}	M	[0.25, 2]
Flow rate of methanol	F_{ME}	ccm	[3.5, 5.5]
Flow rate of air	F_{AIR}	ccm	[81.2, 140.8]

5.6.2 Case Study 1: Selection of Initial Sample Size for Adaptive Metamodeling Based Optimization

The Case Study 1 focuses on identification of the appropriate initial sample size for adaptive metamodeling based optimization to improve the computation efficiency.

As shown in Figure 5.7, a maximum power density can be identified for each I-V curve. Each I-V curve is achieved based on four operating conditions. The objective of the Case Study 1 is to obtain the values of four operating parameters, such that the maximum power density for this operating condition can reach its maximum value.

In this work, 20 evenly distributed current density values from 0.0003A to 0.08A are selected for each I-V curve, and the power densities corresponding to these current densities are calculated using Equation (5.40). Among these power densities, the maximum one at the optimal current density is selected as the best solution considering this operating condition. The process to identify the optimal current density with the maximum power density for a given operating condition can be defined by an optimization problem:

$$\max_{w.r.t.I} P = \max_{w.r.t.I}(VI) = \max_{w.r.t.I}\left(f\left(I, T, C_{ME}, F_{ME}, F_{AIR}\right)I\right) \tag{5.42}$$

In Equation (5.42), the four operating parameters are considered as constants. The identified optimal current density and its corresponding maximum power density are described by I^* and P_{max}. Since one maximum power density can be identified for each operating condition, the maximum power density, P_{max}, can be defined as a function of the four operating parameters by:

$$P_{\max} = P_{\max}(T, C_{ME}, F_{ME}, F_{AIR}) \tag{5.43}$$

Therefore the problem to identify the optimal operating parameters in the case study can be defined by:

$$\max_{w.r.t.T, C_{ME}, F_{ME}, F_{AIR}} P_{\max}(T, C_{ME}, F_{ME}, F_{AIR}) \tag{5.44}$$

Based on the findings from this comparative study, the adaptive metamodeling is designed as follows.

- Since influences of noises are not considered, kriging is used as the metamodel.
- Since the optimization problem is defined by 4 input parameters, the initial sample size is selected as 4 based on the results shown in Figure 5.4.

The optimization results are summarized in Table 5.10.

Table 5.10. Optimization results.

Category	**Result**
Optimal operating parameters	T = 342.9054 K C_{ME} = 0.2515 M F_{ME} = 5.4977 ccm F_{AIR} = 140.7195 ccm
Maximum power density	P_{max}^{**} = 0.0151 W/cm^2
Initial sample size	4
Total sample size	17

The efficiency of the adaptive metamodeling with the proper initial sample size has also been compared with the two cases where the initial sizes are not selected properly, as shown in Table 5.11. Improvement of adaptive metamodeling efficiency measures have also been summarized in Table 5.11. The improvement of efficiency is defined by:

$$\eta = \frac{n - n^*}{n} \tag{5.45}$$

where n is the total size when initial sample size is not properly selected, and n^* is the sample size when initial sample size is properly selected.

Table 5.11. Improvement on efficiency of adaptive metamodeling for optimization.

Metamodeling case	Initial sample size	Total sample size	Efficiency improvement
With too small sample size	2	18	5.56%
With large sample size	8	40	57.5%

5.6.3 Case Study 2: Selection of Metamodel for Adaptive Metamodeling Considering Uniformity in Specific Output Space

The Case Study 2 focuses on selection of appropriate metamodels for adaptive metamodeling considering uniformity in a specific output space.

The objective of this case study is to obtain the metamodel such that batteries with certain voltage requirements can be designed by controlling the operating parameters. To simplify the problem, only two operating parameters, including methanol concentration, C_{ME}, and flow rate of methanol, F_{ME}, are selected as the input parameters in this case study. The cell voltage is selected as the output parameter. The other two operating parameters, the temperature, T, and the flow rate of air, F_{AIR}, and the current density, I, are selected as constants. The relationship given in Equation (5.39) is changed into:

$$V = g\left(C_{ME}, F_{ME}\right) \tag{5.46}$$

The specific cell voltage space is selected as [0.35V, 0.40V]. The cells are connected in series to form a stack to deliver the required voltage. The two constant operating parameters are selected as T = 333 K and F_{AIR}= 140.8 ccm. The current density is selected at I = 0.03 A cm^{-2}.

In adaptive metamodeling, the initial sample size is selected as 10 based on the results in Table 5.8 and Figure 5.5, and the total sample size is selected as 145. In addition, 100 evaluation points are selected to evaluate the quality of the established metamodel. The next input position in adaptive metamodeling at the ($m+1$)-th iteration is identified by:

$$\max_{w.r.t.C_{ME},F_{ME}} \; uniformity \;\; \{V_1, V_2, ..., V_m, g_m(C_{ME}, F_{ME})\} \tag{5.47}$$

In this case study, both the samples without noises and samples with noises are considered.

Samples without noises

When the samples are accurately created, kriging should be selected for metamodeling. The average error and average relative error based on kriging method are summarized in Table 5.12.

Table 5.12. Improvement of quality in adaptive metamodeling for uniform in specific output space without considering influence of noises.

Category	**Metamodel**	**Average error** $\bar{\delta}$	**Improvement in average error** $\eta_{\bar{\delta}}$	**Average relative error** $\bar{\lambda}$ **(%)**	**Improvement in relative error** $\eta_{\bar{\lambda}}$
With correctly selected metamodel	kriging	5.9000×10^{-6}	99.84%	1.67×10^{-4}	99.98%
With wrongly selected metamodel	RBF	0.0037		0.9800	

The result achieved using kriging method has been compared with the result achieved using RBF method when the wrong metamodel is selected.

Improvements in average error and average relative error are also summarized in Table 5.12. The improvement of average error is defined by:

$$\eta_{\bar{\delta}} = \frac{\bar{\delta} - \bar{\delta}^*}{\bar{\delta}} \tag{5.48}$$

where $\bar{\delta}$ is the average error when wrong metamodel is selected, and $\bar{\delta}^*$ is the average error when appropriate metamodel is selected. The improvement of average relative error is defined by:

$$\eta_{\bar{\lambda}} = \frac{\bar{\lambda} - \bar{\lambda}^*}{\bar{\lambda}} \tag{5.49}$$

where $\bar{\lambda}$ is the average relative error when wrong metamodel is selected, and $\bar{\lambda}^*$ is the average relative error when appropriate metamodel is selected.

Samples with noises

When the samples are created with noises, RBF should be selected for metamodeling. In this work, the noise factor α is selected as 0.002. The average error and average relative error based on RBF method are summarized in Table 5.13.

The result achieved using RBF method has been compared with the result achieved using kriging method when the wrong metamodel is selected. Improvements in average error and average relative error are also summarized in Table 5.13.

Table 5.13. Improvement of quality in adaptive metamodeling for uniform in specific output space considering influence of noises.

Category	**Metamodel**	**Average error $\bar{\delta}$**	**Improvement in average error $\eta_{\bar{\delta}}$**	**Average relative error $\bar{\lambda}$ (%)**	**Improvement in relative error $\eta_{\bar{\lambda}}$**
With correctly selected metamodel	RBF	0.0035	97.21%	0.9200	97.52%
With wrongly selected metamodel	kriging	0.1254		34.74	

5.7 Summary

Two adaptive metamodeling cases considering the best output point for optimization and the best fit in a specific output parameter space were considered. Three different metamodels, kriging, radial basis function and multivariate polynomial, were employed in this study. Influences of noise level of samples and initial size of samples on efficiency and accuracy of different adaptive metamodeling methods were investigated in this research through comparative study. Various test functions were used to create the sample data and evaluate the accuracy and efficiency of the adaptive metamodeling methods considering influences of noise and initial size of the samples.

The theoretical contributions and findings identified through this research are summarized as follows.

(1) A new type of adaptive metamodeling problem considering uniformity in specific output space was introduced in this research. As the uniformity in input parameter space is usually considered in the traditional metamodeling methods to improve metamodeling quality, the adaptive metamodeling methods considering uniformity in specific output space can improve the quality of metamodeling in that specific space such that better input parameter values can be identified to achieve a given target output parameter value than the traditional metamodeling methods.

(2) The influences of noise level on different adaptive metamodeling methods were studied in this research. When noise level in samples is low, kriging method is usually more efficient than RBF for adaptive metamodeling based optimization with less number of optimization iterations. Kriging method can provide better quality than RBF in adaptive metamodeling for uniformity in specific output space with smaller errors. When noise level is high, RBF is usually more efficient than kriging for adaptive metamodeling based optimization. RBF method can provide better quality than kriging in adaptive metamodeling for uniformity in specific output space with smaller errors. Multivariate polynomial method is effective when the change of the output parameter is smooth.

(3) The influences of initial sample size on different adaptive metamodeling methods were analyzed in this work. For both adaptive metamodeling for optimization and adaptive metamodeling for uniformity in specific output space, large initial sample size and too small initial sample size can lead to large total sample size. Therefore selecting of an appropriate small sample size can improve the efficiency and quality in adaptive metamodeling.

CHAPTER 6 A WEIGHTED SEQUENTIAL SAMPLING METHOD CONSIDERING INFLUENCES OF SAMPLE QUALITIES IN INPUT AND OUTPUT PARAMETER SPACES FOR GLOBAL METAMODELING AND OPTIMIZATION

6.1 Introduction

Metamodeling is an effective approach to build the relationship between input and output parameters using the sample data collected for these input and output parameters through approximation (Simpson et al., 2001). When extensive experimental and computational efforts are required to collect the sample data, efficiency and accuracy of the metamodeling methods have to be considered. The research on comparative studies of different metamodeling methods considering influencing factors has been introduced in Chapter 5. Since a metamodel is constructed using the sample data, an improvement in quality of the sample data can also lead to the improvement of quality of the metamodel.

The adaptive metamodeling is usually carried out with the process of sequential sampling. In the developed sequential sampling methods considering sample qualities in both input and output parameter spaces, contributions of the sample qualities in input and output parameter spaces are not changed in the whole adaptive metamodeling process. With the increase of sample size in adaptive metamodeling, accuracy of the constructed metamodel is also improved and the sample data are more scatted in the input parameter space. Therefore a new sequential sampling method needs to be developed to put more weight on quality of the samples in input parameter space at early iterations in the adaptive metamodeling process while to put more weight on quality of samples in output parameter space at late iterations in the adaptive metamodeling process.

The adaptive metamodeling method with sequential sampling considering different contributions of the sample qualities in input and output parameter spaces at different sampling stages is also effective to improve the quality of global optimization. The traditional adaptive metamodeling methods based on evaluation of sample quality in output parameter space can be used to identify the optimal solution efficiently. Since sample quality in the input parameter space is not considered, the constructed metamodel may only be accurate at specific locations. Therefore the true global optimal solution may not be identified properly. The objective of the research presented in this chapter is to develop a new weighted sequential sampling (WSS) method and a

two-step global optimization method based on adaptive metamodeling with weighted sequential sampling.

6.2 Comparison of Sampling Methods Considering Sample Quality in Either Input Parameter Space or Output Parameter Space

Since sample qualities in both the input and output parameter spaces are considered in the weighted sequential sampling (WSS) method, influences of sample qualities in input and output parameter spaces on quality of the metamodel are first studied considering different sampling methods and different test functions. In this research, the popular metamodeling scheme, kriging, is selected due to its high accuracy and efficiency in metamodeling. Details of the kriging method have been given in Section 5.3.2.

6.2.1 Two Sampling Methods Considering Sample Quality in Either Input or Output Parameter Space

In this research, the Latin hypercube sampling (LHS) method (McKay et al., 1979) is selected as the one considering sample quality in input parameter space, and the mean squared error (MSE) method (Jin et al., 2002) is selected as the one considering sample quality in output parameter space.

The Latin hypercube sampling (LHS) method

The basic idea for the LHS method (McKay et al., 1979) is to divide the design space C_s into n strata with equal marginal probability 1/n and then sample once from each stratum (Fang et al., 2006). The goal is to ensure that each input variable has all portions of its range represented (Jin et al., 2002). The LHS method has some obvious advantages over other sampling methods (McKay et al., 1979): its sample mean has a relatively smaller variance, it can be used for generating design points when the number of input variables is large and a great many runs are required, and it is cheap in computing and easy for implementation.

The mean squared error (MSE) method

The MSE method (Jin et al., 2002) aims at identifying the new sample point $\mathbf{x_C}$ with the largest estimation of prediction error using the relationship between the input and output parameters defined in the currently developed kriging metamodel which is constructed from the existing sample set. Suppose the mean squared error at $\mathbf{x}$ can be predicted by $s^2(\mathbf{x})$ using the metamodel, location of the next sample point, $\mathbf{x_C}$, can be achieved through an optimization process defined by:

$$\max_{w.r.t.\,\mathbf{x_C}} s^2(\mathbf{x_C}) \tag{6.1}$$

6.2.2 Test Functions

In this research, four test functions have been selected to evaluate the newly developed weighted sequential sampling method and compare it with other sampling methods. These test functions have also been used to evaluate the new global optimization method and compare it with the traditional adaptive metamodeling-based optimization method.

(1) Six-hump camel back function

$$f(x_1, x_2) = (4 - 2.1x_1^2 + \frac{x_1^4}{3})x_1^2 + x_1x_2 + (-4 + 4x_2^2)x_2^2, \quad x_1 \in [-3,3], x_2 \in [-2,2] \tag{6.2}$$

(2) Rosenbrock function

$$f(x_1, x_2) = (1 - x_1)^2 + 100(x_2 - x_1^2)^2, \quad x_1 \in [-5,10], x_2 \in [-5,10] \tag{6.3}$$

(3) Goldstein-Price function

$$\begin{aligned} f(x_1, x_2) = {} & [1 + (x_1 + x_2 + 1)^2(19 - 14x_1 + 3x_1^2 - 14x_2 + 6x_1x_2 + 3x_2^2)] \\ & \times [30 + (2x_1 - 3x_2)^2(18 - 32x_1 + 12x_1^2 + 48x_2 - 36x_1x_2 + 27x_2^2)], \\ & x_1 \in [-2,2], x_2 \in [-2,2] \end{aligned} \tag{6.4}$$

(4) Colville function (n=4)

$$
\begin{aligned}
f(x_1, x_2, x_3, x_4) = {} & 100(x_2 - x_1^2)^2 + (1 - x_1)^2 + 90(x_4 - x_3^2)^2 + (1 - x_3)^2 \\
& + 10.1((x_2 - 1)^2 + (x_4 - 1)^2) + 19.8(x_2 - 1)(x_4 - 1), \\
& x_i \in [-10,10],\ i=1,2,3,4
\end{aligned}
\tag{6.5}
$$

Selection of test functions to evaluate the influences of sample qualities in input and output parameter spaces is based on the following considerations and assumptions.

(1) When the output response surface is smooth, the sample quality in input parameter space plays an important role to influence the quality of the metamodel. When the output response surface has sharp changes, influence of the sample quality in output parameter space has to be considered.

(2) For a test function with many local optima, the sample quality in input parameter space plays an important role to scatter the sample points to well cover the regions with these local optima. For a test function with few local optima, the sample quality in output parameter space plays an important role to identify the optimal solution efficiently.

Characteristics of the four selected test functions are summarized in Table 6.1. The six-hump camel back function has six minima and two of them are global optima in the whole design space. The response surface of this function is relatively smooth. The six-hump camel back function is used to study the influence of sample quality in input parameter space. The global minimum for the Rosenbrock function lays inside a long, narrow, parabolic shaped flat valley. To find the valley is trivial due to the dramatic change of the surface shape. To converge to the global minimum of this function, however, is difficult. The Rosenbrock function is used to study the influence of sample quality in output parameter space. The Goldstein-Price function has several minima and one of these is the global minimum. The surface is flat in most of the areas and has only one sharp change. The Goldstein-Price function is used to study the influences of sample qualities in both input and output parameter spaces. All the above three 2-D test functions are also used to test the new global optimization method. The Colville function is primarily used to evaluate the new global optimization method considering large input parameter space.

Table 6.1. Test functions and their characteristics.

Test function	Number of input parameters	Output surface	Minima	Main testing purpose
Six-hump camel back	2	Smooth	6 minima, 2 global minima	Influence of sample quality in input parameter space
Rosenbrock	2	Sharp changes	Long narrow valley, 1 global minimum	Influence of sample quality in output parameter space
Goldstein-Price	2	Smooth in general with one sharp change	Several minima, 1 global minimum	Influence of sample qualities in both input and output parameter spaces
Colville	4	Sharp changes	1 global minimum	Influence of large input parameter space

6.2.3 Evaluation of the Constructed Metamodel

Quality of the constructed metamodel is evaluated by comparing the predicted output values using the metamodel and the true output values at the selected input parameter locations. To ensure this evaluation independent of the samples created using the selected sampling method, another set of samples, called *test samples*, is created to evaluate the quality of the metamodel. The Latin hypercube sampling (LHS) method is used to create the test samples. In this research, the relative prediction error (RPE) is selected for evaluating the quality of the constructed metamodel at a specific input parameter location. The RPE is defined by:

$$RPE_i = \left| \frac{\hat{y}_i - y_i}{y_i} \right|, \quad i=1,\ldots, n_t \tag{6.6}$$

where $\hat{y}_i$ is the predicted output using the metamodel, y_i is the true output in the test samples, and n_t is the number of test points. Relative errors, rather than absolute errors, are selected because the output values vary significantly with different test functions. The quality of the metamodel considering the whole design space is evaluated by the mean relative prediction error, RPE_{mean}, considering all n_t test points.

$$RPE_{mean} = \frac{1}{n_t} \sum_{i=1}^{n_t} RPE_i \tag{6.7}$$

6.2.4 Comparison between the LHS and MSE Sampling Methods Considering Sample Quality in Either Input or Output Parameter Space

The Latin hypercube sampling (LHS) method is a typical sampling method considering the sample quality in input parameter space in terms of uniformity. The mean squared error (MSE) method, on the other hand, is a typical sampling method considering the sample quality in output parameter space to minimize the prediction error. In this work, three 2-D test functions were used to compare the LHS and MSE sampling methods. The comparative study was conducted considering two cases: (1) with sufficient sample data, and (2) with limited sample data.

Comparative study with sufficient sample data

When the sample points are sufficient, an accurate metamodel can usually be constructed. In this case, selection of the right sampling method does not play an important role to the quality of the metamodel.

In this group of comparative study, the total sample sizes for both the LHS and MSE sampling methods were selected as 200. The samples for the LHS method were created at one time. For the MSE method, the initial sample size was selected as 10. Sequential sampling in the MSE method was stopped when the total number of samples reached to 200. Since the different initial samples may lead to different qualities of the constructed metamodels, each test function for the MSE method was run 10 times.

Each of the constructed metamodel was evaluated by 500 test samples which were created using the LHS method. The results of this comparative study are shown in Table 6.2.

Table 6.2. Comparison between the LHS and MSE methods using sufficient sampling points.

Test function	**Sampling method**			
	LHS		**MSE**	
	Sample size	RPE_{mean}	**Sample size**	RPE_{mean}
Six-hump camel back	n_t = 200	0.10%	n_i = 10, n_t = 200	0.13%
Rosenbrock	n_t = 200	0.33%	n_i = 10, n_t = 200	0.37%
Goldstein-Price	n_t = 200	0.23%	n_i = 10, n_t = 200	0.31%

n_i: initial sample size, n_t: total sample size

From Table 6.2, we can see that when the total sample size is large, the different sampling methods for each of the test functions lead to the similar metamodeling accuracies.

Comparative study with limited sample data

When extensive efforts are required to collect data through experiments or simulations, construction of the metamodel with the required quality using limited sample data has to be conducted. In this case, selection of the appropriate sampling method plays an important role to build the metamodel.

In this work, the comparative study considering limited sample data was conducted in the following way. First the MSE method was used to run the test function. The number of initial samples was selected as 10. In this sequential sampling process, when a new sample was obtained, this new sample was used to update the metamodel. The constructed metamodel was then evaluated using 500 test samples which were created using the Latin hypercube sampling method. The sequential sampling process was continued until the RPE_{mean} for the 500 test samples was less than 5%. The number of total samples, n_t, for a test function was then used to create the samples using the LHS method to evaluate the LHS method for the same test function. Since the different initial samples may lead to different qualities of the constructed metamodels, each test function for the MSE method was run 10 times.

Each of the constructed metamodel was further evaluated by 500 test samples which were created using the LHS method. The results of this comparative study are shown in Table 6.3. The accuracies between the LHS and MSE methods are also compared by a ratio, α, representing how much the LHS method is better than the MSE method.

$$\alpha = \frac{RPE_{mean,MSE} - RPE_{mean,LHS}}{RPE_{mean,LHS}} \tag{6.8}$$

From Table 6.3, we can see that the LHS method is considerable better than the MSE method for the six-hump camel back function. The MSE method is considerable better than the LHS method for the Rosenbrock function. For the Goldstein-Price function, the accuracy measures for the two sampling methods are comparable. The results match well with the assumptions provided in Section 6.2.2 and Table 6.1.

Table 6.3. Comparison between the LHS and MSE methods using limited sampling points.

Test function	**Sampling method**				**α**
	LHS		**MSE**		
	Sample size	RPE_{mean}	**Sample size**	RPE_{mean}	
Six-hump camelback	n_t = 75	1.07%	n_i = 10, n_t = 75	1.55%	44.8%
Rosenbrock	n_t = 47	4.78%	n_i = 10, n_t = 47	2.78%	-41.8%
Goldstein-Price	n_t = 93	2.50%	n_i = 10, n_t = 93	3.04%	21.6%

n_i: initial sample size, n_t: total sample size

This comparison between the LHS and MSE sampling methods for different test functions considering the influences of sample qualities in input and output parameter spaces serves as the foundation to introduce the new sequential sampling method, called the weighted sequential sampling (WSS) method, considering influences of the sample qualities in both the input and output parameter spaces.

6.3 The Weighted Sequential Sampling (WSS) Method

The traditional one-time sampling methods and sequential sampling methods have the following problems.

(1) In the one-time sampling methods such as the LHS method, only influences of the sample qualities in input parameter spaces are considered. In most of the sequential sampling methods such as the MSE method, only influences of the sample qualities in output parameter spaces are considered. These sampling methods may not be effective for the problems with multiple optima and dramatic changes of the output surfaces.

(2) Although some sequential sampling methods, such as the HSS method, have been developed considering influences of the sample qualities in both input and output parameter spaces, the levels of contributions of these quality measures in input and output parameter spaces are not changed during the sequential sampling processes. Since the sample quality in the input parameter space plays a more important role in early sampling stages while the sample quality in the output parameter space plays a more important role in late sampling stages, a new sequential sampling method to automatically adjust the levels of contributions of these quality measures in the input and output spaces in different sampling stages needs to be developed.

The weighted sequential sampling (WSS) method has been developed in this research to address the above two problems.

6.3.1 Principle of the Weighted Sequential Sampling (WSS) Method

In the WSS method, selection of the input parameter location for the next sample point, $\mathbf{x}_{n+1}$, is based on: (1) the quality measures in both input and output parameter spaces, and (2) the weighting factors considering importance of these quality measures.

The algorithm of the weighted sequential sampling method (WSS) is composed of 4 steps.

Step 1: The m initial samples with input parameters $\boldsymbol{x_i}$ (i=1,2,...,m) and output parameter Y_i (i=1,2,...,m) are collected to build the metamodel:

$$Y = f_m(\mathbf{x}) \tag{6.9}$$

Step 2: Suppose the sample quality in the input parameter space is evaluated by $f_i(\mathbf{x}_{n+1})$ ($f_i(\mathbf{x}_{n+1}) \in (0,1)$ from the best to the worst), and the sample quality in the output parameter space is predicted by $f_o(\mathbf{x}_{n+1})$ ($f_o(\mathbf{x}_{n+1}) \in (0,1)$ from the best to the worst), the sample quality considering both the input and output parameter spaces, $f(\mathbf{x}_{n+1})$, in the WSS method is defined by:

$$f(\mathbf{x}_{n+1}) = w_i f_i(\mathbf{x}_{n+1}) + w_o f_o(\mathbf{x}_{n+1}) \tag{6.10}$$

where w_i and w_o are two weighting factors considering importance of the sample quality measures in the input and output spaces. The next sample point is identified through optimization:

$$\underset{w.r.t.\mathbf{x}_{n+1}}{Min} \; f(\mathbf{x}_{n+1}) = \underset{w.r.t.\mathbf{x}_{n+1}}{Min} \left(w_i f_i(\mathbf{x}_{n+1}) + w_o f_o(\mathbf{x}_{n+1})\right) \tag{6.11}$$

Since both the quality measure in the input space, $f_i(\mathbf{x}_{n+1})$, and the quality measure in the output space, $f_o(\mathbf{x}_{n+1})$, need to be minimized in Equation (6.11), this optimization problem is a typical multi-objective optimization problem. The method to associate the different objective functions with weighting factors is a simple and effective way to solve the multi-objective optimization problems.

Step 3: The optimization result of $\boldsymbol{x}^*$ is then selected as the vector of input parameters for the (m+1)-th sample $\boldsymbol{x}_{m+1}$. The output Y_{m+1} corresponding to the $\boldsymbol{x}_{m+1}$ is subsequently obtained based on experiment or simulation.

Step 4: The new pair of data, ($\boldsymbol{x}_{m+1}$, Y_{m+1}), together with all the previously collected sample data are used to update the metamodel into a new relationship f_{m+1}:

$$Y = f_{m+1}(\boldsymbol{x}) \tag{6.12}$$

If the optimization criteria are satisfied, the process is stopped. If not, go to Step 2.

The two weighting factors, w_i and w_o in Equation (6.10), are determined based on the importance levels of sample qualities in input and output parameter spaces in the sequential sampling process. With the increase of the sample size, the constructed metamodel is more reliable to search for the next sample point. Therefore a large w_i and a small w_o are expected at the early stages in WSS while a small w_i and a large w_o are expected at the late stages in WSS. After the initial samples are created, w_i = 1 and w_o = 0 are first assigned. In the process of sequential sampling, the maximum prediction uncertainty calculated using Equation (6.16), which will be introduced in Section 6.3.3., is checked every time when the metamodel is updated. When the maximum prediction uncertainty is smaller than the result obtained in the last iteration, w_1 is scaled down by multiplying it with a scaling factor η between 0 and 1. The weighting factors for the $n+1$ sample, $w_{i,n+1}$ and $w_{o,n+1}$, are updated by:

$$w_{i,n+1} = \eta w_{i,n} \tag{6.13}$$

$$w_{o,n+1} = 1 - w_{i,n+1} \tag{6.14}$$

When the value of w_1 is very small (<0.01), 0 is assigned to w_1 and 1 is assigned to w_2.

In this research, the simulated annealing function called `simulannealbnd()` in Matlab R2013a global optimization toolbox was selected for obtaining the potential input parameters based on Equation (6.11).

6.3.2 Evaluation of Sample Quality Considering Input Parameter Space

The centered L2 discrepancy developed by Hickernell (1998a) is used in this work to evaluate the uniformity of the input data. The equation for calculating the centered L2 discrepancy $(CD(D_n))^2$ is given by Equation (2.12).

The quality measure $f_i(\mathbf{x}_{n+1})$ in Equation (6.10) is therefore defined by:

$$f_i(\mathbf{x}_{n+1}) = (CD(D_n))^2 \tag{6.15}$$

6.3.3 Evaluation of Sample Quality Considering Output Parameter Space

Although errors are effective measures to evaluate quality of the sampling methods using the metamodels constructed from these sampling methods with the known test functions, the actual relationships between input and output parameters are unknown in engineering applications. In this work, the statistically predicted standard deviation, instead of error, is selected to evaluate the sample quality considering the output parameter space.

For the kriging metamodeling method selected in this research, the prediction variance at a location using the developed metamodel can be calculated by (Lophaven et al., 2002):

$$\sigma_{n+1}^2 = \sigma^2\left(1 + \mathbf{u}^T\left(\mathbf{F}^T\mathbf{R}^{-1}\mathbf{F}\right)^{-1}\mathbf{u} - \mathbf{r}^T\mathbf{R}^{-1}\mathbf{r}\right) \tag{6.16}$$

where

$$\mathbf{u} = \mathbf{F}^T\mathbf{R}^{-1}\mathbf{r} - \mathbf{f} \tag{6.17}$$

σ, $\boldsymbol{F}$, $\boldsymbol{R}$, $\boldsymbol{r}$ and $\boldsymbol{f}$ in Equations (6.16) and (6.17) are the same as those in Equations (5.17)-(5.23), and σ_{n+1} in Equation (6.16) is the estimated prediction standard deviation at the input parameter location $\mathbf{x}_{n+1}$.

The quality measure $f_o(\mathbf{x}_{n+1})$ in Equation (6.10) is defined by the normalized predicted standard deviation:

$$f_o(\mathbf{x}_{n+1}) = \frac{\sigma_{n+1}}{\max\{\sigma_{n_i+1}, \sigma_{n_i+2}, \ldots, \sigma_{n+1}\}} \tag{6.18}$$

where n_i is the number of initial samples, and n is the total number of samples collected so far.

6.3.5 Comparative Studies

The newly developed weighted sequential sampling (WSS) method has been compared with the hybrid sequential sampling (HSS) method, a popular method considering sample qualities in both input and output parameter spaces. In addition, the WSS method has also been compared with the LHS and MSE methods considering sample qualities only in input or output parameter space.

The hybrid sequential sampling (HSS) method

The hybrid sequential sampling (HSS) method was introduced by Jin et al. (2002) to search for the next sample point through maximizing the product of the predicted error using the currently constructed metamodel and the minimum distance between the new sample point and the existing sample points. In our research, the predicted error used by Jin et al. (2002) is replaced by the predicted standard deviation. Therefore input location of the next sample point, $\mathbf{x}_{n+1}$, is obtained through optimization:

$$\underset{w.r.t.\mathbf{x}_{n+1}}{Max}\left(\sigma(\mathbf{x}_{n+1})\bullet dis_{\min}(\mathbf{x}_{n+1})\right) \tag{6.19}$$

where $\sigma(\mathbf{x}_{n+1})$ is the predicted standard deviation at the new sample point $\mathbf{x}_{n+1}$ based on the currently constructed metamodel and calculated using Equation (6.16), $dis_{\min}$ is the minimum distance between the new sample point $\mathbf{x}_{n+1}$ and the presently collected all sample points. Contrary to the WSS method where the weighting factors for the sample quality measures in the input and output spaces are changed during the sequential sampling process, the levels of contributions of the sample quality measures in input and output spaces in the HSS method remain the same during the whole sequential sampling process.

Comparison between the WSS method and other two sequential sampling methods, the MSE and HSS methods

The newly developed WSS method has been compared with the two popular sequential sampling methods, the MSE and HSS methods, based on computation efficiency. In this work, the total sampling size under certain accuracy requirement was used as the measure to evaluate the computation efficiency. In sequential sampling, the sample size and the modeling accuracy are

corellated. If the minmum sample size is reduced under the same accuracy requirement, when more data are sampled, the accuracy of the constructed metamodel will also be improved. In other words, improvement in metamodeling efficiency can lead to improvement in metamodeling accuracy.

For each test with a selected sequential sampling method and a test function, 10 sets of different initial sample points were created. The initial sample sizes were selected as 10 for the three 2-D test functions and 15 for the one 4-D test function. After each time of sampling for the new point, the metamodel was updated and then 500 test samples created using the LHS method were used to evaluate the constructed metamodel. When the RPE_{mean} of the 500 test samples was less than 5%, the sequential sampling process was stopped, and the total number of samples, n_t, was recorded.

The average total sampe sizes and their standard deviations for this comparative study are summarized in Table 6.4.

Table 6.4. Comparison among the MSE, HSS and WSS methods based on metamodeling efficiency.

Test function	**Sequential sampling method**								
	MSE			**HSS**			**WSS**		
	n_i	n_t	σ_t	n_i	n_t	σ_t	n_i	n_t	σ_t
Six-hump camel back	10	75	23.6	10	65	5.48	10	57	1.70
Rosenbrock	10	47	12.0	10	41	2.45	10	35	1.29
Goldstein-Price	10	93	1.96	10	92	2.06	10	87	2.32
Colville	15	171	40.5	15	189	32.1	15	142	18.5

n_i: initial sample size, n_t: average total sample size, σ_t: standard deviation of total sample size

From Table 6.4, we can see that the WSS method has higher computation efficiency than the HSS method for all the 4 test functions. The HSS and WSS methods, which consider the influences of sample qualities in both input and output parameter spaces, have better computation efficiencies than the MSE method, which considers the influence of sample quality only in output parameter space. For the six-hump camel back function which is sensitive to the influence of sample quality in the input parameter space, the HSS and WSS methods provide higher computation efficiencies than the MSE method.

Comparison between the WSS and LHS methods

The newly developed WSS method has also been compared with the one-time sampling method, the LHS method, based on metamodeling accuracy. The mean prediction error, RPE_{mean}, was selected as the accuracy measure to evaluate the WSS and LHS methods considering three 2-D test functions and one 4-D test function. For each test function, first the WSS method was used to create the metamodel. The initial sample sizes for the WSS method were selected as 10 for the three 2-D test functions and 15 for the one 4-D test function. After each time of sampling for the new point in WSS, the metamodel was updated and then 500 test samples created using the LHS method were used to evaluate the constructed metamodel. When the RPE_{mean} of the 500 test samples was less than 5%, the WSS process was stopped, and the total number of samples, n_t, was recorded. Due to the random nature in WSS, each test function was run 10 times, and the average total sample size was used as the n_t and average RPE_{mean} was recorded as the accuracy measure. The n_t was then selected as the total number of samples to build the metamodel using the LHS method. These metamodels were further evaluated using 500 new test samples which were created using the LHS method. The accuracy measures for this comparative study are summarized in Table 6.5.

Table 6.5. Comparison between the LHS and WSS methods based on metamodeling accuracy.

Test function	**Sampling method**				
	LHS		**WSS**		
	n_t	RPE_{mean}	n_i	n_t	RPE_{mean}
Six-hump camel back	57	7.13%	10	57	1.91%
Rosenbrock	35	10.4%	10	35	3.23%
Goldstein-Price	87	10.4%	10	87	3.24%
Colville	142	12.6%	15	142	4.61%

n_i: initial sample size, n_t: average total sample size, RPE_{mean}: mean relative prediction error

From Table 6.5, we can see that the WSS method provides higher metamodeling accuracies than the LHS method for all the 4 test functions.

6.4 A Two-step Global Optimization Method Based on Weighted Sequential Sampling (WSS)

Since the developed weighted sequential sampling (WSS) method can improve the accuracy and efficiency of adaptive metamodeling in the whole design space, the WSS method is employed in this research to develop a new global optimization method to improve the optimization quality.

6.4.1 The Traditional Adaptive Metamodeling-based Optimization Approach and Its Problem in Global Optimization

The traditional adaptive metamodeling-based optimization algorithm is given in Section 5.2.1. It is efficient to identify the optimal solution with small number of sample points. Due to the low accuracy of the initial metamodel, however, this optimization approach often leads to identification of a local optimum, rather than the global one, through improving the metamodeling accuracy only in a specific region by sampling data only in that region. To improve the quality of global optimization, a metamodel with good quality in the whole design space has to be constructed.

6.4.2 The Two-step Global Optimization Method

The new global optimization method based on adaptive metamodeling with weighted sequential sampling (WSS) is conducted in two steps.

Step 1: development of an accurate metamodel based on adaptive metamodeling with weighted sequential sampling

Step 2: minimization of the output parameter through adaptive metamodeling-based search with samples scattered in different regions in the input parameter space

In Step 1, first n_i initial samples are created using the LHS method and these samples are used to build an initial metamodel. Then the WSS method is employed to build the metamodel with a total of n_t samples considering the quality in the whole design space. Details to build an accurate metamodel based on adaptive metamodeling with weighted sequential sampling (WSS) method have been well discussed in Section 6.3.

In Step 2, adaptive metamodeling-based optimization is conducted to minimize the value of the output parameter. The method introduced in Section 6.4.1 can be employed for this purpose.

To further improve the global optimization quality by preventing the solution from falling into a local optimum, the quality measure considering input parameter space can be incorporated into the optimization objective function. In this work, uniformity is used to evaluate the sample quality in the input parameter space to ensure the samples are well scatted in different regions in the input parameter space such that the true global optimum cannot be missed. Suppose the output parameter of the new sample at $\mathbf{X_{m+1}}$ can be calculated using the metamodel constructed with the m samples by:

$$Y = f_m\left(\mathbf{X}_{m+1}\right) \tag{6.20}$$

and the quality of samples in the input parameter space is defined by the centered L2 discrepancy:

$$f_i(\mathbf{x}_{m+1}) = (CD(D_m))^2 \tag{6.21}$$

the objective function in the traditional adaptive metamodeling-based optimization given in Equation (5.4) can then be modified to:

$$\min_{w.r.t.\,\mathbf{X}_{m+1}} \left[w_m f_m\left(\mathbf{X}_{m+1}\right) + w_i f_i(\mathbf{x}_{m+1})\right] \tag{6.22}$$

where w_m and w_i are weighting factors considering the importance of the optimization objective function, $f_m(\mathbf{X_{m+1}})$, and the uniformity of the samples in input parameter space, $f_i(\mathbf{X_{m+1}})$, for the new sample at $\mathbf{X_{m+1}}$. During the optimization process, value of w_m is increased and value of w_i is decreased using a similar method given in Equations (6.13) and (6.14).

6.4.3 Comparative Studies

The developed two-step global optimization method introduced in Section 6.4.2 has been compared with the traditional adaptive metamodeling-based optimization method given in Section 6.4.1 using the four test functions to demonstrate its effectiveness in global optimization.

Optimization with the traditional adaptive metamodeling-based optimization method

The traditional adaptive metamodeling-based optimization approach introduced in Section 6.4.1 is efficient to identify the optimal solution with small number of sample points. Since quality of the samples in input parameter space is not considered, a local optimum, rather than the global one, is often achieved. The conditions and failure rates for global optimization using the traditional adaptive metamodeling based-optimization method considering the four test functions are summarized in Table 6.6. In these optimization processes, the initial sample sizes were selected as 10 for the three 2-D test functions and 15 for the one 4-D test function. The optimization process was stopped when change of the output parameter value in five consecutive iterations was less than 0.05. Since different initial samples may lead to different solutions, each 2-D test function was run 10 times and the 4-D test function was run 5 times.

Table 6.6. Failure rates with the traditional metamodeling based optimization method.

Test function	Initial sample size	Test times	Failure rate to obtain the global optimum
Six-hump camel back	10	10	0%
Rosenbrock	10	10	20%
Goldstein-Price	10	10	0%
Colville	15	5	100%

From Table 6.6, we can see that for the test functions with simpler shapes such as the six-hump camel back function and the Goldstein-Price function, the true global optima can be identified. For the Rosenbrock function, the true global optimum sometimes cannot be identified properly with 20% of the failure rate. The Rosenbrock function is a classical optimization test function, of which the global optimum lays inside a long, narrow, parabolic shaped flat valley and is difficult to reach (Molga and Smutnicki, 2005). For the 4-D Colville function, the global optimum cannot be identified with 100% of the failure rate.

Global optimization with the two-step global optimization method

The two-step global optimization approach introduced in Section 6.4.2 aims at improving the quality of global optimization by first constructing a relatively accurate metamodel and then searching for the new solution by incorporating the sample uniformity in input parameter space

into the optimization objective function. Since the sample data used to construct the metamodel are well scattered in different regions of the input parameter space, the true global optimum has less chance to be missed in the search process. Table 6.7 shows the conditions and failure rates for global optimization using the newly developed two-step global optimization method.

Table 6.7. Failure rates with the two-step global optimization method.

Test function	Initial sample size in Step 1	Total sample size in Step 1	Test times	Failure rate to obtain the global optimum
Six-hump camel back	10	57	10	0%
Rosenbrock	10	35	10	0%
Goldstein-Price	10	87	10	0%
Colville	15	142	5	0%

In Step 1 of these optimization processes, the initial sample sizes were selected as 10 for the three 2-D test functions and 15 for the one 4-D test function. The accurate metamodel for each test function was constructed using the adaptive metamodeling method with WSS introduced in Section 6.3. After each time of sampling for a new point in WSS, the metamodel was updated and then 500 test samples created using the LHS method were used to evaluate the constructed metamodel. When the RPE_{mean} of the 500 test samples was less than 5%, the WSS process was stopped, and the total number of samples, n_t, was recorded.

In Step 2, adaptive metamodeling based-optimization was employed to identify the point with the minimum output. The optimization process was stopped when change of the output parameter value in five consecutive iterations was less than 0.05. In this work, each 2-D test function was run 10 times and each 4-D test function was run 5 times.

From Table 6.7, we can see that in addition to the test functions with simpler shapes such as the six-hump camel back function and the Goldstein-Price function, the two-step global optimization method is effective in global optimization for the 2-D Rosenbrock function with relatively complicated shape and the 4-D Colville function with large input parameter space.

In this comparative study, the initial samples that led to the seven failure cases given in Table 6.6 were used in the two-step global optimization. The identified global optima for these cases are

shown in Table 6.8. From this table, we can see that the two-step global optimization method is effective to achieve the global optima with high quality.

Table 6.8. Comparison between the results of the two optimization methods.

Test function	True global optimum	Test No.	Optimum value found by the adaptive metamodel-based optimization method	Optimum value found by the two-step global optimization method
Rosenbrock	0.0	Test 4	3.9542	0.0012
		Test 10	0.5934	0.0033
Colville	0.0	Test 1	0.5655	0.0186
		Test 2	6.4320	0.0027
		Test 3	6.8199	0.0521
		Test 4	4.9155	0.0051
		Test 5	27.2019	0.0665

6.5 Applications in Modeling of a DMFC System

In this research, the WSS method was used to construct accurate metamodels to describe the relationships between operating parameters and performance measures of a direct methanol fuel cell (DMFC) system. The two-step global optimization method was employed to identify the best global operating conditions for the DMFC system.

6.5.1 An Accurate Metamodel to Describe the Relationship between Operating Parameters and Maximum Power Density through Weighted Sequential Sampling

The direct methanol fuel cell system was introduced in Chapter 3 and Section 5.6.1. The relationship between the four operating parameters and the maximum power density output is described by the metamodel. The adaptive metamodeling with weighted sequential sampling (WSS) method was used in this work to improve metamodeling quality in the whole design space.

As shown in Figure 5.7, a maximum power density can be identified for each I-V curve. Each I-V curve is achieved based on four operating conditions. Therefore when values of the four operating parameters are provided, a maximum power density can be obtained from these four operating parameters. In this case study, a metamodel was used to describe the relationship between the four operating parameters and the maximum power density.

In this work, 20 evenly distributed current density values from 0.0003A to 0.08A were selected for each I-V curve, and the power densities corresponding to these current densities were calculated using Equations (5.40) and (5.41). Among these power densities, the maximum one at the optimal current density was selected as the maximum power density output considering this operating condition. Since one maximum power density can be identified for each operating condition, the maximum power density, P_{max}, can be defined as a function of the four operating parameters by:

$$P_{\max} = P_{\max}(T, C_{ME}, F_{ME}, F_{AIR}) \tag{6.23}$$

Kriging scheme was used to build the metamodel for describing the relationship between the four operating parameters and the maximum power density output. Three sequential sampling methods, the MSE, HSS and WSS methods, were used for collecting data points. For all these three sequential sampling methods, the initial sample size was selected as 15. At each iteration in the sequential sampling process, a constructed metamodel was evaluated by 500 test samples which were created using the LHS method. A sequential sampling process was stopped when the mean relative prediction error of these 500 test points, RPE_{mean}, was less than 0.05. These three sequential sampling methods were evaluated based on the total sample sizes considering the computation efficiency. These total sample sizes for the three sequential sampling methods are summarized in Table 6.9.

Table 6.9. Comparison among the MSE, HSS and WSS methods considering metamodeling efficiency.

Metamodeling relation	**Sampling method**					
	MSE		**HSS**		**WSS**	
	n_i	n_t	n_i	n_t	n_i	n_t
$P_{\max} = P_{\max}(T, C_{ME}, F_{ME}, F_{AIR})$	15	74	15	79	15	27

n_i: initial sample size, n_t: total sample size

From Table 6.9, we can see that the WSS method has a much higher computation efficiency than the MSE and HSS methods to obtain the accurate metamodels to describe the relationships between the four operating parameters and the maximum power density measure.

The WSS method has also been compared with the LHS method considering metamodeling accuracy. In this work, first the WSS method was used to get the metamodel with a total of 27

samples. Then the LHS method was used to create 27 samples to build another metamodel. These two metamodels were further evaluated by 500 test samples. The RPE_{mean} measures of these 500 test sample points for the LHS and WSS methods were then compared. The RPE_{mean} measures for these two methods are given in Table 6.10.

Table 6.10. Comparison between the LHS and WSS methods considering metamodeling accuracy.

Metamodeling relation	Sampling method				
	LHS		WSS		
	n_t	RPE_{mean}	n_i	n_t	RPE_{mean}
$P_{\max} = P_{\max}(T, C_{ME}, F_{ME}, F_{AIR})$	27	0.70%	15	27	0.61%

n_i: initial sample size, n_t: total sample size

From Table 6.10, we can see that the WSS method provides better modeling accuracy than the LHS method.

6.5.2 Identification of the Optimal Operating Parameters to Achieve the Maximum Power Density Using the Two-step Global Optimization Method

The metamodel in Step 1 was constructed with 15 inial sample points and 27 total sample points, as explained in Section 6.5.1. In Step 2, adaptive metamodeling based-optimization approach was employed to obtain the optimal operarting parameter values. The optimization process was stopped when change of five consecutive output measures was smaller than 0.0005. The optimization results are shown in Table 6.11.

Table 6.11. Optimization of the DMFC operating parameters.

Objective function	The optimal input operating parameters				The optimal output parameter
$P_{\max} = P_{\max}(T, C_{ME}, F_{ME}, F_{AIR})$	T	C_{ME}	F_{ME}	F_{AIR}	P_{max}
	342.9 K	0.2500 M	5.500 ccm	140.7 ccm	0.0151W/cm^{-2}

6.6 Summary

A new sequential sampling method, namely weighted sequential sampling (WSS) method, was introduced in this research to improve accuracy and efficiency of adaptive metamodeling considering the different levels of contributions of the sample qualities in input and output

parameter spaces at different stages in the sequential sampling process. The WSS method was employed in the development of a new global optimization method, namely two-step global optimization method, by incorporating the uniformity measure in input parameter space into the optimization process to ensure the sample points are scattered in different regions of the input parameter space.

The contributions and findings through this research are summarized as follows.

(1) As different problems have different relationships between input and output parameters, the influences of sample qualities in input and output parameter spaces on the quality of the metamodel constructed through adaptive metamodeling approach may be different. Thus different sampling methods need to be selected. For the surface with smooth shape and many local optima, the sample quality in the input parameter space plays a more important role. In this case, the sampling methods considering sampling qualities in input parameter spaces, such as the LHS method, should be selected. For the surface with sharp shape and few local optima, the sample quality in the output parameter space plays a more important role. In this case, the sampling methods considering sampling qualities in output parameter spaces, such as the MSE method, should be selected.

(2) The quality measures in input and output parameter spaces at different stages in the sequential sampling process have different magnitudes of contributions. The sample quality in input parameter space plays a more significant role in early sampling stages while the sample quality in output parameter space plays a more significant role in late sampling stages. The newly developed WSS method, which considers both sample qualities in input and output parameter spaces while updating the weighting factors of these quality measures during the sequential sampling process, provides better accuracy and efficiency than the HSS method which also uses the sample qualities in input and output parameter spaces for guiding selection of the new samples without considering the different levels of contributions of these measures at different sampling stages.

(3) The newly developed two-step global optimization method can improve the quality of global optimization. In the first step, an accurate metamodel considering influences of both input and output parameter spaces is developed. Searching for the optimal points by

incorporating the uniformity measure in input parameter space into the optimization objective function is conducted in the second step to ensure that the sample points are well scatted in the input parameter space to prevent the solution from falling into a local optimum.

CHAPTER 7 CONCLUSIONS AND FUTURE WORK

7.1 Conclusions

7.1.1 Summary of This Research

As stated in Chapter 1, the interests on research and applications of direct methanol fuel cell (DMFC) have grown significantly over the recent years. Modeling of fuel cell systems plays an important role for the optimal design and operation of the fuel cell systems. In the presently developed directly methanol fuel cell modeling methods, however, only some of the important operating parameters and simplified geometric structures were considered. In addition, since extensive efforts for experiments and simulations are usually required to build the DMFC models and achieve the DMFC behaviors, effective modeling tools also need to be developed to improve the quality and efficiency in DMFC modeling. To solve these problems, this research work focused on two aspects: (1) modeling of direct methanol fuel cell systems, and, (2) development of adaptive metamodeling methods to improve efficiency and quality for modeling and optimization of DMFC systems.

<u>(1) Modeling of direct methanol fuel cell systems considering both design and operating parameters</u>

<u>(1.1) Development of a semi-empirical model to describe the relationships between operating parameters and performance behaviors of a direct methanol fuel cell system</u>

A systematic approach to model the relationships between the operating parameters and the direct methanol fuel cell performance was introduced in this work and explained in Chapter 3. Four operating parameters, including temperature, methanol concentration, flow rate of methanol, and flow rate of air are considered in this approach. A semi-empirical model was developed to describe the relationships. Experiments were designed and conducted to obtain the coefficients in the semi-empirical model. The accuracy of this semi-empirical model was also analyzed. In addition, the influences of the operating parameters and possible applications of the semi-empirical model were also discussed.

(1.2) Development of a CFD model with semi-empirical electrochemical relationships to study the influences of geometric and operating parameters on DMFC performance

A three-dimensional computational fluid dynamics (CFD) model, as explained in Chapter 4, has been developed through collaboration with Biao Yu, a visiting Ph.D. student at University of Calgary, to study the influences of geometric and operating parameters on the performance of DMFC (Yu et al., 2013). In this model, the electrochemical behaviors are described by semi-empirical relationships. Coefficients for these semi-empirical relationships are obtained using adaptive metamodeling based on data collected from experiments. Two geometric configurations with serpentine channels at the anode and cathode are considered for CFD simulation. My work in the development of the CFD model focuses on the adaptive modeling aspect, while Biao Yu's work focuses on the CFD modeling aspect.

(2) Improvement of accuracy and efficiency of adaptive metamodeling methods

(2.1) Comparative study on influencing factors in adaptive metamodeling

Influences of noise level of samples and initial size of samples on efficiency and quality of different adaptive metamodeling methods were investigated in Chapter 5 through comparative study. Two adaptive metamodeling cases considering the best output point for optimization and the best fit in a specific output parameter space were considered. Three different metamodels, kriging, radial basis functions (RBF) and multivariate polynomial, were employed in this study for comparison. Various test functions were used to create the sample data and evaluate the quality and efficiency of the adaptive metamodeling methods with different noises and initial sizes of the samples. The research results have also been applied to the modeling of a DMFC system

(2.2) Development of a weighted sequential sampling method considering influencing factors of sample qualities in input and output parameter spaces for global optimization

A new weighted sequential sampling (WSS) method was introduced in this research to improve accuracy and efficiency of adaptive metamodeling considering the different levels of contributions of the sample qualities in input and output parameter spaces at different stages in the sequential sampling process. Based on the accurate metamodel built with WSS method, a

new global optimization method, namely two-step global optimization method, was developed by incorporating the uniformity measure in input parameter space into the optimization process to ensure the sample points are scattered in different regions of the input parameter space. The developed methods have been used to identify the optimal operating parameters of a DMFC system.

7.1.2 Research Contributions

Through this study, the problems in DMFC modeling, adaptive metamodeling and applications of adaptive metamodeling methods in DMFC system design have been examined. The major contributions from this research are summarized as follows.

(1) Modeling of direct methanol fuel cell systems

- Modeling of all important operating parameters for optimal DMFC system control

  A semi-empirical model, which is effective to describe the relationships between the operating parameters and the direct methanol fuel cell performance, is introduced. Through an analysis of the influences of operating parameters on the DMFC performance based on the semi-empirical model, a better understanding of the DMFC behaviors has been achieved. In addition, the influences of the four operating parameters on the open circuit voltage, resistance polarization, activation polarization and concentration polarization were also achieved. The modeling of the relationships between the operating parameters and the DMFC performance measures provides a basis to identify the optimal operating parameters of the DMFC system considering different power requirements.

- Modeling of both operating parameters and design parameters for optimal DMFC system design

  CFD is an effective tool to model the relationships between geometric/operating parameters and DMFC performance. In the CFD model, the electrochemical behavior near the membrane can be described by semi-empirical relationships. The efficiency to obtain the values of coefficients in the semi-empirical relationships can be improved through adaptive metamodeling. The developed CFD model with semi-empirical electrochemical relationships

can be used to predict performance based on the geometric and operating parameters. This model also provides a platform for the optimal design and control of DMFC systems. My work in the development of the CFD model focuses on the adaptive modeling aspect, while Biao Yu's work focuses on the CFD modeling aspect.

(2) Adaptive metamodeling considering accuracy and efficiency

- Selection of the adaptive metamodeling method considering characteristics of the selected application

  A new type of adaptive metamodeling problem considering uniformity in specific output space was introduced in this research. Compared to the traditional metamodeling methods where uniformity in input parameter space is considered to improve metamodeling quality, the adaptive metamodeling considering uniformity in specific output space can improve the quality of metamodeling in that specific space to identify better input parameter values for obtaining a given target output parameter value.

  The influences of noise level and initial sample size on different adaptive metamodeling methods were studied in this research. When noise level in samples is low, kriging method is usually more efficient than RBF for adaptive metamodeling based optimization with less number of optimization iterations. Kriging method can provide better quality than RBF in adaptive metamodeling for uniformity in specific output space with smaller errors. When noise level is high, RBF is usually more efficient than kriging for adaptive metamodeling based optimization. RBF method can provide better quality than kriging in adaptive metamodeling for uniformity in specific output space with smaller errors. Multivariate polynomial method is effective when the change of the output parameter is smooth. As to initial sample, for both adaptive metamodeling for optimization and adaptive metamodeling for uniformity in specific output space, large initial sample size and too small initial sample size can lead to large total sample size. Therefore selection of an appropriate small sample size can improve the efficiency and quality in adaptive metamodeling.

- Sequential sampling for adaptive metamodeling considering qualities in both the input and output parameter spaces

  For different problems with different relationships between input and output parameters, sample qualities in input and output parameter spaces have different influences on the quality of the metamodel constructed through adaptive metamodeling approach with different sampling methods. For the surface with smooth shape and many local optima, the sample quality in the input parameter space plays a more significant role. In this case, the sampling methods considering sampling qualities in input parameter spaces, such as the Latin hypercube sampling (LHS) method, should be selected. For the surface with sharp shape and few local optima, the sample quality in the output parameter space plays a more significant role. In this case, the sampling methods considering sampling qualities in output parameter spaces, such as the mean squared error (MSE) method, should be selected.

  The newly developed weighted sequential sampling (WSS) method, which considers both sample qualities in input and output parameter spaces while updating the weighting factors of these quality measures during the sequential sampling process, provides better accuracy and efficiency than the hybrid sequential sampling (HSS) method which also uses the sample qualities in input and output parameter spaces for guiding selection of the new samples without considering the different levels of contributions of these measures at different sampling stages. With the accurate metamodel built using the WSS methods, the newly developed two-step global optimization method can be used to search for the optimal points by incorporating the uniformity measure in input parameter space into the optimization objective function to ensure the sample points are well scatted in the input parameter space to prevent the solution from falling into a local optimum.

7.2 Future Work

Many problems are still left unsolved in modeling of fuel cell systems as well as in adaptive metamodeling considering modeling accuracy and efficiency. The major issues that need to be addressed in our future work are summarized as follows.

7.2.1 Modeling of direct methanol fuel cell systems

- Our current semi-empirical model is limited to the TekStak^{TM} DMFC. When the semi-empirical model for a different DMFC is required, new experiments need to be conducted to obtain the coefficient values of the semi-empirical model.
- To improve the CFD model that describes the relationships between geometric/operating parameters and performance measures, experiments considering significantly different levels of geometric and operating parameters should be conducted to better fit the CFD model for optimal geometric design and optimal operating condition control.

7.2.2 Adaptive metamodeling considering accuracy and efficiency

- Due to the complexity of adaptive metamodeling problems, the results achieved in the comparative study only provide guidelines to make decisions, such as to select the metamodel and initial sample size, for solving engineering problems based on adaptive metamodeling approach. This comparative study can be further improved by considering more influencing factors, metamodel schemes, and test functions with different dimensions.
- For problems with large dimensions of input parameters, the weighted sequential sampling method is low in computation efficiency compared with other popular methods such as the Latin hypercube sampling method. Therefore further improvement of the computation efficiency is required for the WSS method.

REFERENCES

Akaike, H. (1974). "A new look at the statistical model identification." *IEEE Transactions on Automatic Control*, Vol. 19, No. 6, pp. 716-723.

Antony J. (2003). *Design of experiments for engineers and scientists*. Butterworth-Heinemann.

Argyropoulos, P., Scott, K., Shukla, A. K. and Jackson, C. (2003). "A semi-empirical model of the direct methanol fuel cell performance – Part I: model development and verification." *Journal of Power Sources*, Vol. 123, No. 2, pp. 190-199.

Arisetty, S., Jacob, C. A., Prasad, A. K. and Advani, S. G. (2009). "Regulating methanol feed concentration in direct methanol fuel cells using feedback from voltage measurements." *Journal of Power Sources*, Vol. 187, No. 2, pp. 415-421.

Atkinson, A. C. and Donev, A. N. (1992). *Optimum Experimental Designs*. Oxford University Press.

Barton, R. R. (1992). "Metamodels for simulation input-output relations." In: *Proceedings of the 24th Conference on Winter Simulation*, Arlington, VA, USA, pp. 289-299.

Baxter, S. F., Battaglia, V. S. and White, R. E. (1999). "Methanol fuel cell model: anode." *Journal of the Electrochemical Society*, Vol. 146, No. 2, pp. 437-447.

Birgersson, E., Nordlund, J., Ekström, H., Vynnycky, M. and Lindbergh, G. (2003). "Reduced two-dimensional one-phase model for analysis of the anode of a DMFC." *Journal of the Electrochemical Society*, Vol. 150, No. 10, pp. 1368-1376.

Birgersson, E., Nordlund, J., Vynnycky, M., Picard, C. and Lindbergh, G. (2004). "Reduced two-phase model for analysis of the anode of a DMFC." *Journal of the Electrochemical Society*, Vol. 151, No. 12, pp. 2157-2172.

Busby, D., Farmer, C. L. and Iske, A. (2007). "Hierarchical nonlinear approximation for experimental design and statistical data fitting." *SIAM Journal on Scientific Computing*, Vol. 29, No. 1, pp. 49-69.

Celik, S. and Mat, M. D. (2010). “Measurement and estimation of species distribution in a direct methanol fuel cell.” *International Journal of Hydrogen Energy*, Vol. 35, No. 5, pp. 2151- 2159.

Chen, V. C. P., Tsui, K. L., Barton, R. R. and Meckesheimer, M. (2006). “A review on design, modeling and applications of computer experiments.” *IIE Transactions*, Vol. 38, No. 4, pp. 273-291.

Crombecq, K. (2011). Surrogate Modelling of Computer Experiments with Sequential Experimental Design. Ph.D. Thesis, University of Antwerp, Belgium.

Crombecq, K., Gorissen, D., Deschri, D. and Dhaene, T. (2011). “A novel hybrid sequential design strategy for global surrogate modeling of computer experiments.” *SIAM Journal on Scientific Computing*, Vol. 33, No. 4, pp. 1948-1974.

Danilov, V. A., Lim, J., Moon, I. and Chang, H. (2006). “Three-dimensional, two-phase, CFD model for the design of a direct methanol fuel cell.” *Journal of Power Sources*, Vol. 162, No. 2, pp. 992-1002.

Dillon, R., Srinivasan, S., Arico, A. S. and Antonucci, V. (2004). “International activities in DMFC R&D: status of technologies and potential applications.” *Journal of Power Sources*, Vol. 127, Nos. 1-2, pp. 112-126.

Divisek, J., Fuhrmann, J., Gärtner, K. and Jung, R. (2003). “Performance modeling of a direct methanol fuel cell.” *Journal of the Electrochemical Society*, Vol. 150, No. 6, pp. 811-825.

Dohle, H. and Wippermann, K. (2004). “Experimental evaluation and semi-empirical modeling of U/I characteristics and methanol permeation of a direct methanol fuel cell.” *Journal of Power Sources*, Vol. 135, Nos. 1-2, pp. 152-164.

Fang, K. T. (1980). “The uniform design: application of number-theoretic methods in experimental design.” *Acta Mathematicae Applagatae Sinica*, Vol. 3, pp. 363-372.

Fang, K. T., Li, R. and Sudjianto, A. (2006). *Design and Modeling for Computer Experiments*. Chapman & Hall/CRC.

Fang, K. T., Lin, D. K. J., Winker, P. and Zhang, Y. (2000). “Uniform design: theory and applications.” *Technometrics*, Vol. 42, No. 3, pp. 237-248.

Fang, K. T., Shui, W. C. and Pan, J. X. (1999). “Uniform design based on Latin squares.” *Statistica Sinica*, Vol. 9, No. 3, pp. 905-912.

Fang, Y. (1995). “Relationships between uniform design and orthogonal design.” In: *Proceedings of the 3rd International Chinese Statistical Association Statistical Conference*, Beijing, China.

Ge, J. and Liu, H. (2005). “Experimental studies of a direct methanol fuel cell.” *Journal of Power Sources*, Vol. 142, Nos. 1-2, pp. 56-59.

Ge, J. and Liu, H. (2006). “A three-dimensional mathematical model for liquid-fed direct methanol fuel cells.” *Journal of Power Sources*, Vol. 160, No. 1, pp. 413-421.

Ge, J. and Liu, H. (2007). “A three-dimensional two-phase flow model for a liquid-fed direct methanol fuel cell.” *Journal of Power Sources*, Vol. 163, No. 2, pp. 907-915.

Gramacy, R. B. and Lee, H. K. H. (2009). “Adaptive design and analysis of supercomputer experiments.” *Technometrics*, Vol. 51, No. 2, pp. 130-145.

Guo, H. and Ma, C. F. (2004). “2D analytical model of a direct methanol fuel cell.” *Electrochemistry Communications*, Vol. 6, No. 3, pp. 306-312.

Hannan, E. J. and Quinn, B. G. (1979). “The determination of the order of autoregression.” *Journal of the Royal Statistical Society: Series B (Methodological)*, Vol. 41, No. 2, pp. 190-195.

Hardy, R. L. (1971). “Multiquadratic equations of topography and other irregular surfaces.” *Journal of Geophysical Research*, Vol. 76, No. 1, pp. 1905-1915.

Hassing, P. M., Fang, H. and Wang, Q. (2010). “Identification of material parameters for McGinty’s model using adaptive RBFs and optimization.” *Structural and Multidisciplinary Optimization*, Vol. 42, No. 2, pp. 233-242.

He, Y. L., Li, X. L., Miao, Z. and Liu, Y. W. (2009). “Two-phase modeling of mass transfer characteristics of a direct methanol fuel cell.” *Applied Thermal Engineering*, Vol. 29, No. 10, pp. 1998-2008.

Hickernell, F. J. (1998a). “A generalized discrepancy and quadrature error bound.” *Mathematics of Computation*, Vol. 67, No. 221, pp. 299-322.

Hickernell, F. J. (1998b). “Lattice rules: how well do they measure up?” In: P. Bickel (Ed.). *Random and Quasi-Random Point Sets*, Springer-Verlag, pp. 109–166.

Hickernell, F. J. and Liu, M. Q. (2002). “Uniform designs limit aliasing.” *Biometrika*, Vol. 89, No. 4, pp. 893-904.

Hua, L. K. and Wang, Y. (1981). *Applications of Number Theory to Numerical Analysis*. Springer-Verlag.

Jeng, K. T. and Chen, C. W. (2002). “Modeling and simulation of a direct methanol fuel cell anode.” *Journal of Power Sources*, Vol. 112, No. 2, pp. 367-375.

Jeong, S., Murayama, M. and Yamamoto, K. (2005). “Efficient optimization design method using kriging Model.” *Journal of Aircraft*, Vol. 42, No. 2, pp. 413-420.

Jin, R., Chen, W. and Simpson, T. W. (2001). “Comparative studies of metamodelling techniques under multiple modeling criteria.” *Structural and Multidisciplinary Optimization*, Vol. 23, No. 1, pp. 1-13.

Jin, R., Chen, W. and Sudjianto, A. (2002). “On sequential sampling for global metamodeling in engineering design.” In: *Proceedings of the ASME 2002 Design Engineering Technical Conferences and Computer and Information in Engineering Conference*. Montreal, Quebec, Canada.

Johnson, M. E., Morre, L. M. and Ylvisaker, D. (1990). “Minimax and maximum distance designs.” *Journal of Statistical Planning and Inference*, Vol. 26, No. 2, pp. 131-148.

Jones, D. R., Schonlau, A. and Welch, W. J. (1998). “Efficient global optimization of expensive black-box functions.” *Journal of Global Optimization*, Vol. 13, No. 4, pp. 455-492.

Kleijnen, J. P. C. (1987). *Statistical Tools for Simulation Practitioners*. Marcel Dekker.

Ko, J., Chippar, P. and Ju, H. (2010). “A one-dimensional, two-phase model for direct methanol fuel cells - part I: model development and parametric study.” *Energy*, Vol. 35, No. 5, pp. 2149-2159.

Korobov, N. M. (1959). “The approximate computation of multiple integrals.” *Doklady Akademii Nauk SSSR*, Vol. 124, pp. 1207-1210.

Krige, D. G. (1951). *A Statistical Approach to Some Mine Valuations and Allied Problems at the Witwatersrand*. Master Thesis, University of Witwatersrand, South Africa.

Kulikovsky, A. A. (2000). "Two-dimensional numerical modelling of a direct methanol fuel cell." *Journal of Applied Electrochemistry*, Vol. 30, No. 9, pp. 1005-1014.

Larminie, J. and Dicks, A. (2003). *Fuel Cell Systems Explained*, 2nd Ed. John Wiley & Sons.

Le, A. D. and Zhou, B. (2008). "A general model of proton exchange membrane fuel cell." *Journal of Power Sources*, Vol. 182, No. 1, pp. 197-222.

Li, G., Aute, V. and Azarm, S. (2010a). "An accumulative error based adaptive design of experiments for offline metamodeling." *Structural and Multidisciplinary Optimization*, Vol. 40, Nos. 1-6, pp. 137-155.

Li, M., Li, G. and Azarm, S. (2008). "A kriging metamodel assisted multi-objective genetic algorithm for design optimization." *Journal of Mechanical Design, ASME Transactions*, Vol. 130, No. 3.

Li, Y. F., Ng, S. H., Xie, M. and Goh, T. N. (2010b). "A systematic comparison of metamodeling techniques for simulation optimization in decision support systems." *Applied Soft Computing*, Vol. 10, No. 4, pp. 1257-1273.

Lin, Y. (2004). *An Efficient Robust Concept Exploration Method and Sequential Exploratory Experimental Design*. Ph.D. Thesis, Georgia Institute of Technology, USA.

Liu, W. and Wang, C. Y. (2007). "Electron transport in direct methanol fuel cells." *Journal of Power Sources*, Vol. 164, No. 2, pp. 561-566.

Liu, Y., Chen, Y., Cheng, J. H. and Lu, J. J. (2011). "An adaptive sampling method based on optimized sampling design for fishery – independent surveys with comparisons with conventional designs." *Fisheries Science*, Vol. 77, No. 4, pp. 467-478.

Lophaven, S. N., Nielsen, H. B. and Søndergaard, J. (2002). "DACE - A matlab kriging toolbox - version 2.0." Technical Report, IMMREP-2002-12. Technical University of Denmark, DK-2800, Kgs. Lyngby, Denmark.

Lovison, A. and Rigoni, E. (2010). “Adaptive sampling with a Lipschitz criterion for accurate metamodeling.” *Communications in Applied and Industrial Mathematics*, Vol. 1, No. 2, pp. 110-126.

Lum, K. W. and McGuirk, J. J. (2005). “Three-dimensional model of a complete polymer electrolyte membrane fuel cell – model formulation, validation and parametric studies.” *Journal of Power Sources*, Vol. 143, No. 1, pp. 103-124.

Ma, C. X. and Fang, K. T. (2004). “A new approach to construction of nearly uniform design.” *International Journal of Materials and Product Technology*, Vol. 20, Nos. 1-3, pp. 115-126.

Mallows, C. L. (1973). “Some comments on C_p.” *Technometrics*, Vol. 15, No. 4, pp. 661-675.

Matheron, G. (1963). “Principles of geostatistics.” *Economic Geology*, Vol. 58, No. 8, pp. 1246-1266.

McKay, M. D., Beckman, R. J. and Conover, W. J. (1979). “A comparison of three methods for selecting values of input variables in the analysis of output from a computer code.” *Technometrics*, Vol. 21, No. 2, pp. 239-245.

Meckesheimer, M., Booker, A. J., Barton, R. R. and Simpson, T. W. (2002). “Computationally inexpensive metamodel assessment strategies.” *AIAA Journa*l, Vol. 40, No. 10, pp. 2053-2060.

Miller, A. (2002). *Subset Selection in Regression*. Chapman & Hall/CRC.

Mitchell, T. J. and Morris, M. D. (1992). “Bayesian design and analysis of computer experiments: two examples.” *Statistica Sinica*, Vol. 2, No. 2, pp. 359-379.

Molga, M. and Smutnicki, C. (2005). “Test functions for optimization needs.” http://www.zsd.ict.pwr.wroc.pl/files/docs/functions.

Morris, M. D. and Mitchell, T. J. (1995). “Exploratory design for computational experiments.” *Journal of Statistical Planning and Inference*, Vol. 43, No. 3, pp. 381-402.

Mourelatos, Z., Kuczera, R. and Latcha, M. (2006). “An efficient Monte Carlo reliability analysis using global and local metamodels.” In: *Proceedings of 11th AIAA/ISSMO multidisciplinary analysis and optimization conference*, Portsmouth, VA, USA.

Myers, R. H. and Montgomery, D. C. (1995). *Response Surface Methodology: Process and Product Optimization Using Designed Experiments*. John Wiley & Sons.

Oliveira, V. B., Falcãoa, D. S., Rangel, C. M. and Pinto, A. M. F. R. (2008). "Heat and mass transfer effects in a direct methanol fuel cell: A 1D model." *International Journal of Hydrogen Energy*, Vol. 33, No. 14, pp. 3818-3828.

Oliveira, V. B., Rangel, C. M. and Pinto, A. M. F. R. (2009). "Modelling and experimental studies on a direct methanol fuel cell working under low methanol crossover and high methanol concentrations." *International Journal of Hydrogen Energy*, Vol. 34, No. 15, pp. 6443-6451.

Owen, A. B. (1992). "Randomly orthogonal arrays for computer experiments, integration and visualization." *Statistica Sinica*, Vol. 2, No. 2, pp. 439-452.

Park, J. S. (1994). "Optimal Latin-hypercube designs for computer experiments." *Journal of Statistical Planning and Inference*, Vol. 39, No. 1, pp. 95-111.

Parker. (2006). *TekStak^{TM} Educational Fuel Cell Kit – Instruction Manual and Reference Information*, Parker Hannifin Energy Systems, Cleveland, Ohio, USA.

Picheny, V., Ginsbourger, D., Roustant, O., Haftka, R. H. and Kim, N. H. (2010). "Adaptive designs of experiments for accurate approximation of a target region." *Journal of Mechanical Design, ASME Transactions*, Vol. 132, No. 7.

Powell, M. J. D. (1987). "Radial basis functions for multivariable interpolation: a review." In: J. C. Mason and M. G. Cox (Eds.). *Algorithms for Approximation*, Clarendon Press, pp. 143-167.

Qi, Z. and Kaufman, A. (2002). "Open circuit voltage and methanol crossover in DMFCs." *Journal of Power Sources*, Vol. 110, No. 1, pp. 177-185.

Rice, J. and Faghri, A. (2006). "A transient, multi-phase and multi-component model of a new passive DMFC." *International Journal of Heat and Mass Transfer*, Vol. 49, Nos. 25-26, pp. 4804-4820.

Sacks, J., Welch, W. J., Mitchell, T. J. and Wynn, H. P. (1989). "Design and analysis of computer experiments." *Statistical Science*, Vol. 4, No. 4, pp. 409-423.

Santner, T. J., Williams, B. J. and Notz, W. I. (2003). *The Design and Analysis of Computer Experiments*. Springer-Verlag.

Schwarz, G. (1978). "Estimating the dimension of a model." *Annals of Statistics*, Vol. 6, No. 2, pp. 461-464.

Scott, K. and Argyropoulos, P. (2004). "A one dimensional model of a methanol fuel cell anode." *Journal of Power Sources*, Vol. 137, No. 2, pp. 228-238.

Scott, K., Argyropoulos, P. and Sundmacher, K. (1999). "A model for the liquid feed direct methanol fuel cell." *Journal of Electroanalytical Chemistry*, Vol. 477, No. 2, pp. 97-110.

Scott, K., Jackson, C. and Argyropoulos, P. (2006). "A semi empirical model of the direct methanol fuel cell – Part II: parametric analysis." *Journal of Power Sources*, Vol. 161, No. 2, pp. 885-892.

Shasha, D. and Wilson, M. (2008). *Statistics is Easy*. Morgan & Claypool Publishers.

Shewry, M. C. and Wynn, H. P. (1987). "Maximum entropy sampling." *Journal of Applied Statistics*, Vol. 14, No. 2, pp. 165-170.

Simpson, T. W., Peplinski, J. D., Koch, P. N. and Allen, J. K. (2001). "Metamodels for computer-based engineering design: survey and recommendations." *Engineering with Computers*, Vol. 17, No. 2, pp. 129-150.

Sivertsen, B. R. and Djilali, N. (2005). "CFD-based modelling of proton exchange membrane fuel cells." *Journal of Power Sources*, Vol. 141, No. 1, pp. 65-78.

Sobol, I. M. (1967). "On the distribution of points in a cube and the approximate evaluation of integrals." *USSR Computational Mathematics and Mathematical Physics*, Vol. 7, No. 4, pp. 86-112.

Song, S. Q., Zhou, W. J., Li, W. Z., Sun, G., Xin, Q., Konton, S. and Tsiakaras, P. (2004). "Direct methanol fuel cells: methanol crossover and its influence on single DMFC performance." *Ionics*, Vol. 10, Nos. 5-6, pp. 458-462.

Tang, B. (1993). "Orthogonal array-based Latin hypercubes." *Journal of the American Statistical Association*, Vol. 88, No. 424, pp. 1392-1397.

Vera, M. (2007). “A single-phase model for liquid-feed DMFCs with non-Tafel kinetics.” *Journal of Power Sources*, Vol. 171, No. 2, pp. 763-777.

Villemonteix, J., Vazquez, E. and Walter, E. (2007). “Identification of expensive-to-simulate parametric models using kriging and stepwise uncertainty reduction.” In: *Proceedings of the 46th IEEE conference on decision and control*, New Orleans, LA, USA.

Wang, G. G. and Shan, S. (2007). “Review of metamodeling techniques in support of engineering design optimization.” *Journal of Mechanical Design, ASME Transactions*, Vol. 129, No. 4.

Wang, L., Shan, S. and Wang, G. G. (2004). “Mode-pursuing sampling method for global optimization on expensive black-box functions.” *Engineering Optimization*, Vol. 36, No. 4, pp. 419-438.

Wang, R., Qi, L., Xie, X., Ding, Q., Li, C. and Ma, C. M. (2008a). “Modeling of a 5-cell direct methanol fuel cell using adaptive-network-based fuzzy inference systems.” *Journal of Power* Sources, Vol.185, No. 2, pp. 1201-1208.

Wang, Y., Au, G., Plichta, E. J. and Zheng, J. P. (2008b). “A semi-empirical method for electrically modeling of fuel cell: executed on a direct methanol fuel cell.” *Journal of Power* Sources, Vol. 175, No. 2, pp. 851-860.

Wang, Z. H. and Wang, C. W. (2003). “Mathematical modeling of liquid-feed direct methanol fuel cells.” *Journal of the Electrochemical Society*, Vol. 150, No. 4, pp. A508-A519.

Warnock, T. T. (1972). “Computational investigation of low discrepancy point sets.” In: S. K. Zaremba (Ed.). *Applications of Number Theory to Numerical Analysis*, Academic Press, pp. 319-343.

Wei, X., Wu, Y. and Chen, L. (2012). “A new sequential optimal sampling method for radial basis functions.” *Applied Mathematics and Computation*, Vol. 218, No. 19, pp. 9635–9646.

Wiens, D. P. (1991). “Designs for approximately linear regression: two optimality properties of uniform designs.” *Statistics & Probability Letters*, Vol. 12, No. 3, pp. 217-221.

Xiong, Y., Chen, W. and Tsui, K. L. (2007). “A new variable fidelity optimization framework based on model fusion and objective-oriented sequential sampling.” In: *Proceedings of the ASME 2007 International Design Engineering Technical Conferences and Computers and Information in Engineering Conference*, Las Vegas, NV, USA.

Yang, H. and Zhao, T. S. (2005). “Effect of anode flow filed design on the performance of liquid feed direct methanol fuel cells.” *Electrochimica Acta*, Vol. 50, Nos. 16-17, pp. 3243-3252.

Yang, Q., Kianimanesh, A., Park, S. S., Freiheit, T. and Xue, D. (2011). “A semi-empirical model considering the influence of operating parameters on performance for a direct methanol fuel cell.” *Journal of Power Sources*, Vol. 196, No. 24, pp. 10640-10651.

Yang, S. H., Chen, C. Y. and Wang, W. J. (2010). “An impedance study of an operating direct methanol fuel cell.” *Journal of Power Sources*, Vol. 195, No. 8, pp. 2319-2330.

Yang, W. W. and Zhao, T. S. (2007). “A two-dimensional, two-phase mass transport model for liquid-feed DMFCs.” *Electrochimica Acta*, Vol. 52, No. 20, pp. 6125-6140.

Yang, W. W., Zhao, T. S. and Xu, C. (2007) “Three-dimensional two-phase mass transport model for direct methanol fuel cells.” *Electrochimica Acta*, Vol. 53, No. 2, pp. 853-862.

Yao, W., Chen, X. and Luo, W. (2009). “A gradient-based sequential radial basis function neural network modeling method.” *Neural Computing and Applications*, Vol. 18, No. 5, pp. 477–484.

Ye, K. Q. (1998). “Orthogonal Column Latin hypercubes and their applications in computer experiments.” *Journal of the American Statistical Association*, Vol. 93, No. 444, pp. 1430-1439.

Yu, B., Yang, Q., Kianimanesh, A., Freiheit, T., Park, S. S., Zhao, H. and Xue D. (2013). “A CFD model with semi-empirical electrochemical relationships to study the influence of geometric and operating parameters on DMFC performance.” *International Journal of Hydrogen Energy*, Vol. 38, No. 23, pp. 9873-9885.

Zhang, J. (2008). *PEM Fuel Cell Electrocatalysts and Catalyst Layers: Fundamentals and Applications*. Springer-Verlag.

Zhao, D. and Xue, D. (2010). “A comparative study of metamodeling methods considering sample quality merits.” *Structural and Multidisciplinary Optimization*, Vol. 42, No. 6, pp. 923-938.

PUBLICATIONS

Journal Publications

- Yang, Q., Kianimanesh, A., Park, S. S., Freiheit, T. and Xue, D. (2011). "A semi-empirical model considering the influence of operating parameters on performance for a direct methanol fuel cell." *Journal of Power Sources*, Vol. 196, No. 24, pp. 10640-10651.
- Kianimanesh, A., Yu, B., Yang, Q., Freiheit, T., Xue, D. and Park, S. S. (2012). "Investigation of bipolar plate geometry on direct methanol fuel cell performance." *International Journal of Hydrogen Energy*, Vol. 37, No. 23, pp. 18403-18411.
- Yu, B., Yang, Q., Kianimanesh, A., Freiheit, T., Park, S. S., Zhao, H. and Xue D. (2013). "A CFD model with semi-empirical electrochemical relationships to study the influence of geometric and operating parameters on DMFC performance." *International Journal of Hydrogen Energy*, Vol. 38, No. 23, pp. 9873-9885.
- Kianimanesh, A., Yang, Q., Park, S. S., Xue, D. and Freiheit, T. "Degradation Analysis of a Single-Cell Direct Methanol Fuel Cell System." Accepted by *Fuel Cells*.
- Yang, Q. and Xue, D. "Comparative study on influencing factors in adaptive metamodeling for optimization." Submitted to *Engineering with Computers*.
- Yang, Q. and Xue, D. "A weighted sequential sampling method considering influences of sample qualities in input and output parameter spaces for global optimization." Submitted to *Journal of Optimization Theory and Applications*.
- Yang, X. and Yang, Q. (2009). "A new approach to compound tool path generation based on discrete cutter locations." *Journal of Hunan University* (*Natural Sciences*), Vol. 36, No. 10, pp. 35-39.
- Xia, Q., Zhou, Z., Huang, X. and Yang, Q. (2010). "Simulation and comparison of thermal resource models in surface grinding." *Computer Simulation*, Vol. 27, No. 1, pp. 297-300.

Conference Publication

- Kianimanesh, A., Yang, Q., Freiheit, T., Xue, D., and Park, S. S. (2011). "Experimental Study of a Direct Methanol Fuel Cell (DMFC) System." In: *Proceedings of the 23rd Canadian Congress of Applied Mechanics (CANCAM'11)*, pp. 239-242, Vancouver, B.C., Canada.